

16th International Circumpolar Remote Sensing Symposium

University of Alaska Fairbanks

16-20 May 2022

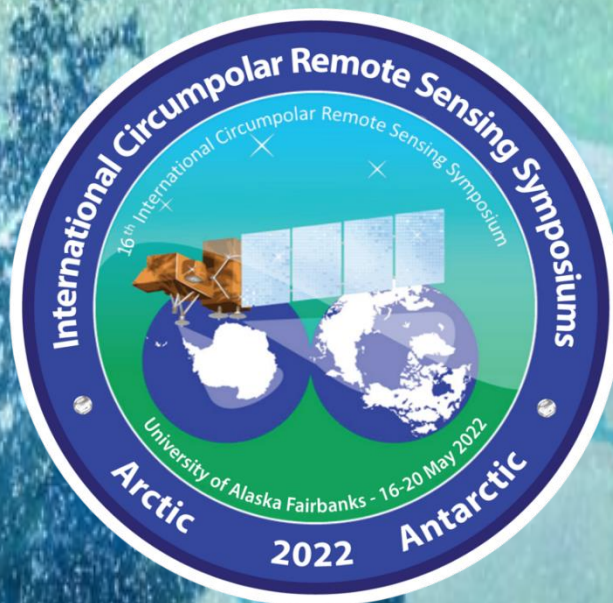


Table of Contents

| | |
|---|----|
| Welcome and | |
| Organizing Committee | 1 |
| Safety Issues | 2 |
| COVID-19..... | 2 |
| Code of Conduct | 2 |
| Maps | 3 |
| University of Alaska Fairbanks | 3 |
| Bus Routes to and from Wedgewood Resort (free) | 4 |
| Program Overview | 5 |
| Schedule | 7 |
| Monday | 7 |
| Tuesday | 9 |
| Wednesday: Excursion Day | 10 |
| Thursday | 11 |
| Friday | 13 |
| Poster Presenters | 14 |
| ABSTRACTS | 16 |
| Session 1: Arctic Land Cover I | 16 |
| 70-year retrospective of remote sensing applied to cumulative impact assessments, Prudhoe Bay Oilfield, Alaska..... | 16 |
| Forty years through the looking glass: spaceborne circumpolar tundra greenness observation enters its 5 th decade..... | 20 |
| An overview of NASA’s Arctic Boreal Vulnerability Experiment (ABOVE): Advances, knowledge gaps and next steps..... | 22 |
| Boreal forests at tree-scale and stand-scale: Exploring the benefits of in-house aerial VNIR/SWIR imaging spectroscopy for Alaska wildfire research | 24 |
| Session 2: Arctic Land Cover II | 26 |
| Time-series maps reveal widespread change in plant functional type cover across arctic and boreal Alaska and Yukon | 26 |
| Unraveling 3D shrub architecture with UAS LIDAR..... | 29 |
| Using Landsat imagery to detect beavers in eastern Nunavik..... | 30 |

| | |
|---|-----------|
| Drought response analysis on a geothermally warmed Sub-Arctic grassland ecosystem using multispectral drone images | 31 |
| Synthesis of observations of boreal forest structure and age: regional patterns of growth | 33 |
| Session 3: Arctic Land Cover III | 34 |
| Discovering data and results from the ABoVE airborne campaign..... | 34 |
| Addressing the hyperspectral data need for the Arctic environment through image simulation | 36 |
| Post-fire tree and shrub cover influences on vegetation indices in Siberian larch forests | 39 |
| Development of an arctic-boreal fire atlas using Visible Infrared Imaging Radiometer Suite active fire data..... | 41 |
| Evolving outburst flood hazards and impacts from glacier-dammed lakes..... | 43 |
| Session 4: New Sensors, Operational Services and Method advancement | 44 |
| NLCD Alaska: Upcoming release supporting NALCMS and the MRLC consortium | 44 |
| NESDIS in the Arctic: | 45 |
| Authoritative climate products from satellite remote sensing | 45 |
| Instrument development for flexible arctic remote sensing | 46 |
| A U-Net based algorithm for automated detection of clouds from medium-resolution satellite imagery | 47 |
| Session 1: Arctic Coasts and its Communities I | 49 |
| Earth observation for permafrost-dominated arctic coasts – contributions to the next generation of the Arctic Coastal Dynamics database..... | 49 |
| Automating coastline measurements of arctic regions from high resolution satellite imagery | 52 |
| Observing permafrost coastal bluff erosion using a high spatial and temporal resolution remote sensing time series at Drew Point, Beaufort Sea Coast, Alaska..... | 54 |
| Remote uncrewed aircraft system (UAS) inspection and response team development in the Bering Strait region | 56 |
| Session 2.1: Arctic Coasts and its Communities II | 58 |
| Shore evidences of a high Antarctic ocean wave event: geomorphology, event reconstruction and coast dynamics through a remote sensing approach | 58 |
| Landscapes and erosion rates of the Alaska Beaufort Sea Coast | 60 |
| Session 2.2: Climate Change and Climate Data Records..... | 61 |
| Low-frequency sea ice variability drives NDVI declines in the Yukon-Kuskokwim Delta | 61 |
| A remote sensing view of Arctic heat anomalies: Spatial-temporal distribution and effects | 64 |
| Early snowmelt and polar jet dynamics drive recent extreme Siberian fire seasons | 67 |
| Session 1: Glaciers and Seasonal Snow Cover | 68 |
| A new 38-year time series of daily, global fractional snow cover maps..... | 68 |

| | |
|--|------------|
| The development and application of a UAS and photogrammetry routine in support of Alaska’s department of transportation effort to elucidate snow height for avalanche risk assessment in Atigun Pass | 70 |
| Session 1.1 : Observing Permafrost I | 72 |
| Deep Learning for mapping retrogressive thaw slumps across the Arctic | 72 |
| Circum-Arctic distribution of topographic asymmetry | 75 |
| Session 2 (11:00-12:20): Observing Permafrost II | 77 |
| Permafrost thaw drives surface water drainage across the pan-Arctic | 77 |
| Multiscale analysis of remotely sensed imagery to quantify spatial and temporal patterns of river bank erosion in floodplains with permafrost..... | 81 |
| Permafrost vulnerability – deriving a vulnerability index from ESA CCI EO-datasets..... | 83 |
| Session 3: Observing Permafrost III | 86 |
| Mapping drained lake basins on a circumpolar scale | 86 |
| The spatio-temporal variability of frost blisters in a perennial frozen lake along the Antarctic coast as indicator of the groundwater supply..... | 88 |
| Mapping retrogressive thaw slumps in High Arctic Canada using high-spatial resolution satellite imagery and deep learning | 90 |
| An approach to inventorying retrogressive thaw slumps on a continental scale | 91 |
| Session 4 : Floating Ice | 93 |
| Sea ice from the ground up using distributed acoustic sensing | 93 |
| Physiographic controls on landfast ice variability from 20 years of maximum extents across the Northwest Canadian Arctic | 95 |
| A neural network-based method for satellite mapping of sediment-laden sea ice in the Arctic..... | 98 |
| Identifying spatial patterns of river ice formation and hazardous open water zones with Synthetic Aperture Radar (SAR) | 100 |
| Session 1 : Microwave Remote Sensing | 102 |
| Potential monitoring of surface organic soil properties in arctic tundra using microwave remote sensing data | 102 |
| Fine-scale ground truth of ground displacement in the Anaktuvuk River Fire (ARF) for satellite and airborne L-band SAR | 105 |
| Monitoring soil water and organic carbon storage patterns in the active layer of the Arctic Foothills using spaceborne InSAR surface deformation data..... | 107 |
| Session 2 : Microwave Remote Sensing II | 109 |
| Synthetic Aperture Radar (SAR) detects large gas seep in lake | 109 |
| Posters Abstracts | 116 |

| | |
|--|-----|
| Baldwin: Utilizing multispectral imagery to assess historic maximum flood heights in remote Alaskan communities and improve flood mitigation strategies | 116 |
| Barth: Earth observation-based time series analysis of retrogressive thaw slump dynamics in the Russian High Arctic..... | 118 |
| Bogardus: Integrating iVR into education and community planning in rural Alaska; a case study from Drew Point, Alaska | 121 |
| Bondurant: Aufeis growth detection on the Sagavanirktok and Dietrich Rivers using unmanned aerial systems and optical photogrammetry | 123 |
| Brown: Identifying spatial patterns of river ice formation and hazardous open water zones with Synthetic Aperture Radar (SAR) | 125 |
| Bryant: Integrating ICESat-2 and optical imagery to measure coastal erosion rates and bluff morphology along the Alaskan Beaufort Sea Coast..... | 126 |
| Burrell: Climate change, fire return intervals and the growing risk of permanent forest loss in boreal Eurasia..... | 128 |
| Czarnecki: The use of remote sensing methods and the capabilities of UAV in polar research – examples of transformation of the shoreline in Kaffiøyra Plain (Svalbard)..... | 130 |
| Czarnecki: Evaluation of the usefulness of Landsat 8 imagery in 2013-2020 on the example of the Aavatsmarkbreen (NW Spitsbergen, Svalbard) | 131 |
| Sobota: Hydrological analysis of Kaffiøyra Plain: Change in areas, coastline and amount of glacial lakes in the light of remote sensing imagery and UAV measurements, Elisebreen sample..... | 132 |
| Dann: Identification of secondary factors controlling Synthetic Aperture Radar (SAR) -derived root-zone soil moisture over the Seward Peninsula using random forest modelling | 133 |
| Farquharson: Permafrost thaw and talik development drives future coastal inundation in North Slope communities..... | 135 |
| Frederick: Space-based observations are critical for validating maps of arctic marine greenhouse gas emissions predicted with numerical models | 137 |
| Grosse: A new dynamic land cover classification of the Arctic Lena Delta for scaling methane fluxes | 139 |
| Hanston: Scaling spectral and structural characterizations of vegetation and landscape features along permafrost thaw gradients in Arctic tundra | 142 |
| Helder: Exploring the reliability and scalability of automated shoreline detection tools for the Alaskan Arctic..... | 145 |
| Hessilt: Influences of snowmelt timing on arctic-boreal fire season start across North America.... | 147 |
| Jones: High spatial and temporal resolution remote sensing of a collapsing pingo in northern Alaska | 148 |
| Kelkar: Applying DInSAR for rock glacier inventories | 150 |
| Kuhle: Quantifying peat carbon mass using ground-penetrating radar (GPR) in high-latitude peatlands of the Kenai Peninsula, Alaska | 152 |

| | |
|---|------------|
| Lara: Mapping arctic-boreal peatlands in Alaska: implications for historical peatland fire dynamics | 154 |
| Martin: Estimating tall shrub biomass in southcentral Alaska | 155 |
| Nole: Predicting permafrost greenhouse gas emissions by linking local and space-based observations through large-scale thermo-hydrologic modeling | 157 |
| Raynolds: Vegetation Response to a climate gradient in the eastern Canadian Arctic..... | 159 |
| Rea: Investigating red snow algae resurfacing and distribution patterns | 160 |
| Rettelbach: The evolution of ice-wedge polygon networks in tundra fire scars | 163 |
| Sivaraj: Characterization of arctic sea ice melt pond dynamics with remote sensing..... | 166 |
| Spasova: Interoperability of remote sensing and open data for Arctic and Antarctic ice and climate change monitoring and security | 168 |
| Turner: Detecting the climate-driven disturbances that are influencing aquatic environments in Old Crow Flats, Yukon, Canada..... | 169 |
| Veremeeva: Yedoma surface thaw subsidence (2015-2021) depended on local geomorphological conditions, Bykovsky Peninsula, Laptev Sea region..... | 172 |
| Wong: Calibrating 2000-2020 MODIS and Landsat greening in Northwest Alaska with 1000 km of vegetation transect data..... | 174 |
| Wooten: Estimating Site Index in boreal forests with lidar and very-high resolution stereo imagery | 176 |
| Special Thanks to Our Sponsors! | 177 |

Welcome!

Welcome to the University of Alaska Fairbanks and the 16th International Circumpolar Remote Sensing Symposium. The ICRSS is returning to Fairbanks for the first time in more than two decades. The theme of the 16th ICRSS is Convergence at the Poles – Addressing urgent research questions and management needs through remote sensing in the Arctic and Antarctic.

Organizing Committee



Benjamin Jones
Inst. N. Engineering, UAF



Melissa Ward Jones
Inst. N. Eng., UAF



Jessica Garron
Geophysical Inst., UAF



Guido Grosse
Alfred Weg. Inst.



Simon Zwieback
Geophys. Inst. UAF



Gerald (JJ) Frost
ABR, Inc.



Helena Bergstedt
b.geos, Korneub



Martha Reynolds
Inst. of Arctic Biology, UAF

Safety Issues

COVID-19

All conference attendees have stated that they are vaccinated and have approved the ICRSS Covid Policy.

If you experience any Covid symptoms, please contact the conference organizers (icrss2022@gmail.com), so that we can take appropriate steps to keep other attendees healthy.

Conference name tags are color coded.

- Red: High Sensitivity, please keep your distance and keep masked
- Yellow: OK with < 2 m distance but no physical contact
- Green: Handshakes & hugs OK

Masks, hand sanitizer and a limited number of Rapid Covid tests will be available for conference attendees.

Free, drive-through testing is available on UAF Campus across the street from the hockey rink in the Nenana parking lot - <https://uaf.edu/news/covid-19-testing-trailer-open.php>. Test turn around times are about 1 hour for verbal results.

If you are feeling symptomatic or if you do test positive please also follow this guidance - <https://sites.google.com/alaska.edu/coronavirus/uaf>

Medical care is available at the Tanana Valley First Care Clinic TVC - telemedicine or in person visit at 907-458-2682. Telemedicine is available Monday Friday 8 AM-5 PM.

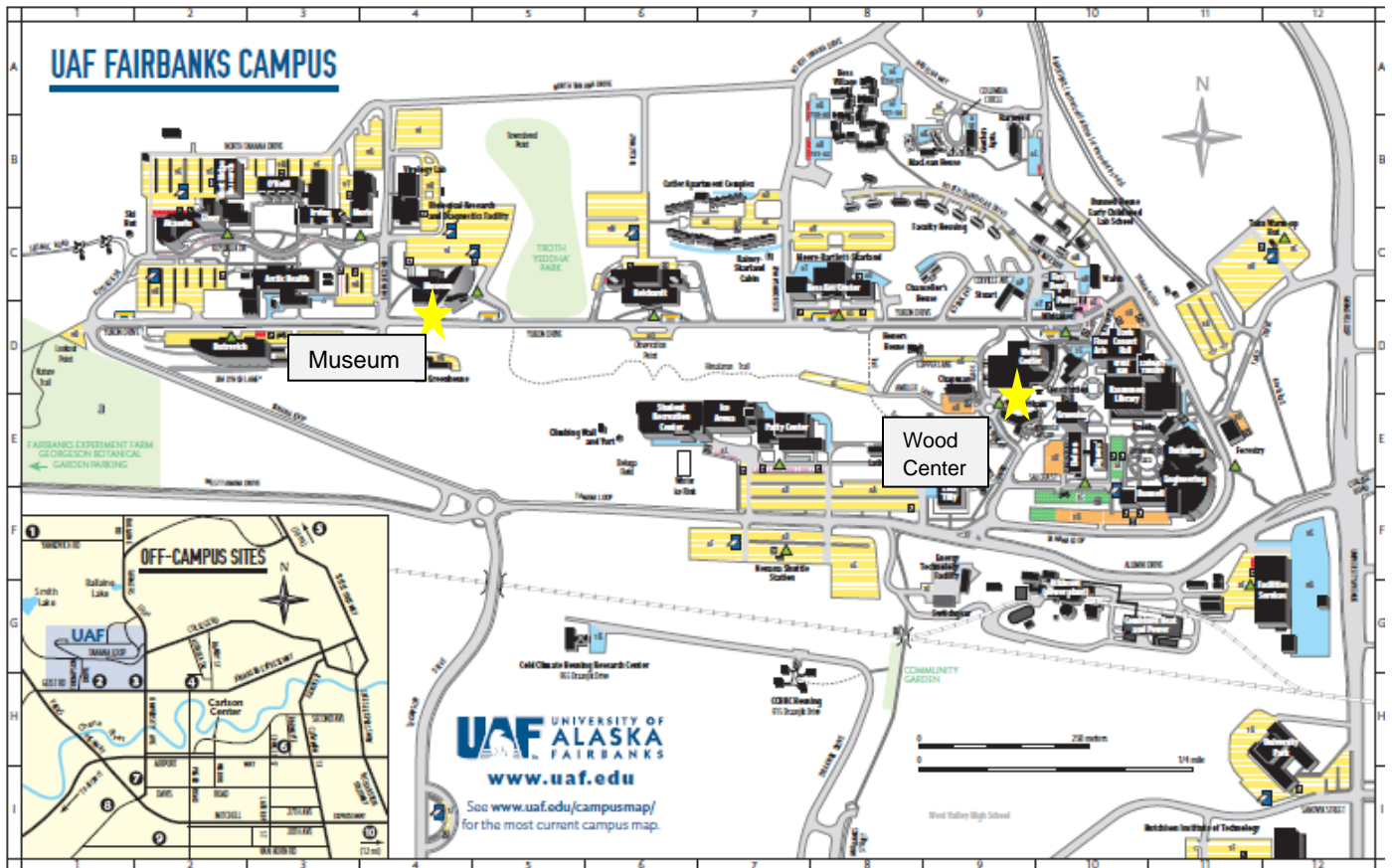
Code of Conduct

The ICRSS follows the University of Alaska guidelines to conduct a meeting that promotes equal opportunities and treatment for all participants, and is free of harassment and discrimination. Participants are expected to treat others with respect and consideration, follow venue rules, and alert conference organizers or security of any dangerous situations or anyone in distress. Speakers are expected to uphold standards of scientific integrity and professional ethics.

Harassment should be reported immediately to Symposium organizers (icrss2022@gmail.com), the UAF Title IX office (website: <https://uaf.edu/titleix/> phone: 1.907.474.7300), UAF Campus security (email: UAF-Police-Dept@alaska.edu phone: 907-474-7721), or 911 in emergency situations.

Maps

University of Alaska Fairbanks



Bus Routes to and from Wedgewood Resort (free)

Blue Line – from Wedgewood to UAF Wood Center (20 minutes). Walk from Wedgewood out Margaret Ave. to College Road, turn left and walk 1 block to bus stop. Get on any bus.

Red Line - from UAF Wood Center to Wedgewood (20 minutes). Get on at bus stop above Wood Center. Get off after light at Antoinette and Margaret Avenue. Cross street and walk back to Margaret Ave. and take Margaret to Wedgewood.

BLUE LINE

Transit Center 1 2 3 4 5 6 7 8 Shoppers Forum

Monday through Friday

| | | | | | | | | | |
|-------|-------|-------|-------|-------|-------|-------|-------|-------|-------|
| 6:30 | 6:40 | 6:43 | 6:50 | 7:00 | 7:15 | 7:20 | 7:23 | 7:30 | 7:36 |
| 7:15 | 7:25 | 7:28 | 7:35 | 7:45 | 8:00 | 8:05 | 8:08 | 8:16 | 8:22 |
| 7:45 | 7:55 | 7:58 | 8:05 | 8:15 | 8:30 | 8:35 | 8:38 | 8:46 | 8:52 |
| 8:30 | 8:40 | 8:43 | 8:50 | 9:00 | 9:15 | 9:20 | 9:23 | 9:31 | 9:37 |
| 9:00 | 9:10 | 9:13 | 9:20 | 9:30 | 9:45 | 9:50 | 9:53 | 10:01 | 10:07 |
| 9:45 | 9:55 | 9:58 | 10:05 | 10:15 | 10:30 | 10:35 | 10:38 | 10:46 | 10:52 |
| 10:15 | 10:25 | 10:28 | 10:35 | 10:45 | 11:00 | 11:05 | 11:08 | 11:16 | 11:22 |
| 11:30 | 11:40 | 11:43 | 11:50 | 12:00 | 12:15 | 12:20 | 12:23 | 12:31 | 12:37 |
| 12:15 | 12:25 | 12:28 | 12:35 | 12:45 | 1:00 | 1:05 | 1:08 | 1:16 | 1:22 |
| 12:45 | 12:55 | 12:58 | 1:05 | 1:15 | 1:30 | 1:35 | 1:38 | 1:46 | 1:52 |
| 1:30 | 1:40 | 1:43 | 1:50 | 2:00 | 2:15 | 2:20 | 2:23 | 2:31 | 2:37 |
| 2:00 | 2:10 | 2:13 | 2:20 | 2:30 | 2:45 | 2:50 | 2:53 | 3:01 | 3:07 |
| 2:45 | 2:55 | 2:58 | 3:05 | 3:15 | 3:30 | 3:35 | 3:38 | 3:46 | 3:52 |
| 3:15 | 3:25 | 3:28 | 3:35 | 3:45 | 4:00 | 4:05 | 4:08 | 4:16 | 4:22 |
| 4:00 | 4:10 | 4:13 | 4:20 | 4:30 | 4:45 | 4:50 | 4:53 | 5:01 | 5:07 |
| 4:30 | 4:40 | 4:43 | 4:50 | 5:00 | 5:15 | 5:20 | 5:23 | 5:31 | 5:37 |
| 5:15 | 5:25 | 5:28 | 5:35 | 5:45 | 6:00 | 6:05 | 6:08 | 6:16 | 6:22 |
| 5:45 | 5:55 | 5:58 | 6:05 | 6:15 | 6:30 | 6:35 | 6:38 | 6:46 | 6:52 |
| 6:30 | 6:40 | 6:43 | 6:50 | 7:00 | 7:15 | 7:20 | 7:23 | 7:31 | 7:37 |
| 8:00 | 8:10 | 8:13 | 8:20 | 8:30 | 8:45 | 8:50 | 8:53 | 9:01 | 9:07 |
| 9:15 | 9:25 | 9:28 | 9:35 | 9:45 | | | | | |

Saturday

| | | | | | | | | | |
|-------|-------|-------|-------|-------|-------|-------|-------|-------|-------|
| 9:15 | 9:25 | 9:28 | 9:35 | 9:45 | 10:00 | 10:05 | 10:08 | 10:16 | 10:22 |
| 10:30 | 10:40 | 10:43 | 10:50 | 11:00 | 11:15 | 11:20 | 11:23 | 11:31 | 11:37 |
| 11:45 | 11:55 | 11:58 | 12:05 | 12:15 | 12:30 | 12:35 | 12:38 | 12:46 | 12:52 |
| 1:00 | 1:10 | 1:13 | 1:20 | 1:30 | 1:45 | 1:50 | 1:53 | 2:01 | 2:07 |
| 2:15 | 2:25 | 2:28 | 2:35 | 2:45 | 3:00 | 3:05 | 3:08 | 3:16 | 3:22 |
| 3:30 | 3:40 | 3:43 | 3:50 | 4:00 | 4:15 | 4:20 | 4:23 | 4:31 | 4:37 |
| 4:45 | 4:55 | 4:58 | 5:05 | 5:15 | 5:30 | 5:35 | 5:38 | 5:46 | 5:52 |
| 6:00 | 6:10 | 6:13 | 6:20 | 6:30 | 6:45 | 6:50 | 6:53 | 7:01 | 7:07 |
| 7:15 | 7:25 | 7:28 | 7:35 | 7:45 | | | | | |

No Sunday Service

BLUE LINE

How to Ride the Bus

First, look at the map on the back of this brochure to find which color bus line (Red, Blue, Green, etc.) takes you to where you want to go. You may need to ride more than one bus to get to your final destination. Let the driver know if you need to connect with another bus. You must pay the fare each time you change buses, unless you purchase a Day or Monthly Pass. Once you know the color bus line, go to www.macstransit.com or pick up that route's brochure to see what time the bus will stop near where you want to board. Timed stops are listed in the schedules. The maps show timed and other bus stops as well as popular destinations.

Finally, look for the roadside bus stop signs. They are usually two to three blocks apart. Each bus stop has a schedule and map posted for your convenience. Try to be at the stop about five minutes early. If you have any questions, please ask the driver. Welcome aboard!

MACS
Fairbanks North Star Borough
Metropolitan Area Connector System
www.macstransit.com

RED LINE

Transit Center 1 2 3 4 5 6 Shoppers Forum

Monday through Friday

| | | | | | | | |
|-------|-------|-------|-------|-------|-------|-------|-------|
| 6:15 | 6:21 | 6:29 | 6:39 | 7:00 | 7:07 | 7:18 | 7:25 |
| | | | | 7:30 | 7:37 | 7:48 | 7:55 |
| 7:30 | 7:36 | 7:44 | 7:54 | 8:15 | 8:22 | 8:33 | 8:40 |
| 8:00 | 8:06 | 8:14 | 8:24 | 8:45 | 8:52 | 9:03 | 9:10 |
| 8:45 | 8:51 | 8:59 | 9:09 | 9:30 | 9:37 | 9:48 | 9:55 |
| 9:15 | 9:21 | 9:29 | 9:39 | 10:00 | 10:07 | 10:18 | 10:25 |
| 10:30 | 10:36 | 10:44 | 10:54 | 11:15 | 11:22 | 11:33 | 11:40 |
| 11:15 | 11:21 | 11:29 | 11:39 | 12:00 | 12:07 | 12:18 | 12:25 |
| 11:45 | 11:51 | 11:59 | 12:09 | 12:30 | 12:37 | 12:48 | 12:55 |
| 12:30 | 12:36 | 12:44 | 12:54 | 1:15 | 1:22 | 1:33 | 1:40 |
| 1:45 | 1:51 | 1:59 | 2:09 | 2:30 | 2:37 | 2:48 | 2:55 |
| 2:15 | 2:21 | 2:29 | 2:39 | 3:00 | 3:07 | 3:18 | 3:25 |
| 3:00 | 3:06 | 3:14 | 3:24 | 3:45 | 3:52 | 4:03 | 4:10 |
| 3:30 | 3:36 | 3:44 | 3:54 | 4:15 | 4:22 | 4:33 | 4:40 |
| 4:45 | 4:51 | 4:59 | 5:09 | 5:30 | 5:37 | 5:48 | 5:55 |
| 5:30 | 5:36 | 5:44 | 5:54 | 6:15 | 6:22 | 6:33 | 6:40 |
| 6:00 | 6:06 | 6:14 | 6:24 | 6:45 | 6:52 | 7:03 | 7:10 |
| 6:45 | 6:51 | 6:59 | 7:09 | 7:30 | 7:37 | 7:48 | 7:55 |
| 8:00 | 8:06 | 8:14 | 8:24 | 8:45 | 8:52 | 9:03 | 9:10 |
| 9:15 | 9:19 | 9:30 | 9:36 | 9:45 | | | |

Saturday

| | | | | | | | |
|-------|-------|-------|-------|-------|-------|-------|-------|
| | | | | 9:15 | 9:22 | 9:33 | 9:40 |
| 11:15 | 11:21 | 11:29 | 11:39 | 12:00 | 12:07 | 12:18 | 12:25 |
| 12:30 | 12:36 | 12:44 | 12:54 | 1:15 | 1:22 | 1:33 | 1:40 |
| 1:45 | 1:51 | 1:59 | 2:09 | 2:30 | 2:37 | 2:48 | 2:55 |
| 3:00 | 3:06 | 3:14 | 3:24 | 3:45 | 3:52 | 4:03 | 4:10 |
| 4:15 | 4:21 | 4:29 | 4:39 | 5:00 | 5:07 | 5:18 | 5:25 |
| 5:30 | 5:36 | 5:44 | 5:54 | 6:15 | 6:22 | 6:33 | 6:40 |

No Sunday Service

RED LINE

How to Ride the Bus

First, look at the map on the back of this brochure to find which color bus line (Red, Blue, Green, etc.) takes you to where you want to go. You may need to ride more than one bus to get to your final destination. Let the driver know if you need to connect with another bus. You must pay the fare each time you change buses, unless you purchase a Day or Monthly Pass. Once you know the color bus line, go to www.macstransit.com or pick up that route's brochure to see what time the bus will stop near where you want to board. Timed stops are listed in the schedules. The maps show timed and other bus stops as well as popular destinations.

Finally, look for the roadside bus stop signs. They are usually two to three blocks apart. Each bus stop has a schedule and map posted for your convenience. Try to be at the stop about five minutes early. If you have any questions, please ask the driver. Welcome aboard!

MACS
Fairbanks North Star Borough
Metropolitan Area Connector System
www.macstransit.com

Program Overview

| | Sunday | Monday | Tuesday | Wednesday | Thursday | Friday |
|---------------|--|---|---|-------------------------|--|---|
| Registration | | 8:00-14:00 | 8:30-14:00 | | 8:30-14:00 | 8:30-12:00 |
| Housekeeping | | 8:50-9:00 | 8:50-9:00 | | 9:00-9:10 | 8:50-9:00 |
| Start | | 9:00 AM | 9:00 AM | | 9:00 AM | 9:00 AM |
| Timeslot-1 | | <i>Arctic Land Cover I</i> | <i>Arctic Coasts and its Communities I</i> | <i>Local excursions</i> | <i>Glaciers and Seasonal Snow</i> <i>Observing Permafrost I</i> | <i>Microwave Remote Sensing I</i> |
| Coffee Break | | 10:40 - 11:00 | 10:30-11:00 | | 10:30-11:00 | 10:10-10:45 |
| Timeslot-2 | | <i>Arctic Land Cover II</i> | <i>Arctic Coasts and its Communities II</i> <i>Climate Change and Climate Data Records</i> | | <i>Observing Permafrost II</i> | <i>Microwave Remote Sensing II</i> <i>Closing Ceremony 12:00-12:15</i> |
| Lunch | | 12:40-14:00 | 12:40-14:00 <i>Movement (14:00-14:15)</i> | | 12:20-13:30 | 12:15-13:30 |
| Timeslot-3 | | <i>Arctic Land Cover III</i> | <i>Panel discussion (14:15-15:15)</i> | | <i>Observing Permafrost III</i> | <i>Side Meetings</i> |
| Coffee Break | | 15:40-16:00 | <i>Coffee + Poster Session - transition to the Pub</i> | | 14:50-15:20 | 15:00-15:30 |
| Timeslot-4 | | <i>New Sensors, Operational Services and Method advancement</i> | | | <i>Floating Ice</i> | <i>Side Meetings</i> |
| Housekeeping | | | | | | |
| Evening Event | Ice Breaker Antique Auto Museum 5-8 pm | Banquet – Green’s Bar & Grill, Fairbanks Golf Course 6-9 pm | Campus Pub | Free night | Arctic Research Open House, West Ridge UAF | Post-Conference Gatherings |



ARCTIC RESEARCH



Open house

Learn about science happening in the Fairbanks "neighborhood!" Over a dozen research groups and colleges on the University of Alaska Fairbanks west ridge are holding open houses. Park for free in lots along Koyukuk Drive. More info ► <https://bit.ly/3P15LLz>

Thursday • May 19 • 4–7 pm

UAF west ridge

Who is participating?

Alaska Center for Energy & Power
Alaska EPSCoR
Alaska IDeA Network of Biomedical Research Excellence
Alaska Satellite Facility
Alaska Sea Grant
Biomedical Learning and Student Training
College of Fisheries and Ocean Sciences

College of Rural and Community Development
Geophysical Institute
Honors College
Institute of Agriculture, Natural Resources and Extension
Institute of Arctic Biology
International Arctic Research Center

Large Animal Research Station/
Animal Resources Center
Map Office
National Weather Service
One Health
Toolik Field Station



free • science • ice cream • food truck

Schedule

Monday

Zoom Link - <https://alaska.zoom.us/j/87552431368?pwd=uAjfCoxPxQWPUkn45Mct7EjvGzS6gz.1>

Conference Opening (9:00-9:10)

Session 1 (9:10-10:40): Arctic Land Cover I

Talk 1: Keynote by Skip Walker (30 min)

A 70-year retrospective of remote sensing applied to cumulative impact assessments of infrastructure and climate change, Prudhoe Bay Oilfield, Alaska, and the circumpolar Arctic

Talk 2: JJ Frost (20 min)

Forty years through the looking glass: spaceborne circumpolar tundra greenness observation enters its 5th decade

Talk 3: Scott Goetz (20 min)

An overview of NASA's Arctic Boreal Vulnerability Experiment (ABOVE): Advances, knowledge gaps and next steps

Talk 4: Christine Waigl (20 min)

Boreal forests at tree-scale and stand-scale: Exploring the benefits of in-house aerial VNIR/SWIR imaging spectroscopy for Alaska wildfire research

Coffee Break (10:40-11:00)

Session 2 (11:00-12:40): Arctic Land Cover II

Talk 5: Matthew Macander (20 min)

Time-series maps reveal widespread change in plant functional type cover across arctic and boreal Alaska and Yukon

Talk 6: Christian Andresen (20 min)

Unraveling 3D shrub architecture with UAS LIDAR

Talk 7: Vanessa Caron (virtual?) (20 min)

Using Landsat Imagery to Detect Beavers in Eastern Nunavik

Talk 8: Amir Hamedpour (virtual) (20 min)

Drought response analysis on a geothermally warmed Sub-Arctic grassland ecosystem using multispectral drone images

Talk 9: Paul Montesano (Virtual?) (20 min)

Synthesis of observations of boreal forest structure and age: regional patterns of growth

Lunch Break (12:40-14:00)

Session 3 (14:00-15:40): Arctic Land Cover III

Talk 10: Elizabeth Hoy (20 min)

Discovering data and results from the ABoVE airborne campaign

Talk 11: Anushree Badola (20 min)

Addressing the hyperspectral data need for the Arctic environment through image simulation

Talk 12: Mike Loranty (20 min)

Post-fire tree and shrub cover influences on vegetation indices in Siberian larch forests

Talk 13: Rebecca Scholten (20 min)

Development of an arctic-boreal fire atlas using Visible Infrared Imaging Radiometer Suite active fire data

Talk 14: Jason Amundson (virtual) (20 min)

Evolving outburst flood hazards and impacts from glacier-dammed lakes

Coffee Break (15:40-16:00)

Session 4 (16:00-17:20): New Sensors, Operational Services and Method advancement I

Talk 15: Jon Dewitz (20 min)

NLCD Alaska: upcoming release supporting NALCMS and the MRLC consortium

Talk 16: Jessica Cherry (20 min)

NESDIS in the Arctic: authoritative climate products from satellite remote sensing

Talk 17: Lora Koenig (20 min)

Instrument development for flexible arctic remote sensing

Talk 18: Amit Hasan (20 min)

Tuesday

Zoom Link - <https://alaska.zoom.us/j/81514930024?pwd=3Oe7VgsKbAiQrcyCnboG5lJ95eoxjE.1>

Session 1 (9-10:30): Arctic Coasts and its Communities I

Talk 1: Keynote by Annett Bartsch (30 min)

Earth observation for permafrost-dominated arctic coasts – contributions to the next generation of the Arctic Coastal Dynamics database.

Talk 2: Kristopher Carroll (20 min)

Automating coastline measurements of arctic regions from high resolution satellite imagery

Talk 3: Melissa Ward Jones (20 min)

Monitoring coastal erosion using a high-resolution time series at Drew Point, Beaufort Sea Coast, Alaska

Talk 4: Jessica Garron and John Henry, Jr. (20 min)

Remote uncrewed aircraft system (UAS) inspection and response team development in the Bering Strait Region

Coffee Break (10:30-11:00)

Session 2.1 (11:00-11:40): Arctic Coasts and its Communities II

Talk 5: Stefano Ponti (20 min)

Shore evidences of a high Antarctic ocean wave event: geomorphology, event reconstruction and coast dynamics through a remote sensing approach

Talk 6: Anastasia Piliouras (20 min)

Landscapes and erosion rates of the Alaska Beaufort sea coast

Session 2.2 (11:40- 12:40): Climate Change and Climate Data Records I

Talk 7: Amy Hendricks (20 min)

Low-frequency sea ice variability drives NDVI declines in the Yukon-Kuskokwim Delta

Talk 8: Victoria Miles (20 min)

A remote sensing view of Arctic heat anomalies: Spatial-temporal distribution and effects.

Talk 9: Rebecca Scholten (20 min)

Early snowmelt and polar jet dynamics drive recent extreme Siberian fire seasons

Lunch Break (12:40-14:00)

Movement activity (14:00-14:15)

Session 3 (14:15-15:15): Panel Discussion(s)

Session 4.1. (15:15-15:45): Lightning Talks for Poster presenters

Session 4.2. (15:45-18:00): Poster Session

Adjourn to Pub – adjacent to poster venue

Wednesday: Excursion Day

Thursday

Zoom Link –

https://alaska.zoom.us/j/82851814389?pwd=P2fUT_-ibuoXrZ-x6FsVqka-E6l1nj.1

Session 1 (9:00-9:40): Glaciers and Seasonal Snow Cover I

Talk 1: Rune Solberg (virtual) (20 min)

A new 38-year time series of daily, global fractional snow cover maps

Talk 2: Eyal Saitet (20 min)

The development and application of a UAS and photogrammetry routine in support of Alaska's department of transportation effort to elucidate snow height for avalanche risk assessment in Atigun Pass

Session 1.1. (9:40-10:30): Observing Permafrost I

Talk 3: Keynote by Ingmar Nitze (30 min)

Deep Learning for mapping retrogressive thaw slumps across the Arctic

Talk 4: Simon Zwieback (20 min)

Circum-Arctic distribution of topographic asymmetry

Coffee Break (10:30-11:00)

Session 2 (11:00-12:20): Observing Permafrost II

Talk 5: Elizabeth Webb (20 min)

Permafrost thaw drives surface water drainage across the pan-Arctic

Talk 6: Katreen Wikstrom Jones (20 min)

Climate & Cryosphere Hazard Program

Talk 7: Joel Rowland (20 min)

Multiscale analysis of remotely sensed imagery to quantify spatial and temporal patterns of river bank erosion in floodplains with permafrost

Talk 8: Alexandra Runge (20 min)

Permafrost vulnerability – deriving a vulnerability index from ESA CCI EO-datasets

Lunch Break (12:20-13:30)

Session 3 (13:30-14:50): Observing Permafrost III

Talk 9: Helena Bergstedt (20 min)

Mapping drained lake basins on a circumpolar scale

Talk 10: Stefano Ponti (20 min)

The spatio-temporal variability of frost blisters in a perennial frozen lake along the Antarctic coast as indicator of the groundwater supply

Talk 11: Amit Hasan for Rajitha Udawalpola (20 min)

Mapping retrogressive thaw slumps in High Arctic Canada using high-spatial resolution satellite imagery and deep learning

Talk 12: Lingcao Huang (20 min)

An approach to inventorying retrogressive thaw slumps on a continental scale

Coffee Break (14:50-15:20)

Session 4 (15:20-16:40): Floating Ice

Talk 13: Robert Abbott (20 min)

Sea Ice from the ground up using distributed acoustic sensing

Talk 14: Eleanor Wratten (virtual) (20 min)

Physiographic controls on landfast ice variability from 20 years of maximum extents across the Northwest Canadian Arctic

Talk 15: Hisatomo Waga (20 min)

A neural network-based method for satellite mapping of sediment-laden sea ice in the Arctic

Talk 16: Dana Brown (20 min)

Identifying spatial patterns of river ice formation and hazardous open water zones with Synthetic Aperture Radar (SAR)

Friday

Zoom Link - <https://alaska.zoom.us/j/82798828755?pwd=sTL0xsCiLGwWpR77S-RXto-C127Aag.1>

Session 1 (9-10:10): Microwave Remote Sensing I

Talk 1: Keynote by Yonghong Yi (virtual) (30 min)

Potential monitoring of surface organic soil properties in arctic tundra using microwave remote sensing data

Talk 2: Go Iwahana (20 min)

Fine-scale ground truth of ground displacement in the Anaktuvuk River Fire (ARF) for satellite and airborne L-band SAR

Talk 3: Sophy Yue Wu (20 min)

Monitoring soil water and organic carbon storage patterns in the active layer of the Arctic Foothills using spaceborne InSAR surface deformation data

Coffee Break (10:10-10:45)

Session 2 (10:45-11:45): Microwave Remote Sensing II

Talk 4: Melanie Engram (20 min)

Synthetic Aperture Radar (SAR) detects large gas seep in lake

Talk 5: Alex Lewandowski (20 min)

SAR data, on-demand processing and analysis tools, and other user support services available at the Alaska Satellite Facility

Talk 6: Natalie Tyler (20 min)

A potential SAR-based approach to remote sensing methane superseeps in Arctic lakes

Closing Ceremony (12:00 – 12:15)

Lunch Break (12:15-13:30)

Session 3 (13:30-15:00): Side Meetings

Coffee Break (15:00-15:30)

Session 4 (15:30-17:00): Side Meetings

Poster Presenters

- Guido Grosse: *A new dynamic land cover classification of the Arctic Lena Delta for scaling methane fluxes*
- Russell Wong: *Calibrating 2000-2020 MODIS and Landsat greening in Northwest Alaska with 1000 km of vegetation transect data*
- Kaili Martin: *Estimating tall shrub biomass in southcentral Alaska*
- Martha Reynolds: *Vegetation response to a climate gradient in the Eastern Canadian Arctic*
- Temenuzhka Spasova: *Interoperability of remote sensing and open data for Arctic and Antarctic ice and climate change monitoring and security*
- Mark Lara: *Mapping arctic-boreal peatlands in Alaska: Implications for historical peatland fire dynamics*
- Micheal Nole: *Predicting permafrost greenhouse gas emissions by linking local and space-based observations through large-scale thermo-hydrologic modeling*
- Cameron Kuhle: *Quantifying peat carbon mass using ground-penetrating radar (GPR) in high-latitude peatlands of the Kenai Peninsula, Alaska*
- Dana Brown: *Identifying spatial patterns of river ice formation and hazardous open water zones with Synthetic Aperture Radar (SAR)*
- Allen Bondurant: *Aufeis growth detection on the Sagavanirktok and Dietrich Rivers using unmanned aerial systems and optical photogrammetry*
- Jennifer Frederick: *Space-based observations are critical for validating maps of Arctic marine greenhouse gas emissions predicted with numerical models*
- Sophia Barth: *Earth observation-based time series analysis of retrogressive thaw slump dynamics in the Russian High Arctic*
- Tabea Rettelbach: *The evolution of ice-wedge polygon networks in tundra fire scars*
- Marnie Bryant: *Integrating ICESat-2 and optical imagery to measure coastal erosion rates and bluff morphology along the Alaskan Beaufort Sea Coast*
- Louise Farquharson: *Permafrost thaw and talik development drives future coastal inundation in North Slope Communities*
- Kamil Czarnecki: *Changes in the glaciers of Kaffiøyra region in the light of remote sensing imagery and UAV measurements, Svalbard, the Arctic;*

Hydrological analysis of Kaffiøyra Plain: Change in areas, coastline and amount of glacial lakes in the light of remote sensing imagery and UAV measurements, Elisebreen sample;

Evaluation of the usefulness of Landsat 8 imagery in 2013-2020 on the example of the Aavatsmarkbreen (NW Spitsbergen, Svalbard);

The use of remote sensing methods and the capabilities of UAV in polar research – examples of transformation of the shoreline in Kaffiøyra Plain (Svalbard)

- Madeleine Rea: *Investigating red snow algae resurfacing and distribution patterns*
- Kaytan Kelkar: *Applying DInSAR for rock glacier Inventories*
- Noelle Helder: *Exploring the reliability and scalability of automated shoreline detection tools for the Alaskan Arctic*
- Harper Baldwin: *Utilizing multispectral imagery to assess historic maximum flood heights in remote Alaskan communities and improve flood mitigation strategies*
- Reyce Bogardus: *Integrating iVR into education and community planning in rural Alaska; a case study from Drew Point, Alaska*
- Dan Hayes: *Scaling spectral and structural characterizations of vegetation and landscape features along permafrost thaw gradients in Arctic tundra*
- Margaret Wooten: *Estimating Site Index in boreal forests with lidar and very-high resolution stereo imagery*
- Arden Burrell: *Climate change, fire return intervals and the growing risk of permanent forest loss in boreal Eurasia*
- Alexandra Veremeeva: *Yedoma surface thaw subsidence (2015-2021) depended on local geomorphological conditions, Bykovsky Peninsula, Laptev Sea region*
- Benjamin M. Jones: *High spatial and temporal resolution remote sensing of a collapsing pingo in northern Alaska*
- Julian Dann: *Identification of secondary factors controlling Synthetic Aperture Radar (SAR) - derived root-zone soil moisture over the Seward Peninsula using random forest modelling*
- Kavya Sivaraj: *Characterization of arctic sea ice melt pond dynamics with remote sensing*
- Thomas Duchnik Hessilt: *Influences of snowmelt timing on Arctic-boreal fire season start across North America*

ABSTRACTS

Session 1: Arctic Land Cover I

70-year retrospective of remote sensing applied to cumulative impact assessments, Prudhoe Bay Oilfield, Alaska

Donald A. Walker¹, Annett Bartsch², Helena Bergstedt², Uma S. Bhatt³, Jerry Brown⁴, Ronald P. Daanen⁵, Howard E. Epstein⁶, Gerald V. Frost⁷, Benjamin M. Jones⁸, Janet C. Jorgenson⁹, M. Torre Jorgenson¹⁰, Mikhail Kanevsky⁸, Anna K. Liljedahl¹¹, Dmitry Nikolsky³, Jana L. Peirce¹, Martha K. Reynolds¹, Vladimir E. Romanovsky³, Thomas Schneider von Deimling¹², Yuri Shur⁸, Patrick J. Webber¹³, Lisa Wirth³, Chandi Witharana¹⁴, Simon Zwieback³

¹Alaska Geobotany Center, Institute of Arctic Biology, University of Alaska Fairbanks, Fairbanks, AK, 99775 USA

²b.geos, Industriestrasse 1, 2100 Korneuburg, Austria

³Geophysical Institute, University of Alaska Fairbanks, Fairbanks, AK, 99775 USA

⁴International Permafrost Association, PO Box 7, Woods Hole, 02543 USA

⁵Alaska Division of Geological & Geophysical Surveys, Alaska Department of Natural Resources, 3354 College Rd., Fairbanks, AK 99709 USA

⁶Department of Environmental Sciences, University of Virginia, 291 McCormick Rd, Charlottesville, VA 22904 USA

⁷Alaska Biological Research, Inc., 2842 Goldstream Rd, Fairbanks, AK, 99709 USA

⁸Institute of Northern Engineering, University of Alaska Fairbanks, Fairbanks, AK, 99775 USA

⁹Arctic National Wildlife Refuge, U.S. Fish and Wildlife Service, Fairbanks, AK, 99701 USA

¹⁰Alaska Ecoscience, 2332 Cordes Way, Fairbanks, AK, 99709 USA

International Arctic Research Center, University of Alaska Fairbanks, Fairbanks, AK, 99775 USA

¹¹Woodwell Climate Research Center, 149 Woods Hole Road, Falmouth, MA 02540 USA

¹²Alfred Wegener Institute Helmholtz Centre for Polar and Marine Research, 14473 Potsdam, Germany
Alfred Wegener Institute, Telegrafenberg, Gebäude A45, 14473 Potsdam, Germany

¹³Emeritus, Kellogg Biological Station, Michigan State University, East Lansing, MI 48824

¹⁴Department of Natural Resources and the Environment, University of Connecticut, Storrs, CT 06269 USA

Abstract

Cumulative impact assessments (CIAs) for new Arctic oilfields have not adequately addressed the potential landscape impacts of climate change or the indirect impacts of infrastructure in areas with ice-rich permafrost (IRP) (e.g., Reynolds et al. 2020). The main goals of this paper are: (1) trace the history of remote sensing for assessing past cumulative impacts in the

Prudhoe Bay Oilfield (PBO), Alaska (Fig. 1); (2) discuss some promising new remote-sensing and modeling tools; and (3) point toward improved capability to predict future changes.

We first define IRP and cumulative impacts (CIs) and distinguish direct impacts (footprint) of infrastructure from the indirect impacts that follow construction. Aerial photographs (U.S. Navy 1948–1949) provided images of PBO landscapes before development occurred. The oil industry initiated annual high-resolution aerial-photograph missions of the PBO in 1968. In the same year, the International Biological Program (IBP) Tundra Biome started geocological investigations that used these images to map landforms, soils, and vegetation of the PBO (Walker et al. 1980). The maps were later adapted to GIS approaches in three highly impacted 25-km² areas of the PBO, which included several years of changes to tundra areas adjacent to infrastructure (Walker et al. 1987). The National Research Council later updated these three landscape-scale maps to 2001 and contracted the oil companies and Quantum Spatial Inc. to produce a regional-scale historical analysis of the network of roads, pipelines and other forms of infrastructure in all the North Slope Oilfields (NRC 2003). The regional- and landscape-scale maps used for NRC analysis were updated again in 2010 when unexpected rapid expansion of ice-wedge thermokarst was detected (Raynolds et al. 2014, 2016).

Up to this time, CIAs of the PBO relied on aerial photographs and maps produced by the oil industry. The spatial resolution of available satellite-based remote-sensing data was insufficient to discern the details of periglacial landforms (e.g., ice-wedge polygons and nonsorted circles) or of roads, pipelines, or changes to land surfaces adjacent to infrastructure. Industry-sponsored studies that used remote-sensing products included studies of oil-pipeline spills, reserve-pits leaks (e.g., Jorgenson et al. 1995), off-road vehicles trails, and recovery following removal of gravel pads. Highlighted studies for this talk include a new NSF project that is part of the NSF Navigating the New Arctic initiative that is using integrated ground-based studies, advanced remote-sensing tools, and improved modeling approaches to examine climate- and infrastructure-related changes (Walker et al. 2022, Bergstedt 2022). Other projects that use PBO datasets for calibration, include an analysis of long-term impacts from a catastrophic flood (Shur et al. 2016, Zwieback et al. 2021) and studies that are using massive amounts of high-resolution imagery and pattern-recognition tools to detect and map ice-wedge polygons, water bodies, and infrastructure across the circumpolar Arctic (Bartsch et al. 2020; Witherrana et al. 2021). These tools combined with improved modeling approaches that bridge the gap between regional and engineering scales (e.g., Deimling et al. 2021) promise to greatly improve our ability to predict and monitor future infrastructure and landscape changes in areas with IRP.

References

- Bartsch A, Pointner G, Ingeman-Nielsen T, Lu W. Towards circumpolar mapping of Arctic settlements and infrastructure based on Sentinel-1 and Sentinel-2. *Remote Sensing*, 2020, 12, 2368. <https://doi.org/10.3390/rs12152368>.
- Bergstedt H, Jones BM, Walker DA, Peirce J, Kanevskiy MZ, Raynolds MK, Buchhorn M. 2022 submitted. Quantifying the spatial and temporal influence of infrastructure on seasonal

- snowmelt timing and its influence on vegetation productivity and early season surface water cover in the Prudhoe Bay Oilfield. *Arctic Science*.
- Jorgenson M, Cater TC, Smith M, Anderson BA. 1995. Remote sensing of salinity and gravel impacts to tundra ecosystems using vegetation indicators at four drill sites in the Kuparuk Oilfield, 1994. Final report for ARCO Alaska, Inc., Anchorage, AK, by ABR, Inc., Fairbanks, AK.
- Jorgenson, MT, Kanevskiy M, Shur Y, Moskalenko N, Brown DRN, Wickland D, Striegl R, Koch J. 2015. Role of ground ice dynamics and ecological feedbacks in recent ice wedge degradation and stabilization. *Journal of Geophysical Research: Earth Surface*, 120:2280–2297. doi: [10.1002/2015jf003602](https://doi.org/10.1002/2015jf003602).
- NRC (National Research Council). 2003. Cumulative Environmental Effects of Oil and Gas Activities on Alaska's North Slope. National Academies Press. <https://doi.org/10.17226/10639>.
- Raynolds MK, Jorgenson JC, Jorgenson MT, Kanevskiy M, Liljedahl AK, Nolan M, Sturm M, Walker DA. 2020. Landscape impacts of 3D-seismic surveys in the Arctic National Wildlife Refuge, Alaska. *Ecological Applications*, 30:e02143. <https://doi.org/10.1002/eap.2143>
- Raynolds MK, Walker DA, Ambrosius KJ, Brown J, Everett KR, Kanevskiy M, Kofinas GP, Romanovsky VE, Shur Y, Webber PJ. 2014. Cumulative geocological effects of 62 years of infrastructure and climate change in ice-rich permafrost landscapes, Prudhoe Bay Oilfield, Alaska. *Global Change Biology*, 20(4):1211–24. <https://onlinelibrary.wiley.com/doi/pdf/10.1111/gcb.12500>.
- Raynolds MK, Walker DA. 2016. Increased wetness confounds Landsat-derived NDVI trends in the central Alaska North Slope region, 1985–2011. *Environmental Research Letters*, 11:085004. <http://iopscience.iop.org/1748-9326/11/8/085004>.
- Schneider von Deimling T, Lee H, Ingeman-Nielsen T, Westermann S, Romanovsky V, Lamoureux S, Walker DA, Chadburn S, Trochim E, Cai L, Nitzbon J, Jacobi S, Langer M. 2021. Consequences of permafrost degradation for Arctic infrastructure – bridging the model gap between regional and engineering scales. *The Cryosphere*, 15:2451–2471. doi: [10.5194/tc-15-2451-2021](https://doi.org/10.5194/tc-15-2451-2021).
- Shur Y, Kanevskiy M, Walker DA, Jorgenson MT, Buchhorn M, Raynolds MK. 2016. Permafrost-related causes and consequences of Sagavanirktok River flooding in Spring 2015, Abstract 1065. Pages 1014–1016 in F. Gunther and A. Morgenstern, editors. 11th International Conference on Permafrost, Potsdam, Germany.
- Walker DA, Everett KR, Webber PJ, Brown J. 1980. *Geobotanical atlas of the Prudhoe Bay region, Alaska*. Hanover, NH: Cold Regions Research and Engineering Laboratory, CRREL Report 80-14. Available from: <https://erdc-library.erdcdren.mil/jspui/handle/11681/9008>.
- Walker DA, Webber PJ, Binnian EF, Everett KR, Lederer ND, Nordstrand EA, and Walker MD. 1987. Cumulative impacts of oil fields on northern Alaskan landscapes. *Science*, 238(4828):757–61. Available from: <http://www.jstor.org/stable/1700351>.

Walker DA, Reynolds MK, Kanevskiy MZ, Shur YS, Romanovsky VE, Jones BM, Buchhorn M, Jorgenson MT, Šibík J, Breen AL, Kade A, Watson-Cook E, Bergstedt H, Liljedahl AK, Daanen RP, Connor B, Nicolsky D, and Peirce JL. 2022. Cumulative impacts of a gravel road and climate change in an ice-wedge polygon landscape, Prudhoe Bay, AK. *Arctic Science*. <https://doi.org/10.1139/AS-2021-0014>.

Zwieback, S. et al. 2022 submitted. Disparate permafrost terrain changes after a large flood observed from space. *International Journal of Applied Earth Observation and Geoinformation*.

Acknowledgements US National Science Foundation (Grant Nos. 1263854, 1720875, 1722572, 1927723, 1927872, 1928237, 2051888, 2052107) with contributions from the US National Aeronautics and the Space Administration (NASA Grant Nos. NNX14AD90G and NNX13AM20G), the Bureau of Ocean Energy Management, and US Geological Survey. Special BP Alaska Exploration, Hillcorp, the Prudhoe Bay Unit, NV5 GeoSpatial, contributors to the Rapid Arctic Transitions due to Infrastructure and Climate (RATIC) initiative of the International Arctic Science Committee (IASC). Many others made major contribution to earlier geocological mapping and cumulative effects analyses in the Prudhoe Bay region and northern Alaska, including William Acevedo, John Adams, Nancy Auerbach, Emily Binnian, Vicky Dow, Kaye Everett, Len Gaydos, Jiong Jia, Julie Knudson, Gary Kofinas, Leanne Lestack, Hilmar Meier, Pam Miller, Don Mills, Steve Muller, Earl Nordstrand, Chris Snyder-Conn, Stephen Sparks, Bill Streever, and Marilyn Walker.

Forty years through the looking glass: spaceborne circumpolar tundra greenness observation enters its 5th decade

Gerald V. Frost¹, Uma S. Bhatt², Matthew J. Macander¹, Howard E. Epstein³, Martha K. Raynolds⁴, and Donald A. Walker⁴

¹Alaska Biological Research, Inc., Fairbanks, AK USA

²Geophysical Institute, University of Alaska Fairbanks, Fairbanks, AK USA

³Department of Environmental Sciences, University of Virginia, Charlottesville, VA USA

⁴Institute of Arctic Biology, University of Alaska Fairbanks, Fairbanks, AK USA

Abstract

The summer of 2021 marked the fortieth consecutive season of spaceborne circumpolar tundra greenness observation using the Normalized Difference Vegetation Index (NDVI), a spectral metric of fundamental importance to studies of environmental change in the terrestrial Arctic. In the late 1990s, a strong increase in the productivity of tundra vegetation emerged in observations by the Advanced Very High Resolution Radiometer (AVHRR), a phenomenon now widely known as “the greening of the Arctic.” Over the latter half of the AVHRR record, what began as a seemingly straightforward trend of Arctic greening has become more nuanced, due in part to the responses of varied Arctic landscapes to climate change, the proliferation of more advanced spaceborne sensors which often do not agree, and the emergence of increased climatic variability as a component of Arctic climate change.

Since 2000, two sensors with daily temporal resolution—AVHRR and MODIS—have formed the backbone of circumpolar greenness observation. Many of the trends observed are consistent between both sensors, but others are not. Nonetheless, in the big picture, both records portray an increasingly productive, greener Arctic. For example, the five highest circumpolar greenness values in the 40-year AVHRR record have all been observed in the last ten years, and for MODIS, circumpolar peak greenness has exceeded the 2000–2020 mean for eleven consecutive growing seasons. In 2020, both sensors recorded the highest average circumpolar greenness measurements in both records (since 1982 and 2000, respectively). The ability to monitor and contextualize Arctic greening trends relies on the continuity of legacy spaceborne records into the future, the harmonization of VIIRS and MODIS, and the continued integration of more advanced sensors that typically possess higher spatial, but lower temporal resolution (e.g., Landsat, Sentinel).

In this presentation, we present a brief retrospective of Arctic greenness dynamics since 1982, and seek to prompt a community discussion concerning the use of spaceborne NDVI as a “grand integrator” of Arctic biological and physical processes, how to ensure continuity in the long-term record going forward, and how best to apply existing and planned sensor capabilities in an increasingly maritime, less frozen Arctic.

Keywords: Arctic tundra, Normalized Difference Vegetation Index, greening

References: Frost, G. V., M. J. Macander, U. S. Bhatt, L. T. Berner, J. W. Bjerke, H. E. Epstein, B. C. Forbes, S. J. Goetz, M. J. Lara, T. Park, G. K. Phoenix, S. P. Serbin, H. Tømmervik, D. A. Walker, and D. Yang. 2021. Tundra greenness. *Arctic Report Card 2021*. T. A. Moon, M. L. Druckenmiller, and R. L. Thoman (eds.). <<https://doi.org/10.25923/8n78-wp73>>.

Acknowledgements: We thank current and former coauthors on annual reports concerning Arctic tundra greenness trends issued as part of the annual NOAA Arctic Report Card and Bulletin of the American Meteorological Society (BAMS) State of the Climate reports. We also thank Jorge Pinzon at the Biospheric Sciences Laboratory, NASA Goddard Space Flight Center for his ongoing work with the Global Inventory Modeling and Mapping Studies 3g (GIMMS-3g+) dataset derived from the AVHRR satellite record.

An overview of NASA's Arctic Boreal Vulnerability Experiment (ABOVE): Advances, knowledge gaps and next steps

Scott J. Goetz¹, Charles Miller², Peter Griffith³, Abhishek Chatterjee^{3,4}, Natalie Boelman⁵, Laura Bourgeau-Chavez⁶, David Butman⁷, Howard Epstein⁸, Joshua Fisher⁹, Nancy French⁶, Elizabeth Hoy¹⁰ John S. Kimball¹¹, Elisabeth Larson², Tatiana Loboda¹², Michelle Mack¹³, Mahta Moghaddam¹⁴, Paul Montesano², Laura Prugh⁷, Michael Rawlins¹⁵, Adrian V. Rocha¹⁶, Brendan M. Rogers¹⁷, Kevin Schaefer¹⁸

¹School of Informatics and Computing, Northern Arizona University, Flagstaff AZ, USA

²Jet Propulsion Laboratory, California Institute of Technology, Pasadena CA, USA

³NASA Goddard Space Flight Center / SSAI, Greenbelt MD, USA

⁴Universities Space Research Association, Columbia, MD, USA.

⁵Lamont-Doherty Earth Observatory and Department of Earth and Environmental Sciences, Columbia University, Palisades NY, USA

⁶Michigan Technological University Research Institute, Ann Arbor MI, USA

⁷School of Environmental and Forest Sciences, University of Washington, Seattle WA, USA

⁸Department of Environmental Sciences, University of Virginia, Charlottesville VA, USA

⁹Joint Institute for Regional Earth System Science and Engineering, University of California, Los Angeles CA, USA

¹⁰NASA Goddard Space Flight Center / GST, Greenbelt MD, USA

¹¹Numerical Terradynamics Simulation Group, University of Montana, Missoula MT, USA

¹²Department of Geographical Sciences, University of Maryland, College Park MD, USA

¹³Center for Ecosystem Science and Society, Northern Arizona University, Flagstaff AZ, USA

¹⁴School of Engineering, University of Southern California, Los Angeles CA, USA

¹⁵Department of Geosciences, University of Massachusetts, Amherst MA, USA

¹⁶Department of Biological Sciences, University of Notre Dame, South Bend IN, USA

¹⁷Woodwell Climate Research Center, Falmouth MA, USA

¹⁸National Snow and Ice Data Center, University of Colorado, Boulder CO, USA

Abstract

NASA's Arctic Boreal Vulnerability Experiment (ABOVE) is a large coordinated multi-disciplinary research effort addressing ecosystem changes taking place in biomes of the Arctic and boreal region. Although the geographic focus of the field campaigns centers on northwestern North America, ABOVE research is ultimately designed to address scaling from field measurements to multi-sensor airborne data acquisitions to satellite remote sensing and ultimately to terrestrial biosphere models. As such, ABOVE has pan-Arctic and pan-boreal implications and applications. We will provide an overview of ABOVE research progress and findings at the midpoint of its planned ten-year effort. We briefly highlight a selection of some key publications and findings, as well as identified knowledge and data gaps that still need to be addressed. These gaps are critical research areas for further advancing our understanding of the interactions and feedbacks between the climate system and changes in the spatial and temporal environmental drivers of dynamics in carbon, hydrology, snow, permafrost, disturbance and vegetation composition, structure and function. Addressing these gaps will

also advance our ability to map changes using remote sensing and to capture these dynamics in prognostic models.

Keywords: ecosystem, interdisciplinary, vulnerability

References: Goetz et al. 2022. Environmental Research Letters (forthcoming)

Acknowledgements: ABoVE is supported by the NASA Terrestrial Ecology (TE) program, led by program scientists Hank Margolis and Mike Falkowski. We thank all members of the CCE Office for their assistance and support of the science team. We acknowledge early contributions of Eric Kasischke, lead principal investigator of the 2008 ABoVE scoping study proposal and the Science Definition Team. We thank every active member of the Science Team for what they have done and continue to contribute to the collaborative and collective effort that is at the heart of ABoVE research and applications.

Boreal forests at tree-scale and stand-scale: Exploring the benefits of in-house aerial VNIR/SWIR imaging spectroscopy for Alaska wildfire research

Christine F Waigl^{1,*} (cwaigl@alaska.edu), Martin Stuefer², Anushree Badola², Christopher Smith², Santosh K Panda^{3,2} and Uma S Bhatt^{1,2}

¹ International Arctic Research Center, University of Alaska Fairbanks, Fairbanks, AK, USA

² Geophysical Institute, University of Alaska Fairbanks, Fairbanks, AK, USA

³ Department of Natural Resources and Environment and Institute of Agriculture, Natural Resources and Extension, University of Alaska Fairbanks, Fairbanks, AK, USA

* presenting author

Abstract

Starting during the 2019 Alaska wildfire season, the Boreal Fires team of the Alaska EPSCoR “Fire & Ice” project has carried out a program of hyperspectral imagery data acquisition over wildfire-related target sites. The study areas include well-characterized boreal forest (Caribou-Poker Creeks Research Watershed, Bonanza Creek Experimental Forest), post-fire burn scars including the 2019 McKinley and Shovel Creek and the 2021 Munson Creek fires, vegetation recovery locations on the Kenai Peninsula, and active fire imagery acquired over multiple fire incidents varying in intensity from extremely active to nearly extinguished.

The camera system in use consists in dual HySpex VNIR/SWIR imaging spectrometers: a VNIR-1800 (410-1000 nm) and a SWIR-384 (960-2500 nm) camera, mounted within a fixed-wing single-engine piloted aircraft (Cristóbal et al., 2021). We transformed the data obtained from this instrumentation into spectral reflectance (or, for active fire, spectral radiance) imagery that is corrected for terrain, atmospheric, and (where applicable) illumination and observation geometry effects. The intrinsic spatial resolutions at flight elevations of approx. 2000 m, is slightly more than 50 cm (VNIR) and 1.5 m (SWIR). Imagery rasters are sampled at a spatial resolution of 1 m in 459 regularly spaced spectral bands.

The dataset allows for the extraction of spectral libraries of boreal forest canopies for a wide range of relevant vegetation species including deciduous trees (*Betula papyrifera*, *Populus tremuloides*, *Populus balsamifera*), coniferous trees (*Picea mariana*, *Picea glauca*), as well as large shrubs and meadow and understory vegetation types. The vegetation was identified based on field survey data, which we also used to train and validate supervised classifiers. Outputs of this effort include maps of vegetation types (Alaska Fuel Model Guide Task Group, 2018; Badola et al., 2021; Smith et al., 2021) species distribution, estimates of live biomass, canopy density and related wildfire fuel characteristics, which were correlated with spectral vegetation indices. Furthermore, post and active fire imagery delivered burn pattern maps and observations of active fire behavior (Waigl et al., 2019).

A key insight of this research is that while the best choice of classification approach (Random Forest classifier, spectral angle mapping, spectral mixture analysis, etc.) can be somewhat site-dependent, useful wildfire fuel classes and post-fire recovery categories are inherently defined

on the scale of a stand, not a single pixel or even single tree. We therefore applied aggregation strategies that delivered a stand-scale output while still taking advantage of the high spatial resolution of our imagery spectroscopy data. In general, such strategies are necessary to scale the high-resolution data from crewed or uncrewed aerial sensors to the conceptual categories and level of detail and that users, such as fire managers, require to inform their decision-making processes.

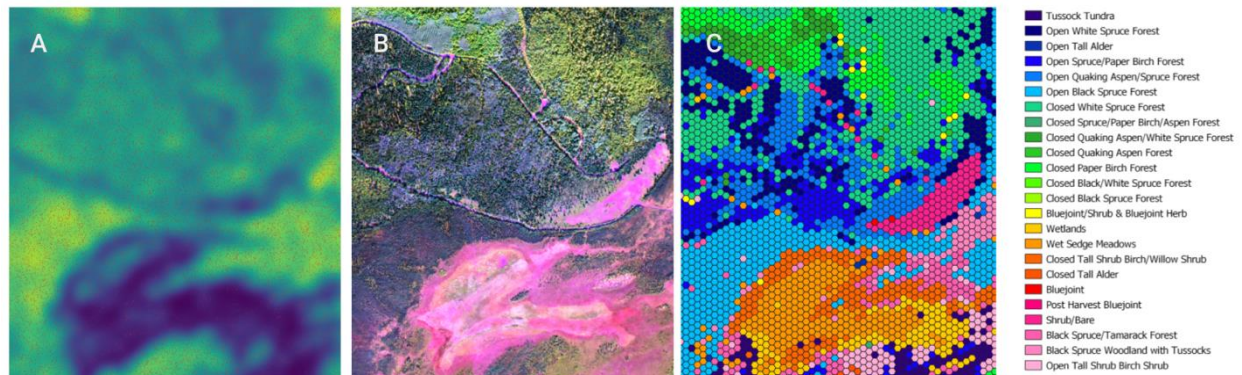


Figure 1: HySpex-derived imagery products (Bonanza Creek Experimental Forest, 2021): A – tree crown density; B – RGB composite (1600/850/470 nm); C – Alaska vegetation type classification on a hexagonal grid.

Keywords: wildfire, boreal forest, imaging spectroscopy

Acknowledgements: This material is based upon work supported by the National Science Foundation and under the award OIA-1757348 and by the State of Alaska.

References:

- Alaska Fuel Model Guide Task Group. (2018). *Fuel Model Guide to Alaska Vegetation* (Unpublished Report) (p. 105). Fairbanks, AK. Retrieved from <https://www.frames.gov/catalog/56055>
- Badola, A., Panda, S. K., Roberts, D. A., Waigl, C. F., Bhatt, U. S., Smith, C. W., & Jandt, R. R. (2021). Hyperspectral Data Simulation (Sentinel-2 to AVIRIS-NG) for Improved Wildfire Fuel Mapping, Boreal Alaska. *Remote Sensing*, 13(9), 1693. <https://doi.org/10.3390/rs13091693>
- Cristóbal, J., Graham, P., Prakash, A., Buchhorn, M., Gens, R., Guldager, N., & Bertram, M. (2021). Airborne Hyperspectral Data Acquisition and Processing in the Arctic: A Pilot Study Using the HySpex Imaging Spectrometer for Wetland Mapping. *Remote Sensing*, 13(6), 1178. <https://doi.org/10.3390/rs13061178>
- Smith, C. W., Panda, S. K., Bhatt, U. S., & Meyer, F. J. (2021). Improved Boreal Forest Wildfire Fuel Type Mapping in Interior Alaska Using AVIRIS-NG Hyperspectral Data. *Remote Sensing*, 13(5), 897. <https://doi.org/10.3390/rs13050897>
- Waigl, C. F., Prakash, A., Stuefer, M., Verbyla, D., & Dennison, P. (2019). Fire detection and temperature retrieval using EO-1 Hyperion data over selected Alaskan boreal forest fires. *International Journal of Applied Earth Observation and Geoinformation*, 81, 72–84. <https://doi.org/10.1016/j.jag.2019.03.004>

Session 2: Arctic Land Cover II

Time-series maps reveal widespread change in plant functional type cover across arctic and boreal Alaska and Yukon

Matthew J Macander¹, Peter R Nelson², Timm W Nawrocki³, Gerald V Frost¹, Kathleen M Orndahl⁴, Eric C Palm⁵, Aaron F Wells⁶, and Scott J Goetz⁴

¹ ABR, Inc.—Environmental Research & Services, Fairbanks, Alaska

² The Schoodic Institute, Winter Harbor, ME 04693, USA

³ Alaska Center for Conservation Science, University of Alaska Anchorage, Anchorage, AK 99508, USA

⁴ Northern Arizona University, Flagstaff, AZ 86011, USA

⁵ Department of Ecosystem and Conservation Sciences, W. A. Franke College of Forestry and Conservation, University of Montana, Missoula, MT 59812, USA

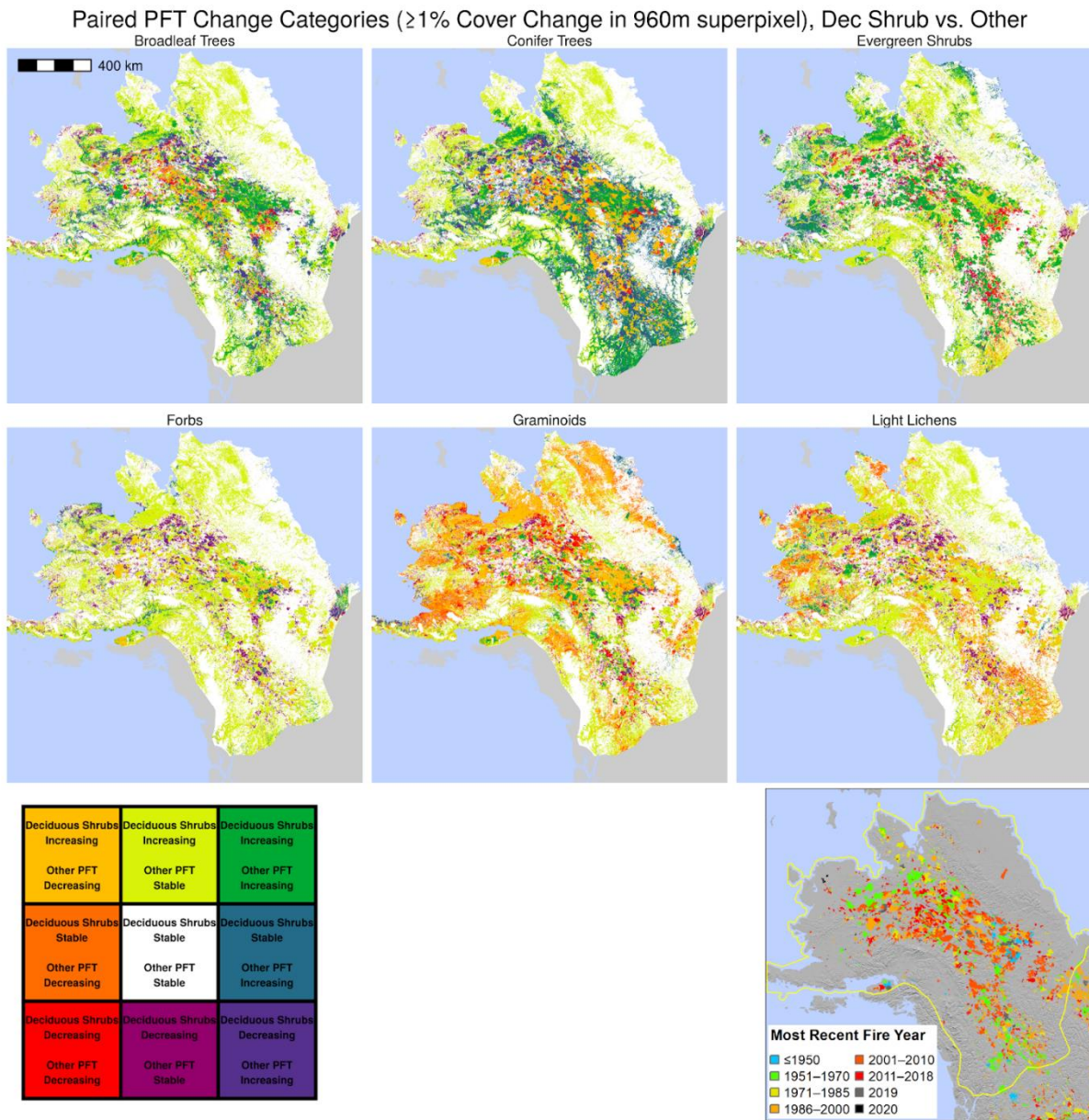
⁶ ABR, Inc.—Environmental Research & Services, Anchorage, AK 99518, USA

Abstract

Widespread changes in the distribution and abundance of plant functional types (PFTs) are occurring in Arctic and boreal ecosystems due to the intensification of disturbances, such as fire, and climate-driven vegetation dynamics, such as tundra shrub expansion. To understand how these changes affect boreal and tundra ecosystems, we need to first quantify change for multiple PFTs across recent years. While landscape patches are generally composed of a mixture of PFTs, most previous moderate resolution (30-m) remote sensing analyses have mapped vegetation distribution and change within land cover categories that are based on the dominant PFT; or else the continuous distribution of one or a few PFTs, but for a single point in time.

Here we map a 35-year time-series (1985–2020) of top cover (TC) for seven PFTs across a 1.77 x 106 km² study area in northern and central Alaska and northwestern Canada. We improve on previous methods of detecting vegetation change by modeling TC, a continuous measure of plant abundance. The PFTs collectively include all vascular plants within the study area as well as light macrolichens, a nonvascular class of high importance to caribou management. We identified net increases in deciduous shrubs (66 x 10³ km²), evergreen shrubs (20 x 10³ km²), broadleaf trees (17 x 10³ km²), and conifer trees (16 x 10³ km²), and net decreases in graminoids (-40 x 10³ km²) and light macrolichens (-13 x 10³ km²) over the full map area, with similar patterns across Arctic, Oroarctic, and Boreal bioclimatic zones. Model performance was assessed using spatially blocked, nested 5-fold cross-validation with overall root mean square errors ranging from 8.3–19.0%. Most net change occurred as succession or plant expansion within areas undisturbed by recent fire, though PFT TC change also clearly resulted from fire disturbance. These maps have important applications for assessment of surface energy

budgets, permafrost changes, nutrient cycling, and wildlife management and movement analysis.



~/programming/abr/nasa-veg-data-ingest-r/pft_manuscript/maps/visualize_change_combinations.Rmd, 2022-02-01

Figure 1. Patterns of deciduous shrub top cover change, 1985–2020, coincident with top cover change in other plant functional types at 960-m superpixel scale and fire history. Changes at the 960-m superpixel scale $\leq 1\%$ top cover are categorized as stable. 30-m pixels where change was less than the magnitude of model RMSE were set to zero before aggregation, in order to emphasize areas with higher confidence of change.

Keywords

Plant functional type, Landsat

References

Macander, M J, Peter R Nelson, Timm W Nawrocki, Gerald V Frost, Kathleen M Orndahl, Eric C Palm, Aaron F Wells, and Scott J Goetz. In review. Time-series maps reveal widespread change in plant functional type cover across arctic and boreal Alaska and Yukon.

Macander, M J. In Review. Modeled Plant Functional Type Top Cover, Arctic and Boreal Alaska and Yukon. ORNL DAAC, Oak Ridge, Tennessee, USA.

Acknowledgements

This work was supported by NASA ABoVE grants NNX17AE44G and 80NSSC19M0112 and Strategic Environmental Research and Development Program (SERDP) award RC18-1183. In addition to reference data provided by co-authors, we thank Carl Roland, Dave Swanson and Kyle Joly (NPS), Sarah Burnett (BLM), Nadele Flynn, Marcus Waterreus, and Caitlin Willier (Yukon Government), Bill Collins (Alaska Department of Fish and Game), Todd Mahon (Environmental Dynamics Inc.), and Emily Holt (University of Northern Colorado) for sharing reference data to use in our mapping, and the numerous field biologists who collected those data and the project managers who supported their efforts.

Unraveling 3D shrub architecture with UAS LIDAR

Christian G. Andresen¹, Jaccob May¹

¹Geography Department, University of Wisconsin-Madison, USA

Abstract

The Arctic is characterized by dwarf vegetation that has been challenging to characterize in 3D from satellite and airborne platforms. Advances in LIDAR technology have opened a new window into understanding ecosystem structure at fine scales and associated ecosystem processes. Representation of the type, shape and composition of the canopy is a key component for estimation and modeling of tundra land-atmosphere water and carbon interactions. The ability to gather multi-return LiDAR data allows the full detection of the vegetation 3D structure from the top of the canopy to the understory at a very fine scale. We employed multi-return UAS LIDAR technology with densities of 500+ pts/m² to characterize 3D shrub architecture and developed shrub-specific deep learning neural networks to map and quantify individual shrub structural properties at cm scale. This study will serve as a novel approach into understanding shrub ecology, heterogeneity, biomass and associated environmental feedbacks.

Keywords shrubs, UAS LIDAR, ecosystem structure

Using Landsat imagery to detect beavers in eastern Nunavik

Vanessa Caron¹, Mikhaela Neelin², Oumer Ahmed³, Ralf Ludwig⁴

^{1,4} Department of Geography, Ludwig-Maximilians-Universität, Munich, Germany

² McGill University, Montreal, Canada, and Nunavik Hunting Fishing Trapping Association, Tasiujaq, QC, Canada

³ Department of Environment, Wildlife, and Research, Makivik Corporation, Montreal, QC, Canada

Abstract

As beavers move north of the treeline and start colonizing low arctic tundra regions of Canada, there is growing interest from both Inuit land-users and regional governments to develop a cost-effective tool to monitor beaver populations and their impact on the Arctic landscape. Beavers are widely considered ecosystem engineers and there is concern that their dams could have an adverse effect on the seasonal migrations of Arctic char, a species of key importance to the traditional food security of Inuit fishermen. Evidence also suggests that the ponds they create could exacerbate permafrost degradation (Jones et al., 2020). Previous studies have shown that satellite remote sensing can be used to detect beaver ponds in both tundra and boreal ecozones, establishing the potential of satellite imagery to monitor beavers (Tape et al., 2018). In this study, we evaluated the feasibility of using remote sensing data to detect new beaver activity in streams around Tasiujaq, a coastal Inuit village in Northern Quebec. We used breakpoint detection algorithms to detect beaver pond formation by identifying abrupt changes to arctic riparian habitats in time series of Landsat satellite imagery. Our method leveraged open access data, powerful change detection techniques, and rapid cloud computing capabilities in Google Earth Engine, and allowed our research team to successfully identify the year of colonization of most beaver colonies in the study. This research also highlighted the challenges of detecting small, temporally and spatially complex beaver disturbances in tundra landscapes, and provided groundwork for the further development of a remote sensing approach to monitor beaver's range expansion into the Arctic.

Keywords Beavers, Remote Sensing, Change Detection

References

- Jones, B.M., Tape, K.D., Clark, J.A., Nitze, I., Grosse, G., Disbrow, J., 2020. Increase in beaver dams controls surface water and thermokarst dynamics in an Arctic tundra region, Baldwin Peninsula, northwestern Alaska. *Environ. Res. Lett.* 15, 075005.
<https://doi.org/10.1088/1748-9326/ab80f1>
- Tape, K.D., Jones, B.M., Arp, C.D., Nitze, I., Grosse, G., 2018. Tundra be dammed: Beaver colonization of the Arctic. *Glob. Change Biol.* 24, 4478–4488.

Drought response analysis on a geothermally warmed Sub-Arctic grassland ecosystem using multispectral drone images

Amir Hamedpour^{1,2}, Bjarni D. Sigurdsson², Josep Peñuelas^{3,4}, Iolanda Filella^{3,4}, Hafsteinn Einarsson⁵, Steven Latré⁶, Tryggvi Stefánsson¹

¹ Svarmi, Data Company Specialized in Remote Sensing and Drones, Árleyni 22, IS-112 Reykjavík, Iceland

² Agricultural University of Iceland, Fac. of Environmental and Forest Sciences, Hvanneyri, IS-311 Borgarnes, Iceland

³ CSIC, Global Ecology Unit CREAM-CSIC-UAB, Bellaterra, Barcelona 08193, Catalonia, Spain

⁴ CREAM, Cerdanyola del Vallès, Barcelona 08193, Catalonia, Spain

⁵ University of Iceland, IS-101 Reykjavik, Iceland

⁶ imec - University of Antwerp, Sint-Pietersvliet 7, 2000 Antwerp, Belgium

Abstract

The effects of climate change are expected to be most severe in the Arctic and sub-Arctic regions of the world [1] so studying the effects of temperature rise and drought on these ecosystems is crucial [2]. Natural geothermal soil temperature gradients in Iceland offer a unique opportunity to study these effects [3]. In this study, we analyzed the phenological responses of grasslands located in southern Iceland, close to the village of Hveragerdi encompassing geothermally heated natural grasslands [4]. Our main goal was to understand how warming affected the onset and the duration of the active growing season in this Sub-Arctic environment and if we could detect any drought response through remote sensing data analysis.

We established 20 plots with different soil temperatures, installed a weather station and sensors to record the various parameters such as precipitation, air temperature, wind speed, soil water content, etc. We then conducted an intensive fieldwork consisting of 15 repeated measurement campaigns, starting in April 2021 and ending in December 2021. And we used a 10-band multispectral MicaSense dual-camera sensor to map the field sites with a drone.

Data collection with drones in our field site had major challenges due to the weather condition in Iceland, which are usually windy and rainy, and the remote location of the field site. Another challenge was the small hummocks that characterize Sub-Arctic grasslands, which together with the low solar angles at high latitudes produce microscale shading patterns on their surface when exposed to varying sunlight. Because of the sensitivity of the multispectral data to these shadow-patterns, measurements had to take place on completely cloud-free or on completely overcast days, which was difficult to find in Icelandic unstable weather conditions. Sloping terrain also made a standardized drone elevation of 30 m challenging, but it was required to have ca. 2 cm resolution in the images.

We had a few periods of less than 10 days without rain in early June and July and only one period of more than 10 days without rain in early August, which is within the main growing season for the subarctic grasslands [5]. After processing the multispectral data and georeferencing them accurately, analysis performed by deriving the Normalized Difference Vegetation Index (NDVI) and the Photochemical Reflectance Index (PRI) showed clear shifts in the active growing season of the Sub-Arctic grasslands with increased warming. Further, we were able to see temporary reductions in NDVI and PRI indices of grassland plots during periods of no rain, which allows us to calculate the relative seasonal changes in reflectance, closely related to the seasonal changes in productivity [6], due to drought. And PRI seems to be more sensitive than NDVI, showing a severe decrease during drought conditions in which NDVI did not change that much.

Keywords: Sub-Arctic grassland, soil warming, multispectral images

References

- N. Verbrugghe et al., "Long-term warming reduced microbial biomass but increased recent plant-derived C in microbes of a subarctic grassland," *Soil Biology and Biochemistry*, vol. 167, p. 108590, 2022, doi: <https://doi.org/10.1016/j.soilbio.2022.108590>
- E. Dorrepaal et al., "Carbon respiration from subsurface peat accelerated by climate warming in the subarctic," *Nature*, vol. 460, no. 7255, pp. 616–619, 2009, doi: <https://doi.org/10.1038/nature08216>
- N. I. W. Leblans et al., "Phenological responses of Icelandic subarctic grasslands to short-term and long-term natural soil warming," *Global Change Biology*, vol. 23, no. 11, pp. 4932–4945, 2017, doi: <https://doi.org/10.1111/gcb.13749>
- B. D. Sigurdsson et al., "Geothermal ecosystems as natural climate change experiments: The ForHot research site in Iceland as a case study," *Icelandic agricultural sciences*, vol. 29, pp. 53–71, 2016, doi: <https://doi.org/10.16886/IAS.2016.05>
- S. Lett and A. Michelsen, "Seasonal variation in nitrogen fixation and effects of climate change in a subarctic heath," *Plant and Soil*, vol. 379, no. 1, pp. 193–204, 2014, doi: <https://doi.org/10.1007/s11104-014-2031-y>
- Y. Gu et al., "Mapping grassland productivity with 250-m eMODIS NDVI and SSURGO database over the Greater Platte River Basin, USA," *Ecological Indicators*, vol. 24, pp. 31–36, 2013, doi: <https://doi.org/10.1016/j.ecolind.2012.05.024>
-

Synthesis of observations of boreal forest structure and age: regional patterns of growth

Paul Montesano^{1,2}, Christopher S.R. Neigh¹, Laura Duncanson³, Amanda Armstrong³, Min Feng⁴, Joseph O. Sexton⁴, Panshi Wang⁴

¹ NASA Goddard Space Flight Center, Greenbelt, MD, USA

²ADNET Systems, Inc., Bethesda, MD, USA.

³Dept. of Geographical Sciences, University of Maryland-College Park, College Park, MD, USA

⁴TerraPulse, Inc., North Potomac, MD, USA

A current map of forest stand age has been compiled for the circumpolar boreal forest domain for 2020. This map captures the stand age of young boreal forests disturbed during the Landsat TM record (1984-2020). We linked this map with forest stand height estimates from airborne lidar and a suite of climate variables to show the magnitude and variation in forest growth rates in the western North American boreal at regional scales. These growth rates, together with a new map of aboveground forest biomass density for the circumpolar boreal domain, provide a basis for mapping the high resolution patterns in the current potential for carbon accumulation in boreal forests and validating modelling results.

Keywords boreal, forest, structure, stand, age

Session 3: Arctic Land Cover III

Discovering data and results from the ABoVE airborne campaign

Elizabeth Hoy¹, Charles Miller², Scott Goetz³, Peter Griffith⁴, Hank Margolis⁵, Mike Falkowski⁵, Libby Larson⁴, Dan Hodkinson⁴

¹NASA Goddard Space Flight Center/Global Science & Technology, Inc., Greenbelt, MD, USA

²Jet Propulsion Laboratory, California Institute of Technology, Pasadena CA, USA

³School of Informatics and Computing, Northern Arizona University, Flagstaff AZ, USA

⁴NASA Goddard Space Flight Center/SSAI, Greenbelt, MD, USA

⁵NASA Headquarters, Washington, D.C., USA

Abstract

The Arctic-Boreal Vulnerability Experiment (ABoVE) is a NASA Terrestrial Ecology field, airborne, and remote sensing campaign designed to understand environmental change in western North America. Research from ABoVE has resulted in over 300 publications, with results across multiple science themes such as carbon dynamics, fire disturbance, hydrology, and permafrost. As part of ABoVE, an airborne campaign (the ABoVE Airborne Campaign, or AAC) was initially conducted from April through November 2017, with follow-on measurements made in 2018 and 2019, and additional measurements planned for 2022 (see map of the AAC). Many flights during the AAC were coordinated with same-day ground-based measurements to link process-level studies with geospatial data products derived from satellite sensors. The data collected spans the critical intermediate space and time scales that are essential for a comprehensive understanding of scaling issues across the ABoVE Study Domain and extrapolation to the pan-Arctic. Recent results using this scaling strategy showed the fine-scale spatial distribution of intense methane emission hotspots near water bodies within the ABoVE domain (Elder et al., 2020); while others have developed maps of active layer thickness, soil moisture, and subsidence (Schaefer et al., 2022). Many of the datasets developed as part of ABoVE – both airborne data and derived data products – are freely available for download and use. Here we present an overview of airborne data products, highlight recent results, and discuss methods to discover and download available datasets.

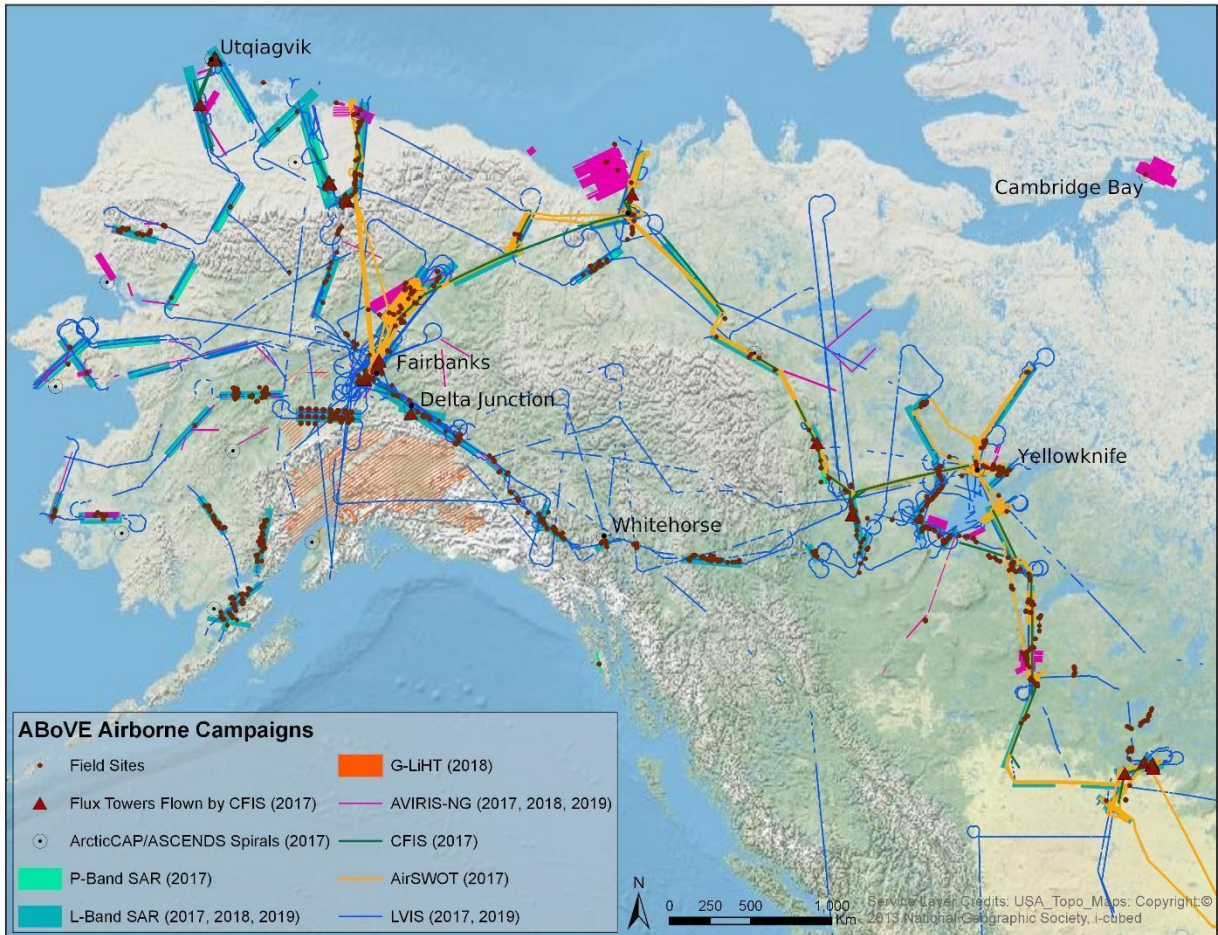


Figure 1. The ABoVE Airborne Campaign (AAC) has included measurements from >10 aircraft over multiple years.

Keywords airborne, scaling, ABoVE

Addressing the hyperspectral data need for the Arctic environment through image simulation

Anushree Badola¹, Santosh k. Panda^{1,2}, Dar A. Roberts³, Christine F. Waigl⁴, Uma S. Bhatt¹, Randi R. Jandt⁵

¹Geophysical Institute, University of Alaska Fairbanks, Fairbanks, AK 99775, USA abadola@alaska.edu (corresponding author) skpanda@alaska.edu usbhatt@alaska.edu

²Department of Natural Resources and Environment and Institute of Agriculture, Natural Resources and Extension, University of Alaska Fairbanks, Fairbanks, AK 99775, USA skpanda@alaska.edu

³Department of Geography, University of California, Santa Barbara, CA 93106, USA dar@geog.ucsb.edu

⁴International Arctic Research Center, University of Alaska Fairbanks, Fairbanks, AK 99775, USA cwaigl@alaska.edu

⁵Alaska Fire Science Consortium, International Arctic Research Center, University of Alaska Fairbanks, Fairbanks, AK 99775, USA rjandt@alaska.edu

Abstract

The Arctic region has been undergoing a dramatic change in response to accelerated warming over the last half-century. Declining sea ice extent, widespread permafrost thaw, increasing wildfires, and unprecedented insect outbreaks and diseases are changing the arctic environment with severe societal impacts. Remote sensing is an ideal approach to document and monitor widespread change at daily to seasonal timescale. Particularly, hyperspectral remote sensing is immensely effective in detecting and quantifying biogeochemical changes in land, water, and vegetation because of imaging in hundreds of narrow spectral bands. Many studies have highlighted the unique advantages of hyperspectral remote sensing in detecting and quantifying vegetation change, wildfire impacts, sea ice extent, and permafrost thickness [1–3]. However, the paucity of hyperspectral data for the Arctic region limits its application. On the other hand, moderate-coarse resolution multispectral image data (consisting of a few spectral bands) is widely available from different satellite platforms e.g., Landsat 8 - 9, Sentinel-2, Terra, and Aqua. They provide global coverage but have a coarser spectral resolution that limits their usefulness in detecting and quantifying subtle biogeochemical changes.

To address the paucity of hyperspectral image data for the Arctic region, we developed a novel approach to simulate Airborne Visible InfraRed Imaging Spectrometer - Next Generation (AVIRIS-NG) hyperspectral image from the widely available Sentinel-2 image data. We used the Universal Pattern Decomposition Method (UPDM) [4], a spectral unmixing technique that uses ground spectra as endmembers, and the Spectral Response Functions (SRF) of AVIRIS-NG and Sentinel-2 sensors to simulate AVIRIS-NG imagery. We employed the Iterative Endmember Selection (IES) algorithm [5] on the ground spectra collected using a handheld spectrometer to obtain the ideal endmember spectra for black spruce, birch, and gravel. The simulated image data (at 10 m pixel size) has the same number of bands and spectral resolution as the AVIRIS-NG image. We validated our simulation results by comparing spectral signatures extracted from known pixels of birch and black spruce (RMSE of 0.03 and 0.02 for birch and black spruce spectra, respectively). We further validated the simulated image data by performing vegetation classification using the Random Forest model.

We observed a 33% improvement in vegetation map accuracy compared to the existing maps generated from Landsat multispectral image (LANDFIRE Existing Vegetation Type and Alaska Vegetation and Wetlands Map). Our novel simulation algorithm paves the way for generating science-ready hyperspectral images from Sentinel 2 images that can be used in a variety of Arctic focus applications, including vegetation, geology, cryosphere, and land use land cover studies.

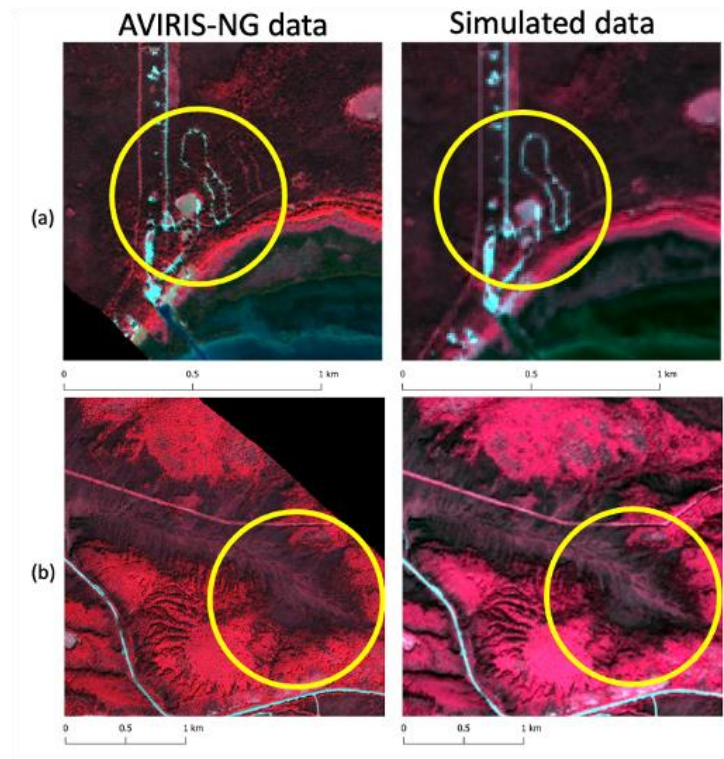


Figure 1. Visual comparison of the simulated image (pixel size: 10 m) and AVIRIS-NG image (pixel size: 5 m) using Colored InfraRed image composites (R: 843 nm, G: 662 nm, B: 557 nm). The top panel (a) shows accurate capture of trails and the built-up area in the simulated data, and the bottom panel (b) shows accurate capture of coniferous and deciduous vegetation cover.

Keywords

Simulation, hyperspectral, endmembers

References

1. Han, Y.; Li, J.; Zhang, Y.; Hong, Z.; Wang, J. Sea Ice Detection Based on an Improved Similarity Measurement Method Using Hyperspectral Data. *Sensors (Basel)*. **2017**, *17*, 10.3390/S17051124.
2. Wang, Q.; Zhang, J. Hyperspectral image vegetation change detection based on biochemical parameters inversion. *Lect. Notes Electr. Eng.* **2019**, *463*, 629–637. 10.1007/978-981-10-6571-2_77.
3. Zhang, C.; Douglas, T.A.; Anderson, J.E. Modeling and mapping permafrost active layer thickness using field measurements and remote sensing techniques. *Int. J. Appl. Earth Obs. Geoinf.* **2021**, *102*, 102455. 10.1016/J.JAG.2021.102455.

4. Zhang, L.; Furumi, S.; Muramatsu, K.; Fujiwara, N.; Daigo, M.; Zhang, L. Sensor-independent analysis method for hyperspectral data based on the pattern decomposition method. *Int. J. Remote Sens.* **2006**, *27*, 4899–4910. 10.1080/01431160600702640.
5. Roth, K.L.; Dennison, P.E.; Roberts, D.A. Comparing endmember selection techniques for accurate mapping of plant species and land cover using imaging spectrometer data. *Remote Sens. Environ.* **2012**, *127*, 139–152. 10.1016/J.RSE.2012.08.030.

Acknowledgments

This material is based upon work supported by the National Science Foundation and under the award OIA-1757348 and by the State of Alaska. A heartfelt thanks to Chris Smith, Malvika Shriwas, and Brooke Kubby for assisting in fieldwork. Thanks to the NASA JPL and ESA for collecting and providing access to AVIRIS-NG scenes and Sentinel-2 data, respectively.

Post-fire tree and shrub cover influences on vegetation indices in Siberian larch forests

Nadav S. Bendavid¹, Michael M. Loranty^{1}, Heather D. Alexander², Sergey P. Davydov³, Heather Kropp⁴, Michelle C. Mack⁵, Susan M. Natali⁶, Seth A. Spawn-Lee⁷, Nikita S. Zimov³*

¹Department of Geography, Colgate University, Hamilton, NY, USA

²School of Forestry and Wildlife Sciences, Auburn University, Auburn, AL, USA

³Pacific Institute for Geography, Far East Branch, Russian Academy of Sciences, Northeast Science Station, Cherskiy, Russia

⁴Environmental Studies Program, Hamilton College, Clinton, NY, USA

⁵Center for Ecosystem Science and Society, Northern Arizona University, Flagstaff, AZ, USA

⁶Woodwell Climate Research Center, Falmouth, MA, USA

⁷Department of Geography, University of Wisconsin, Madison, WI, USA

*Presenting Author

Abstract

Arctic greening is among the most prominent and widespread ecological responses to global climate change. This greening has been observed across a wide range of boreal forest and tundra ecosystem types using decadal time series of proxies of vegetation productivity derived from optical satellite data. Field observations of northward tree and shrub encroachment as well as dendrochronological measures of productivity corroborate ecological interpretations of these greening trends. Such changes, especially tree and shrub encroachment, will alter a wide range of ecosystem services. Productivity increases directly affect carbon storage in vegetation biomass, and indirectly impact permafrost soil carbon through myriad impacts on soil thermal dynamics. Increases in vegetation act as a positive climate feedback through reduced albedo. Vegetation change also alters a wide range of ecosystem provisioning services such as wildlife habitat that are important for Arctic communities. Despite the multifaceted importance of Arctic greening, quantifying the magnitude and extent of different types of vegetation change remains challenging due to concurrent effects of disturbances such as permafrost degradation and wildfire, as well as confounding factors that operate at spatial scales too fine to be resolved using long-term satellite records ([Myers-Smith et al., 2020](#)).

Here we examine the relationships between heterogeneous forest cover and commonly used satellite proxies of vegetation productivity in northeastern Siberian larch forests. Our study site includes 26 forest stands situated within the perimeter of a fire that occurred ca. 1940. At each stand we measured canopy cover, inventoried trees and erect shrubs (*Betula* spp. and *Salix* spp.), and developed genera and density specific allometric relationships to calculate leaf area from either basal diameter (shrubs) or diameter at breast height (trees). All stands are approximately 60 years old, and canopy cover ranges from 25% to 90%. Our previous work at these sites revealed that the Normalized Difference Vegetation Index (NDVI) and Enhanced Vegetation Index (EVI) derived from Landsat and PlanetScope satellite imagery did not capture variability in

tree biomass or canopy cover ([Loranty et al., 2018](#)). In this study we quantify tree and shrub leaf area across the density gradient, and compare these data to vegetation indices from Landsat and PlanetScope. We find that increases in understory shrubs compensate for declines in tree leaf area across the density gradient. Both tree and shrub leaf area index (LAI) vary significantly across the gradient, but total LAI does not. Interestingly, NDVI and EVI are positively associated with shrub LAI. Our results show that understory shrubs compensate for reduced tree leaf area in low density forests, and that shrubs are crucial for understanding variation of vegetation indices in these systems. The ecological and climatic implications of tree- and shrub-driven greening are quite different, therefore continued research should aim to improve our ability to differentiate trees and shrubs in Siberian larch forests and elucidate the process drivers of postfire vegetation dynamics.

Keywords: Siberia, larch, greening

References

- [Loranty, M. M., Davydov, S., Kropp, H., Alexander, H., Mack, M., Natali, S., & Zimov, N. \(2018\). Vegetation Indices Do Not Capture Forest Cover Variation in Upland Siberian Larch Forests. *Remote Sensing*, 10\(11\), 1686. <https://doi.org/10.3390/rs10111686>](#)
- [Myers-Smith, I. H., Kerby, J. T., Phoenix, G. K., Bjerke, J. W., Epstein, H. E., Assmann, J. J., John, C., Andreu-Hayles, L., Angers-Blondin, S., Beck, P. S. A., Berner, L. T., Bhatt, U. S., Bjorkman, A. D., Blok, D., Bryn, A., Christiansen, C. T., Cornelissen, J. H. C., Cunliffe, A. M., Elmendorf, S. C., ... Wipf, S. \(2020\). Complexity revealed in the greening of the Arctic. *Nature Climate Change*, 10\(2\), 106–117. <https://doi.org/10.1038/s41558-019-0688-1>](#)

Acknowledgements

This project was supported by funding from the National Science Foundation (NSF) Office of Polar Programs to MML (PLR-1304464, PLR-1417745, and OPP-1708322)

Development of an arctic-boreal fire atlas using Visible Infrared Imaging Radiometer Suite active fire data

Rebecca C. Scholten¹, Yang Chen², James T. Randerson², Sander Veraverbeke¹

¹ Faculty of Science, Vrije Universiteit Amsterdam, the Netherlands

² Department of Earth System Science, University of California, Irvine, CA, USA

Abstract

Intensifying wildfires in high-latitude forest and tundra ecosystems are a major source of greenhouse gas emissions, releasing carbon through direct combustion and long-term degradation of permafrost soils and peatlands. Several remotely sensed burned area and active fire products have been developed, yet these do not provide information about the ignitions, growth and size of individual fires. Such object-based fire data is urgently needed to disentangle different anthropogenic and bioclimatic drivers of fire ignition and spread. This knowledge is required to better understand contemporary arctic-boreal fire regimes and to constrain models that predict changes in future arctic-boreal fire regimes.

Here, we developed an object-based fire tracking system to map the evolution of circumpolar arctic-boreal fires at a sub-daily scale. Our approach harnesses the improved spatial resolution of 375m Suomi-NPP Visible Infrared Imaging Radiometer Suite (VIIRS) active fire detections. The arctic-boreal fire atlas includes ignitions and sub-daily perimeters of individual fires between 2012 and 2021, which are corrected using finer-scale information on waterbodies. It also provides information on the abundance of unburned land areas within fire perimeters, which may serve as an important refugia for tree species. In the future this information will be complemented with information on ignition sources, and may help improve fire models by providing better understanding of drivers and limits of fire ignition and spread.

Keywords: Boreal fire, fire tracking, fire spread dynamics

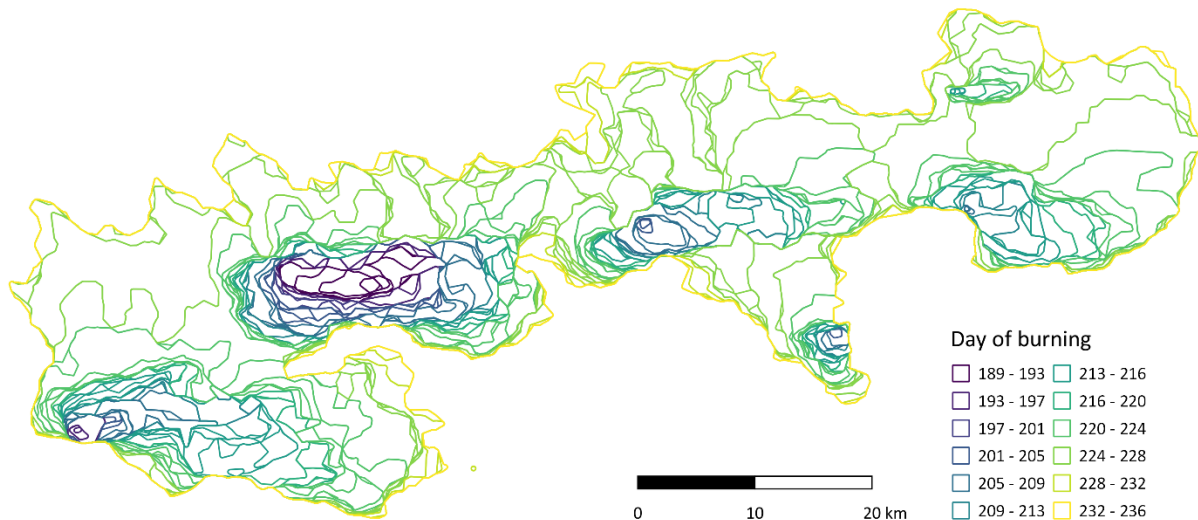


Figure 1. Daily perimeters of an exemplary fire in the Northwest Territories, which burned between July 8, 2017 (Julian day: 189) and August 24, 2017 (Julian day: 236). Perimeters were derived with the fire tracking system and are based on Suomi NPP VIIRS active fire data.

Evolving outburst flood hazards and impacts from glacier-dammed lakes

Jason M. Amundson¹, Eran Hood¹, Christian Kienholz¹, Gabriel J. Wolken^{2,3}, Amy Jenson^{1,4}

¹Department of Natural Sciences, University of Alaska Southeast, Juneau, Alaska, USA

²International Arctic Research Center, University of Alaska Fairbanks, Fairbanks, Alaska, USA

³Alaska Division of Geological and Geophysical Surveys, Fairbanks, Alaska, USA

⁴Department of Mathematical Sciences, Montana State University, Bozeman, Montana, USA

Abstract Glacier outburst floods are a common hazard in glacierized landscapes. These floods can threaten infrastructure and cause semi-regular but short-lived perturbations to downstream ecosystems. The largest of these floods create major erosional features during glacial periods; smaller, more frequent outburst floods are also important in driving landscape change. Outburst flood theory dictates that flood characteristics, such as event timing and peak discharge, depend on glacier and basin geometry, both of which evolve as glaciers advance or retreat. Consequently, outburst floods can be viewed as semi-periodic disturbances to glaciated landscapes that switch on/off and evolve in response to climate change. Understanding how these floods evolve over decadal timescales is challenging due to difficulties with instrumenting marginal basins, which are often surrounded by steep terrain and crevassed glacier ice and are filled with ice rubble. Here, using Mendenhall Glacier, Alaska, as a test case, we demonstrate how high resolution orthoimagery and digital elevation models produced from UAV imagery can provide valuable information on basin bathymetry and storage capacity, and suggest that further development of UAV and small satellite technologies will enable much broader investigation of outburst flood hazards and impacts.

Keywords glacier; outburst floods; hazards

Acknowledgements This project has been supported by funding from the Alaska Climate Adaptation Science Center.

Session 4: New Sensors, Operational Services and Method advancement

NLCD Alaska: Upcoming release supporting NALCMS and the MRLC consortium

Jon Dewitz

NLCD Production Manager, U.S. Geological Survey (USGS) Earth Resources Observation and Science (EROS) Center

Abstract

The National Land Cover Database (NLCD) is a product of the Multi-Resolution Land Characteristics Consortium (MRLC) and provides consistent and accurate land cover monitoring for the United States. NLCD also creates a modified version of its Land Cover product to support the continental mapping efforts of the North American Land Change Monitoring System (NALCMS). NLCD will be remapping Alaskan Land Cover from 2001 to 2021 at a five-year interval to take advantage of Landsat's Collection 2 release. This release has updated orthorectification, creating large pixel shifts from previously mapped products. This presentation will touch on future deliverables, timelines, strategies, and methodologies for this upcoming release.

Keywords NLCD, Alaska, NALCMS

NESDIS in the Arctic: Authoritative climate products from satellite remote sensing

*Jessica Cherry*¹

¹Regional Climate Services Director for Alaska, National Environmental Satellite Data and Information Service (NESDIS), National Oceanic and Atmospheric Administration (NOAA), Anchorage, AK, USA

Abstract This overview talk describes the different types of remote sensing datasets at the National Environmental Satellite Data and Information Service's (NESDIS) National Centers for Environmental Information (NCEI) archive, including those core climate data records developed within the agency, as well as data archived at NCEI by individual researchers. Use of these datasets as indicators of climate change processes, including strengths and limitations, will be reviewed. Finally, the talk will outline NESDIS's planned products for the future, used to meet the needs of decision-makers as diverse as those in Tribal land management, subsistence fisheries, research, commerce, and defense.

Keywords Climate Data Records, NOAA, data archive, weather, land surface

Instrument development for flexible arctic remote sensing

Lora S Koenig¹, Cassie Lee², Samantha Edgington¹ and Clemens Tillier¹.

¹Lockheed Martin, Advanced Technologies Center, Palo Alto, CA, USA

²Lockheed Martin, Civil and Commercial Space, Littleton, CO, USA

Abstract

The Arctic is the fastest-warming region on the planet. The dramatic reduction of ice and substantial land surface change has presented the world with a new set of poorly characterized risks. Lockheed Martin is designing instruments to help our stakeholders and partners understand, respond, and adapt to these risks. Lockheed Martin's Flexible Hosted Imager (FHI) is a compact multi-spectral infrared weather imaging payload that can be hosted on a platform in a highly elliptical orbit providing long-duration imaging over the Arctic at mesoscale resolution. FHI was developed to add agility and resiliency to future hybrid weather imaging constellations. FHI is distinguished from legacy weather imagers by its ability to dynamically vary the observing timeline as best suited for scientific observations and objectives. It replaces prescribed scan modes constrained to imaging all bands using constant repeating timelines, with flexible step-stare imaging over configurable areas in selected bands at the desired update rate.

Keywords Hyperspectral Imaging, Remote Sensing

Acknowledgements Lockheed Martin would like to thank NOAA and NASA for their support and feedback under GEO/XO instrument concept study contract 1332KP20CNEEP0068

A U-Net based algorithm for automated detection of clouds from medium-resolution satellite imagery

Amit Hasan¹, Chandi Witharana², Rajitha Udawalpola³, Anna K. Liljedahl⁴.

^{1,2,3}Department of Natural Resources and the Environment, University of Connecticut, Storrs, Connecticut, USA

⁴Woodwell Climate Research Center, Falmouth, Massachusetts, USA

Abstract

Cloud detection is an inextricable pre-processing step in remote sensing image analysis workflows. Most of the traditional rule-based band machine-learning-based algorithms utilize low-level features of the clouds and classify individual cloud pixels based on their spectral signatures. Cloud detection using such approaches can be challenging due to a multitude of factors including harsh lighting conditions, the presence of thin clouds, the context of surrounding pixels, and complex spatial patterns. In recent studies, deep convolutional neural networks (CNNs) have shown outstanding results in the computer vision domain. These methods are practiced for better capturing the texture, shape as well as context of images. In this study, we propose a deep learning CNN approach to detect cloud pixels from medium-resolution satellite imagery. We repurposed the U-Net architecture, which performs well in medical image analysis tasks with record low segmentation errors. We have built and trained a modified version of the U-Net from scratch. The proposed CNN accounts for both the low-level features, such as color and texture information as well as high-level features extracted from successive convolutions of the input image. We prepared a cloud-pixel dataset of approximately 7273 randomly sampled 320 by 320 pixels image patches taken from a total of 121 Landsat-8 (30m) and Sentinel-2 (20m) image scenes. These satellite images come with cloud masks. From the available spectral channels, only blue, green, red, and NIR bands are fed into the model. The CNN model was trained and validated on 5300 and 1973 image patches, respectively. As the final output from our model, we extract a binary mask of cloud pixels and non-cloud pixels. The results are benchmarked against established cloud detection methods using standard accuracy metrics.

Keywords

Deep learning, Cloud-detection

References

Li, Z., Shen, H., Cheng, Q., Liu, Y., You, S., & He, Z. (2019). Deep learning based cloud detection for medium and high resolution remote sensing images of different sensors. *ISPRS Journal of Photogrammetry and Remote Sensing*, 150, 197-212.
<https://doi.org/10.1016/j.isprsjprs.2019.02.017>

Ronneberger, O., Fischer, P., & Brox, T. (2015). U-Net: Convolutional Networks for Biomedical Image Segmentation. *Medical Image Computing and Computer-Assisted Intervention – MICCAI 2015*, 234–241. https://doi.org/10.1007/978-3-319-24574-4_28

Acknowledgements

This research was supported by the US National Science Foundation grants 1720875, 1722572, 1927872, 1927723, and 1927729.

Session 1: Arctic Coasts and its Communities I

Earth observation for permafrost-dominated arctic coasts – contributions to the next generation of the Arctic Coastal Dynamics database.

Annett Bartsch¹, Anna Irrgang², Julia Boike², Julia Martin², Guido Grosse², Hugues Lantuit², Ingmar Nitze², Gonçalo Vieira³, Benjamin M. Jones⁴, Barbara Widhalm¹, Clemens v. Baeckmann¹

¹ b.geos (Department, Institute, City, State/Territory/Country)

² Permafrost Research Section, Alfred Wegener Institute Helmholtz Centre for Polar and Marine Research, Potsdam, Germany

³ Centre of Geographical Studies, Institute of Geography and Spatial Planning, University of Lisbon, Lisbon, Portugal

⁴ Institute of Northern Engineering, University of Alaska Fairbanks, Fairbanks, Alaska, USA

Abstract

The multifaceted impacts of coastal environmental change on local communities, ecosystem services, and socio-economic dynamics have not yet been quantified in an integrated framework at the circum-Arctic scale (Fritz et al., 2017). Also the NRC (2014) report on ‘Opportunities to Use Remote Sensing in Understanding Permafrost and Related Ecological Characteristics’ calls for the development of maps that delineate areas at risk of permafrost degradation and coastal erosion, to produce vulnerability maps for determining safe building locations, and to provide information where mitigation efforts should be focused to protect Arctic coastal areas.

We propose the following Earth Observation (EO)-guided activities in order to address these issues with the possibilities offered by remote sensing:

1. Creation of the first circumpolar consistent dataset of coastal erosion trends.
2. Creation of the first circumpolar consistent dataset of infrastructure at risk along the coasts.
3. Validation of the circumpolar datasets of (1) and (2) as well as permafrost time series which are already available through permafrost_cci
4. Significantly enhancing the current Arctic Coastal Dynamics database (ACD, Lantuit et al. 2012) through ingestion of results from (1), (2), (3) and Permafrost_cci for full coastal environment characterization.
5. Development of a roadmap for future EO based updates of the ACD

The retrieval of coastal erosion will be based on Landsat-data for the last 20 years following the approach of Bartsch et al. (2020b; Figure 1). The long observation period allows the detection of erosion rates larger than 2m/year despite of the comparably low spatial resolution of Landsat (30m). Detection of infrastructure potentially at risk has recently been shown feasible

for 10m datasets from Sentinel-1/2 using machine learning (AI) methodology (Bartsch et al. 2020a).

We will present our strategy for the entire initiative and will specifically discuss validation and calibration steps.

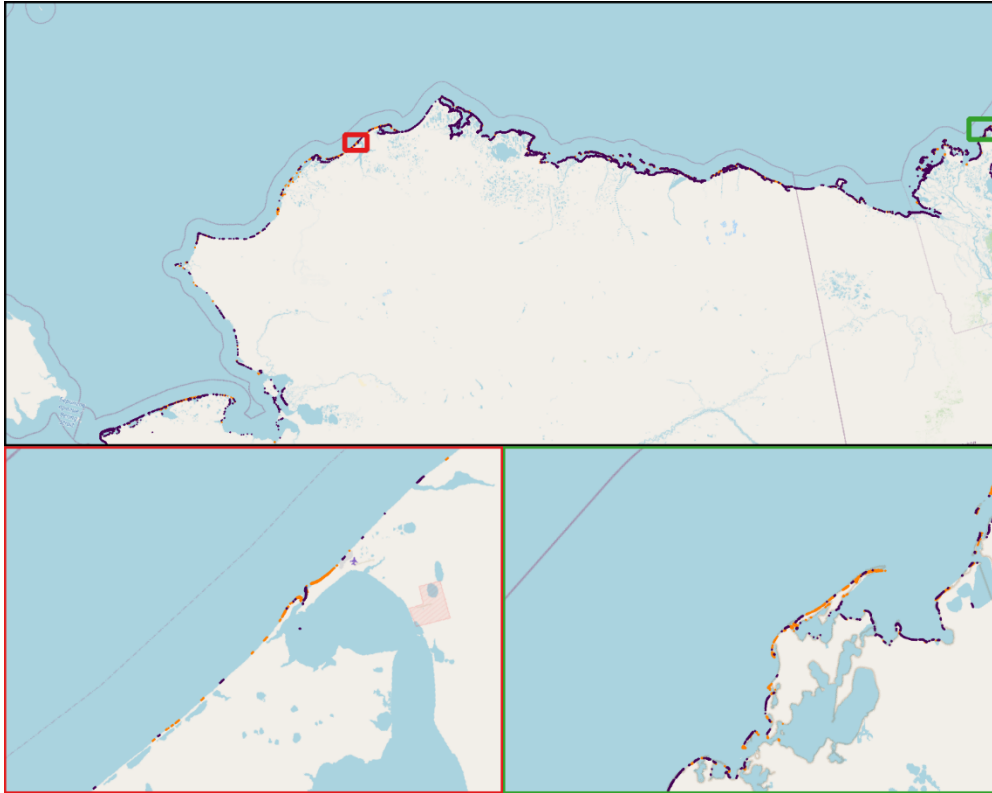


Figure 1. Example of regions with erosion and accretion derived from Landsat (1999-2014) for Northern and northwestern Alaska. Orange – accretion, purple – erosion. Prototype based on Bartsch et al. (2020a). Dataset: Bartsch and Nitze (2021)

Keywords

Coastal erosion, permafrost, infrastructure

References

- Fritz, M., Vonk, J. & Lantuit, H. Collapsing Arctic coastlines. *Nature Clim Change* **7**, 6–7 (2017). <https://doi.org/10.1038/nclimate3188>
- Lantuit, Hugues; Overduin, Pier Paul; Couture, Nicole; Wetterich, Sebastian; Are, Felix; Atkinson, David; Brown, Jerry; Cherkashov, Georgy A; Drozdov, Dimitry S; Forbes, Donald Lawrence; Graves-Gaylord, Allison; Grigoriev, Mikhail N; Hubberten, Hans-Wolfgang; Jordan, James; Jorgenson, M Torre; Ødegård, Rune Strand; Ogorodov, Stanislav; Pollard, Wayne H; Rachold, Volker; Sedenko, Sergey; Solomon, Steve; Steenhuisen, Frits; Streletskaia, Irina; Vasiliev, Alexander (2012): The Arctic Coastal Dynamics Database: A New Classification Scheme and Statistics on Arctic Permafrost Coastlines. *Estuaries and Coasts*, 35(2), 383-400, <https://doi.org/10.1007/s12237-010-9362-6>
- Bartsch, A., Pointner, G., Ingeman-Nielsen, T., Lu, W. (2020a): Towards Circumpolar Mapping of Arctic Settlements and Infrastructure Based on Sentinel-1 and Sentinel-2. *Remote Sensing*, 12, 2368. , <https://doi.org/10.3390/rs12152368>.

Bartsch A., Ley S. Nitze I., Pointner G., Vieira G. (2020b): Feasibility Study for the Application of Synthetic Aperture Radar for Coastal Erosion Rate Quantification Across the Arctic. *Frontiers in Environmental Science* 8, 143 <https://www.frontiersin.org/article/10.3389/fenvs.2020.00143>
Bartsch, Annett, & Nitze, Ingmar. (2021). Coastal erosion and accretion areas along the Beaufort Sea and Laptev Sea Coasts based on Landsat 1999 - 2014 (Version v01) [Data set]. Zenodo. <https://doi.org/10.5281/zenodo.5195621>

Acknowledgements

The work is funded primarily through the European Space Agency Polar Science Cluster Program (project EO4PAC). Further funding was received from ESA's Climate Change Initiative (Permafrost_cci), the European Union's Horizon 2020 Research and Innovation Programme (No. 773421, Nunataryuk) and the US National Science foundation grant OISE-1927553 (PerCS-Net).

Automating coastline measurements of arctic regions from high resolution satellite imagery

Kristopher J. Carroll¹, Frank D.W. Witmer², Matthew Kupilik³

¹Interdisciplinary Graduate Student, University of Alaska Anchorage

²Department of Computer Science, University of Alaska Anchorage

³Department of Electrical Engineering, University of Alaska Anchorage

Abstract

Coastal erosion is a threat to many of the world's coastlines, particularly in Arctic regions where reduced sea ice leaves coastlines more vulnerable to wave action from storms. Modeling historical and future coastline morphology is of great value to communities and ecosystems prone to coastal erosion. Such models require accurate representations of coastline locations over time. For areas where coastline data are unavailable or sparse, an automated process for coastline extraction is preferable to the time intensive process of manual extraction via photo interpretation.

Using high temporal and spatial resolution imagery from PlanetLabs, we examined the efficacy of traditional methods of image segmentation and modern convolutional neural networks to automate coastline measurements for the area of Deering, Alaska. For the traditional methodology, we used the Normalized Difference Water Index (NDWI) followed by thresholding to segment images into water and land areas. Convolutional neural networks (CNN) were built on the design of DeepWaterMap which processed large datasets to produce probability maps indicating the likelihood of a pixel being water. Each of these methods was then subject to active contour analysis to generate vectorized coastlines. We then attempted to enhance the accuracy of the CNN by applying data augmentation techniques such as rotation and flipping of images to expand the dataset significantly as well as testing the production of a reliable training label set in a resolution corresponding to the satellite imagery we were using. As other water label datasets were only available for the area in a resolution an order of magnitude lower than the satellite imagery available, we used a moving window NDWI thresholding technique to generate training labels and compared the results of the CNN trained on these higher resolution labels to the CNN using label data from the coarser resolution Global Surface Water (GSW) dataset. To assess the accuracy of our coastlines, we compared them to coastal measurements from USGS, ground measurements via high accuracy GPS, and manual digitization of coastlines from high resolution imagery using the root mean square error (RMSE) metric.

We present the comparisons of the traditional NDWI methods against both the CNN using lower resolution label data as well as the CNN using the novel label technique.

Keywords:

Deep learning, convolutional neural networks, data augmentation

References:

- Gibbs, Ann E., Alexander G. Snyder, and Bruce M. Richmond. 2019. "National Assessment of Shoreline Change - Historical Shoreline Change Along the North Coast of Alaska, Icy Cape to Cape Prince of Wales: U.S. Geological Survey Open-File Report." Open-File Report. U.S. Geological Survey. <https://doi.org/10.5066/P9H1S1PV>
- Isikdogan, Furkan, Alan C. Bovik, and Paola Passalacqua. 2017. "Surface Water Mapping by Deep Learning." *IEEE Journal of Selected Topics in Applied Earth Observations and Remote Sensing* 10 (11): 4909–18. <https://doi.org/10.1109/JSTARS.2017.2735443>.
- Isikdogan, Leo F., Alan Bovik, and Paola Passalacqua. 2019. "Seeing Through the Clouds With DeepWaterMap." *IEEE Geoscience and Remote Sensing Letters*, 1–5. <https://doi.org/10.1109/LGRS.2019.2953261>.
- Liu, H., and K. C. Jezek. 2004. "Automated Extraction of Coastline from Satellite Imagery by Integrating Canny Edge Detection and Locally Adaptive Thresholding Methods." *International Journal of Remote Sensing* 25 (5): 937–58. <https://doi.org/10.1080/0143116031000139890>.
- Paravolidakis, Vasilis, Lemonia Ragia, Konstantia Moirogiorgou, and Michalis Zervakis. 2018. "Automatic Coastline Extraction Using Edge Detection and Optimization Procedures." *Geosciences* 8 (11): 407. <https://doi.org/10.3390/geosciences8110407>.

Acknowledgements:

We would like to thank the Alaska Sea Grant and the National Oceanic and Atmospheric Administration for their support and funding for the research presented here. Additionally, we would like to thank Jack Carroll and Brandon Mommsen for their efforts in finalizing this project.

Observing permafrost coastal bluff erosion using a high spatial and temporal resolution remote sensing time series at Drew Point, Beaufort Sea Coast, Alaska

Melissa K. Ward Jones¹, Benjamin M. Jones¹, Ingmar Nitze², Matthias Gessner³, Guido Grosse²

¹Institute of Northern Engineering, University of Alaska Fairbanks, USA

²Alfred Wegener Institute Helmholtz Centre for Polar and Marine, Potsdam, Germany

³Deutsches Zentrum für Luft- und Raumfahrt e.V. (DLR), Berlin, Germany

Arctic coastlines are eroding at different rates due to the spatial and temporal variability from factors such as permafrost conditions, sediment composition, ground ice content, hydrometeorological conditions and ocean forcing (Lantuit et al., 2012). Ice-rich coastlines, such as those along the Beaufort Sea in Alaska, are eroding the most rapidly due to its high ground ice content. The dominant mechanisms of erosion of ice-rich coastlines are thermal denudation (i.e., slumping) and thermal abrasion (i.e., block failure). High temporal and spatial resolution time series can provide insights into better understanding the processes driving erosion rates along ice-rich permafrost coastlines (Jones et al., 2018). We present a 15-image time series using high-resolution satellite imagery, airborne multispectral imagery and UAV surveys spanning the full 2018 and 2019 open-water seasons along a 1.5 km section of Drew Point, Beaufort Sea Coast, Alaska. We measured erosion using transects lines spaced 1 m apart using the Digital Shoreline Analysis System v.5 (DSAS) ArcGIS Desktop software extension tool (Thieler et al., 2009). Mean erosion was 10.5 m in 2018 and 28.7 m in 2019. Put into context of mean annual erosion rates measured between 2007 and 2019 along a 9 Km coastline that includes the 1.5 Km stretch, the 2018 season represents the second lowest mean erosion (11.2 m) and the 2019 season, the highest erosion (34.5 m). We further explored erosion mechanisms by determining erosion rates of thermal abrasion (i.e., block failure) and thermal denudation (i.e., slumping), as well as rates along protected (i.e., block present) and exposed (i.e., no blocks present) sections. The 2018 season had a higher number of blocks present (between 98 and 122 present) leading to a higher percentage of protected coast (36 % to 51 %) compared to 2019 (25 to 70 blocks present) with a lower percentage of protected coastline (9% to 48 %). Our research shows the importance of accounting for block presence at the foot of the bluff in understanding erosion rates and processes along ice-rich permafrost coastlines.

Keywords: Coastal processes, permafrost, UAV, high resolution time series

References

Jones, B.M., Farquharson, L.M., Baughman, C.A., Buzard, R.M., Arp, C.D., Grosse, G., Bull, D.L., Günther, F., Nitze, I., Urban, F. and Kasper, J.L., 2018. A decade of remotely sensed observations

highlight complex processes linked to coastal permafrost bluff erosion in the Arctic. *Environmental Research Letters*, 13(11), p.115001.

Lantuit, H., Overduin, P.P., Couture, N., Wetterich, S., Aré, F., Atkinson, D., Brown, J., Cherkashov, G., Drozdov, D., Forbes, D.L. and Graves-Gaylord, A. (2012). The Arctic coastal dynamics database: a new classification scheme and statistics on Arctic permafrost coastlines. *Estuaries and Coasts*, 35(2), pp.383-400. <https://doi.org/10.1007/s12237-010-9362-6>

Theiler, E., Himmelstoss, E., Zichichi, J., and Ergul, A. (2017). Digital Shoreline Analysis System (DSAS) Version 4.0-An ArcGIS Extension for Calculating Shoreline Change (Ver. 4.4). *US Geological Survey Open-File Report*, 1278.

Acknowledgements: Funding for this research was provided by two grants from the National Science Foundation - OISE-1927553 (BMJ) and OIA-1929170 (BMJ and MKWJ). Funding for the Polar-6 airborne operations was provided through AWI base funds for the ThawTrend-Air 2019 campaign. We thank Martin Gehrman, Maximilian Stöhr, Daniel Steinhage, and Birgit Heim (all AWI) as well as Torsten Sachs (GFZ) for technical help during the Polar-6 campaign and the pilots of Kenn Borek Air for safe operations under adverse weather conditions in 2019. We thank Daniel Hein (DLR) for remote support with the MACS image acquisition toolbox during the Polar-6 campaign. Additional support was provided by Sandia National Laboratory.

Remote uncrewed aircraft system (UAS) inspection and response team development in the Bering Strait region

Jessica Garron^{1}, John Henry, Jr.^{2*}, Margy Hall³, Jereme Altendorf⁴*

¹ Jessica Garron (jgarron@alaska.edu) (Alaska Climate Adaptation Science Center, International Arctic Research Center, University of Alaska Fairbanks, Fairbanks, AK, USA)

² John Henry, Jr. (john.henry@unkira.org) (Native Village of Unalakleet, Unalakleet, AK, USA)

³ Margaret Hall (margy@mfpp.org) (Model Forest Policy Program, Sagle, ID, USA)

⁴ Jereme Altendorf (Jereme.m.altendorf@uscg.mil) (Marine Safety Task Force, Sector Anchorage, United States Coast Guard, Anchorage, AK, USA)

*Presenting authors

Abstract

Remote-sensing tools are critical components of environmental observations in support of decision-making across remote Alaska. Understanding this capacity, the Native Village of Unalakleet, Alaska, located in western Alaska, completed a feasibility study in 2021 about using uncrewed aircraft systems (UAS) and on-line data tools to support community adaptation planning in response to climate change and to support emergency response activities. Also in Alaska, the United States Coast Guard (USCG) is responsible for the inspection of 380 bulk fuel storage facilities in Alaska, 347 of which are only accessible by boat or airplane. Exploring the nexus of needs of these two coastal Alaskan stakeholder groups, this project and subsequent program was designed to train a set of UAS pilots in the remote, coastal, hub community of Unalakleet, Alaska to fly small UAS in support of local decision-making and USCG mission support.

Members of the Bering Strait community of Unalakleet, Alaska applied for participation in the program, received eight-weeks of remote training from University of Alaska Fairbanks drone pilots and researchers on the safe and legal use of these remote sensing tools, followed by the successful completion of their FAA Part 107 Certification exams. Along with UAS flight training, this project included the co-production of infrastructure assessment, environmental monitoring, and emergency response UAS protocols among the pilots, researchers and USCG representatives. Pilots were trained to use both electrooptical and infrared sensors to analyze different targets, and to create 2D orthomosaics and 3D models of infrastructure and landscape features.

The feasibility of expanding this training program regionally, inclusive of the economic challenges and required capacities, is currently under evaluation while the broad dissemination of process and technological knowledge gained to other remote Arctic communities has begun. This project affirmed that technology-based solutions applied to problems associated with climate change, food security, environmental stewardship and emergency response can bolster workforce development opportunities in rural communities while also meeting the needs of regulatory and response agencies. This presentation will highlight the leveraging of

partnerships, adaptation of methodologies, and milestones achieved to make this a successful multidisciplinary project.

Keywords: Drones, Coproduction, Climate Change

Acknowledgements: The presenters would like to highlight the extensive and continued support of our sponsors at the Arctic Domain Awareness Center, a Department of Homeland Security Center of Excellence, the unflagging support from our partnerships with the entire community of Unalakleet, and our regional partners throughout the Norton Sound. Thank you!

Session 2.1: Arctic Coasts and its Communities II

Shore evidences of a high Antarctic ocean wave event: geomorphology, event reconstruction and coast dynamics through a remote sensing approach

Stefano Ponti, Mauro Guglielmin

¹Department of Theoretical and Applied Sciences, Insubria University, 21100 Varese, Italy

Abstract

In the boundary zone between land and ocean, remote sensing can be helpful to define the dynamic of high-latitude coastal environments. These areas are characterized by the role of cryogenic processes like sea-ice or permafrost together with storm surges and wind action. In this study we examined the geomorphological dynamics of a beach located at Edmonson Point (74 S) not far from the Italian Antarctic Station “Mario Zucchelli” between 1993 and 2019 using different remote sensing techniques and field measurements.

Our data demonstrated that the average rate of the beach surficial increase ($0.002 \pm 0.032 \text{ m yr}^{-1}$) was slightly higher than the uplift rate determined by previous authors ($0\text{--}1 \text{ cm yr}^{-1}$) (Baroni and Orombelli, 1991; Ivins, 2003) in case of pure isostatic rebound. However, we suggest that the evolution of Edmonson Point North Beach (EPNB) is likely due to the couple effect of vertical uplift and high wave-energy events. Indeed, the coastline accumulation could be related to the subsurface sea water infiltration and annually freezing at the permafrost table interface as aggradational ice (Mackay, 1972) as suggested by the electrical resistivity tomography (ERT) carried out in 1996. This ERT suggested the occurrence of saline frozen permafrost or hypersaline brines under the sea level, while permafrost with ice occurred above the sea level. The beach also revealed areas that had quite high subsidence rates (between 0.08 and 0.011 m yr^{-1}) located where ice content was higher in 1996 and where the active layer thickening and wind erosion could explain the measured erosion rates.

In this geomorphological context we also dated at the late morning of 15 February 2019 the coastal flooding and defined a significant wave height of 1.95 m. During the high oceanic wave event, the sea level increased advancing shoreward up to 360 m, three times higher than the previous reported storm surge (81 m) and with a sea level rise almost five times higher than has been previously recorded in the Ross Sea (Goring and Pyne, 2003).

Keywords: beach processes; coastal storm; coastal geomorphology

References:

Baroni, C.; Orombelli, G. Holocene raised beaches at Terra Nova Bay, Victoria Land, Antarctica. *Quat. Res.* 1991, *36*, 157–177.

Goring, D.G.; Pyne, A. Observations of sea-level variability in Ross Sea, Antarctica. *N. Zeal. J. Mar. Freshw. Res.* 2003, 37, 241–249.

Ivins, E.R. Glacial isostatic stress shadowing by the Antarctic ice sheet. *J. Geophys. Res.* 2003, 108.

Mackay, J.R. The world of underground ice. *Ann. Assoc. Am. Geogr.* 1972, 62, 1–22.

Acknowledgements: We want to thank all the logistical people of ENEA that support the research at Mario Zucchelli Station and Helicopter New Zealand and their pilots that allow this research. We also thank Emanuele Forte for a contribution in Figure 11 and Ulrich Neumann for his help in the field.

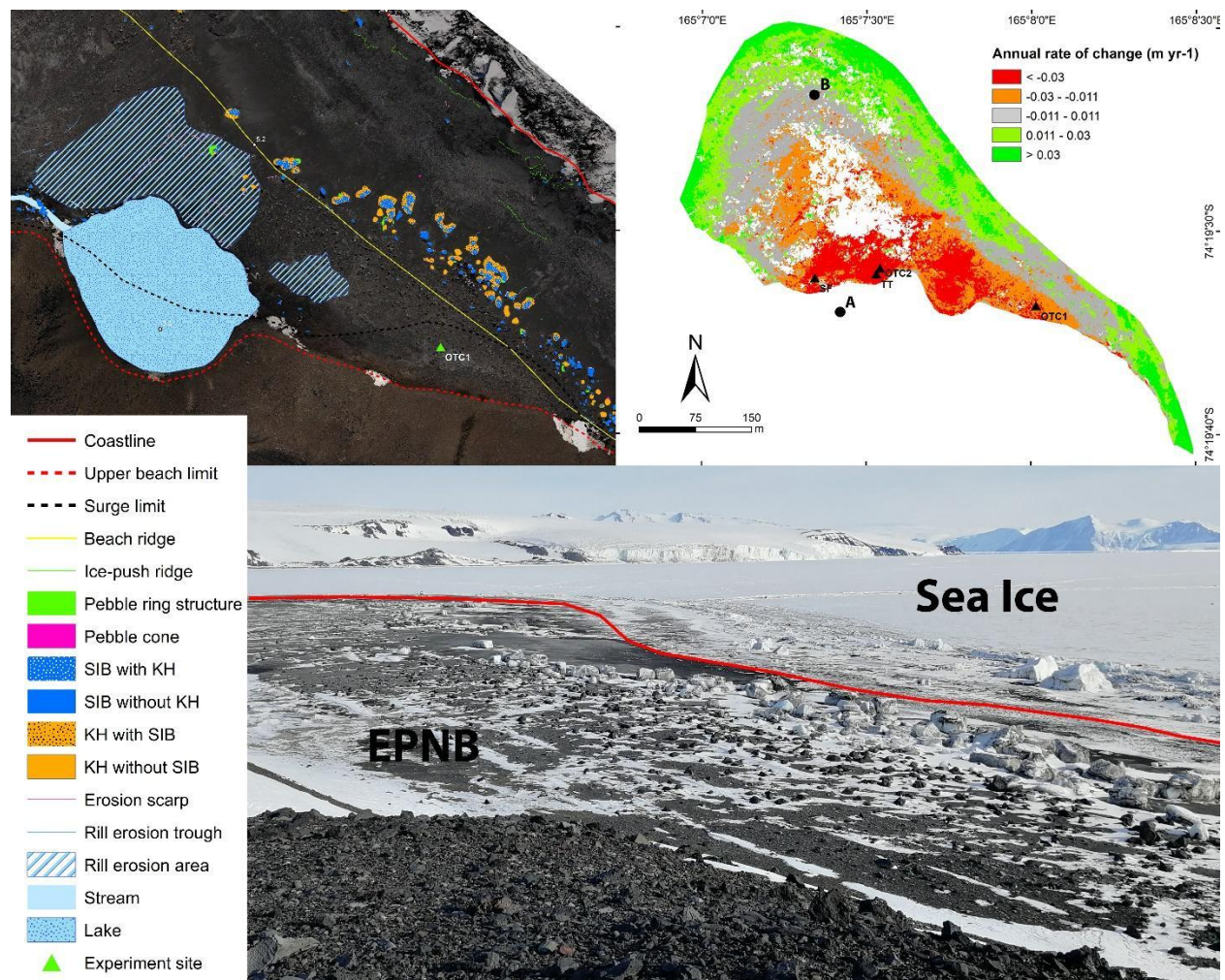


Figure 1. Photogrammetric products of EPNB: the beach geomorphology after the oceanic wave event and the vertical rate of change ($m\ yr^{-1}$) calculated in 26 years.

Landscapes and erosion rates of the Alaska Beaufort Sea Coast

Anastasia Piliouras^{1,2}, Benjamin Jones³, Tabatha Clevenger⁴, Joel C. Rowland¹

¹Earth and Environmental Sciences Division, Los Alamos National Laboratory, Los Alamos, NM USA
(Department, Institute, City, State/Territory/Country)

²Department of Geosciences, Pennsylvania State University, State College, PA USA

³Institute of Northern Engineering, University of Alaska Fairbanks, Fairbanks AK USA

⁴Department of Earth Science and Geography, Vassar College, Poughkeepsie, NY USA

Abstract

Arctic coastal environments are rapidly changing as the Arctic continues to warm, but heterogeneity in landscape and soil conditions makes coastal erosion difficult to predict. We analyzed a compilation of geospatial and remotely sensed datasets along Alaska's Beaufort Sea Coast to understand the heterogeneity in landscape conditions and historical erosion rates, including topography, shoreline orientation, surficial geology, geomorphology, landcover, and ice content. We also used these datasets to develop a set of coastal typologies that capture the variability in environments susceptible to coastal erosion on Alaska's northern coast. We examined the relationships between surface and subsurface characteristics and historical erosion rates, finding that no single variable is a good predictor of erosion rates. Areas along the Alaskan Beaufort Sea Coast that are sheltered by barrier islands had a three times lower erosion rate on average, suggesting that the loss of barrier islands, for example by storms or by sand and gravel mining, could drive more than a tripling in future erosion rates in northern Alaska. Finally, the typologies suggest that areas with the highest erosion rates are not broadly representative of the region, and that high erosion rates are generally associated with bluffs 0-2 m in height, north- to northeast-facing shorelines, a peaty pebbly silty lithology, and glaciomarine deposits with high ice contents. These results can be used to guide future modeling and observational efforts by increasing our understanding of the prevalence of different landscapes and the association of combinations of surface and subsurface conditions with high and low erosion rates.

Keywords: Coastal, Erosion, Geospatial

Acknowledgements

This work was funded by the US Department of Energy Office of Biological and Environmental Research as part of the InterFACE project.

Session 2.2: Climate Change and Climate Data Records

Low-frequency sea ice variability drives NDVI declines in the Yukon-Kuskokwim Delta

Amy Hendricks¹, Uma Bhatt¹, Gerald Frost², Donald Walker³, Peter Bieniek⁴, and Matthew Macander²

¹Department of Atmospheric Sciences, Geophysical Institute, University of Alaska Fairbanks, Fairbanks, Alaska, USA

²ABR, Inc., Fairbanks, Alaska, USA

³University of Alaska Fairbanks, Institute of Arctic Biology and Department of Biology and Wildlife, Fairbanks, Alaska, USA

⁴International Arctic Research Center, University of Alaska Fairbanks, Fairbanks, Alaska, USA

Abstract

Rapidly warming temperatures in the Arctic are driving increasing tundra vegetation productivity, evidenced in both satellite imagery and field studies. However, spatial patterns are not uniform across the circumpolar Arctic. Southwest Alaska's Yukon-Kuskokwim Delta (YKD) is a notable region displaying declining trends in vegetation productivity. Satellite imagery from the Advanced Very High Resolution Radiometer (AVHRR) is used to calculate an index of photosynthetic activity known as the Normalized Vegetation Difference Index (NDVI) (Pinzon and Tucker, 2014). Negative linear trends of NDVI in the YKD region were first noted in analysis conducted over the 1982-2008 period and have been a recurring feature in the spatial trend maps of NDVI as the time series was incrementally extended (Verbyla 2008, Bhatt et al. 2010, 2021; Frost et al. 2021). These trends have been difficult to explain since temperature is a limiting factor for tundra, and Summer Warmth Index (SWI) displays positive trends in this region.

Now that the record is nearly four decades long, analysis over 1982-2021 reveals insights into the operating processes. The time series for NDVI displays a distinct coherent multidecadal variability (Figure 1), showing an increase in NDVI during the first decade, followed by a generally steady decline for two decades, reaching a minimum at the start of the third decade. A sharp rise in NDVI occurs over the most recent decade. A simple linear trend of NDVI in the YKD region over 1982-2021 results in a negative trend, despite a strong positive trend in the past 10 years. This distinct coherent multidecadal variability is also present in SWI and 100-km coastal zone spring sea ice concentrations. SWI does not show as strong of a decadal variability as NDVI and sea ice early in the record, but the trends of NDVI, sea ice, and SWI show increasing similarity over the most recent decade. This indicates that low frequency climate

variations can dominate the variability of NDVI through their influence of the climate drivers of tundra vegetation, namely coastal sea ice concentrations and SWI. This study highlights the importance of examining time series and simple trend analyses spatially, since low-frequency variability can obscure the interpretation of long-term trends. The continued decline of sea ice in the Bering Sea motivates exploring how climate drivers of vegetation productivity are currently changing and will change in the future.

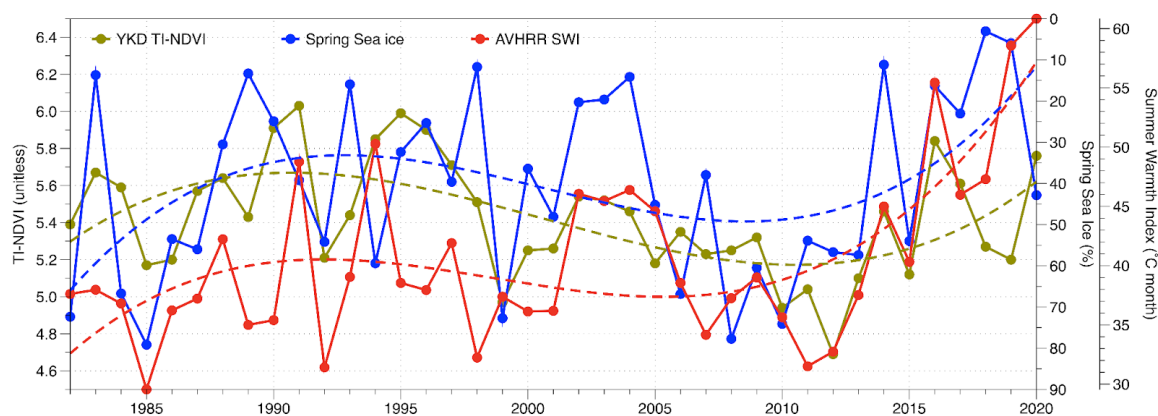


Figure 1. Time series of TI-NDVI (olive), Summer Warmth Index (SWI; red), and 100-km coastal spring sea ice concentration (blue) show similar multidecadal variability, identified by the corresponding dashed cubic-fit lines. Note the scale is reversed for sea ice concentration.

Keywords

NDVI, climate drivers, sea ice variability

References

- Global Ecology and Biogeography Bhatt, U. S., Walker, D. A., Raynolds, M. K., Comiso, J. C., Epstein, H. E., Jia, G., Gens, R., Pinzon, J. E., Tucker, C. J., Tweedie, C. E., & Webber, P. J., (2010). Circumpolar Arctic Tundra Vegetation Change Is Linked to Sea Ice Decline, *Earth Interactions*, 14(8), 1-20.
- Bhatt, U.S., Walker, D.A., Raynolds, M.K., Walsh, J.E., Bieniek, P.A., Cai, L., Comiso, J.C., Epstein, H.E., Frost, G.V., Gersten, R. and Hendricks, A.S., (2021). Climate drivers of Arctic tundra variability and change using an indicators framework. *Environmental Research Letters*, 16(5), p.055019.
- Frost, G.V., Bhatt, U.S., Macander, M.J., Hendricks, A.S. and Jorgenson, M.T., (2021). Is Alaska’s Yukon–Kuskokwim Delta Greening or Browning? Resolving Mixed Signals of Tundra Vegetation Dynamics and Drivers in the Maritime Arctic. *Earth Interactions*, 25(1), pp.76-93.
- Pinzon, J. E., & Tucker, C. J. (2014). A non-stationary 1981–2012 AVHRR NDVI3g time series. *Remote sensing*, 6(8), 6929-6960.
- Verbyla, D. (2008). The greening and browning of Alaska based on 1982–2003 satellite data., 17: 547-555.

Acknowledgements

This research was funded by the NASA Arctic-Boreal Vulnerability Experiment grant award NNX15AT76A. The author would like to thank the University of Alaska Fairbanks Research Computing Services for technical support, and Calista Education and Culture for fruitful discussion about local environmental changes in the Yukon-Kuskokwim Delta. University of Alaska Fairbanks is located on Troth Yeddha' on the ancestral homelands of the Lower Tanana Dené People.

A remote sensing view of Arctic heat anomalies: Spatial-temporal distribution and effects

Victoria V. Miles¹

¹Nansen Environmental and Remote Sensing Center, Bergen, Norway, Bjerknes Centre for Climate Research, Bergen, Norway

Abstract

Arctic climate change is amplified and accelerated, but until recently, the high variability of the Arctic climate has kept a low signal-to-noise ratio of the anthropogenic warming in the region [1]. Recent high temperature extremes in the region are record-breaking and have already been attributed to global warming [2]. The Arctic heat wave impact has both environmental and human perspectives [3]. The last decade has witnessed several unprecedented heat waves in the Arctic, notoriously in 2012, 2016, and 2020 [4].

Enhanced sea ice melt leads to larger heat content of the upper ocean layers and delayed refreezing. It keeps strong warm temperature anomalies in the Arctic throughout November–December. High land temperatures favor wildfires and permafrost thaw; enhance carbon release from soils, and the land disturbances open pathways to afforestation and shrubification of the Arctic [5].

We produced a spatial-temporal analysis of land surface temperature (LST) data. LST is a good indicator of the energy balance at Earth’s surface because it is one of the key parameters in the physics of land surface processes. LST integrates the results of surface-atmosphere interactions and energy fluxes between the atmosphere and the ground. Our study demonstrates the increase of Arctic heat wave occurrences during last decade and show some examples of its effects.

The LST anomaly maps were made using thermal infrared measurements collected by the Moderate Resolution Imaging Spectroradiometer (MODIS) instrument aboard NASA’s Terra satellite. The climatology used for calculating the anomaly spans 2000-2020. The anomalies were calculated for a given month compared to the average conditions during that period between 2000-2020.

The ‘mindboggling’ Arctic heatwave in 2020 was record-breaking, and headlines are full of alarming news. Intense heat also affected several regions in the summer of 2016. The extremely dry and hot weather set in northern Siberia seriously affected local ecosystems, causing severe tundra fires but showing positive anomalies in most northwestern Siberia [5].

The most recent high temperature extremes in the region are record-breaking with all-time record high temperature in 2020. The Arctic “thermometer” – Svalbard – shows summer in 2020 is the warmest on record, well above the old summer record from 2015.

The heatwaves increase the ambient temperatures and also intensify the difference between urban and rural temperatures. As a result, the added heat stress in cities is even higher than the sum of the background urban heat island effect and the heatwave effect (Fig. 1), e.g., extreme urban heat in Nadym (65.5°N, 72.5°E) in Siberia in August 2020.

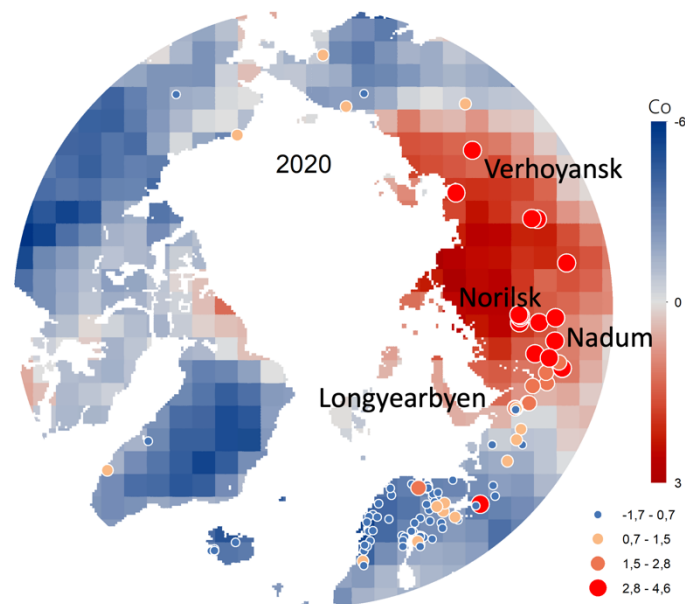


Figure 1. Urban heat island anomalies and Arctic summer LST anomalies in 2020. Higher urban anomalies are in areas with high surface temperature anomalies. Over the past decade, due to the arctic heatwaves, additional heat stress has been created in the cities.

Keywords Arctic amplification, land surface temperature, urban heat island.

References

- [1] Mahlstein et al. (2011). Early onset of significant local warming in low latitude countries. *Environ. Res. Lett.*, 6, 34009.
- [2] Prolonged Siberian Heat Wave 2020. (2020). Retrieved from <https://www.worldweatherattribution.org/siberian-heatwave-of-2020-almost-impossible-without-climate-change>
- [3] see story of the oil reservoir collapse in Norilsk, 29 May 2020, https://en.wikipedia.org/wiki/Norilsk_oil_spill
- [4] Dobricic et al. (2020). Increasing occurrence of heat waves in the terrestrial Arctic. *Environ. Res. Lett.*, 15(2).

[5] Miles, M. W., Miles, V., Esau, I., 2019: Varying climate response across the tundra, forest–tundra and boreal forest biomes in northern West Siberia. *Environ. Res. Lett.*.

<https://doi.org/10.1088/1748-9326/ab2364>.

Acknowledgements

The research is supported by the Belmont Forum's SERUS project and the Bjerknes Climate Research Center's Fast track initiative.

Early snowmelt and polar jet dynamics drive recent extreme Siberian fire seasons

Rebecca C. Scholten¹, Dim Coumou^{1,2}, Fei Luo¹, Sander Veraverbeke¹

¹ Faculty of Science, Vrije Universiteit Amsterdam, Amsterdam, the Netherlands

² Royal Netherlands Meteorological Institute (KNMI), De Bilt, the Netherlands

Abstract

2019, 2020 and 2021 were extreme fire years in the vast larch forests of northeastern Siberia, with many fires burning in permafrost peatlands within the Arctic Circle. These fire extremes have been linked to record-high spring and summer temperatures over the region. 2020 also exhibited exceptionally early snowmelt onsets in large parts of Siberia – a development that is in line with longer-term trends in advancing snowmelt throughout the region.

In mid-latitudes, the pronounced and long-lasting heatwaves of the last decade have been linked to amplified Rossby waves connected with weak atmospheric circulation. These amplified waves tend to phase-lock in preferred positions and thereby lead to more persistent summer weather. Linkages between atmospheric teleconnections and boreal wildfires exist for some regions, yet the influence of jet stream dynamics on arctic-boreal wildfires is unknown. We used MODIS burned area, active fires and snow cover, and ERA5 climate data to explore relationships between the jet stream, snowmelt trends, and unprecedented fire activity in Siberia, with the aim of assessing whether the recent surge in arctic-boreal fires in Siberia is driven by large-scale atmospheric dynamics.

We show that the formation of an anomalous Arctic front jet over northeastern Siberia promoted unusual hot and dry conditions, thereby triggering extreme lightning and fire occurrences. Notably within the Arctic Circle, fire extremes were further reinforced by early seasonal snowmelt. The last decades have seen both, an advancing snowmelt in Siberia and more frequent and persistent Arctic front jets. These compounding climatological drivers promote extreme fires, which accelerate the degradation of carbon-rich permafrost peatlands.

Keywords: Boreal fire, jet stream, Siberia

Session 1: Glaciers and Seasonal Snow Cover

A new 38-year time series of daily, global fractional snow cover maps

Rune Solberg¹, Øystein Rudjord¹, Arnt-Børre Salberg¹, Mari Anne Killie², Steinar Eastwood², Atle Sørensen²

¹Norwegian Computing Center, Section for Earth Observation, Oslo, Norway

² Norwegian Meteorological Institute, Oslo, Norway

Abstract

The ESA CryoClim project previously developed an operational service for long-term systematic climate monitoring of the cryosphere, including snow cover. The project developed a binary snow cover product. The product is based on fusion of AVHRR GAC and SMMR + SSM/I + SSMIS data. The product set consists of a time series (1982-2015) of daily, snow cover maps of 5 km spatial resolution with full global coverage independent of clouds and polar-night darkness. The product includes an estimate of the uncertainty at grid level. The ESA Climate Change Initiative (CCI) Snow ECV project has now developed an advancement to a fractional snow cover (FSC) product. This presentation gives an overview of the algorithm and the validation results and provides the first findings to global and regional changes in snow cover over the entire time series (1982-2019).

The original binary algorithm is based on a hidden Markov model (HMM) simulating snow states based on the satellite observations. The basic idea is to simulate the states the snow surface goes through during the snow season with a state model. The model is described by the different states and the possible transitions between these states. The states are given by probability density functions and the transitions by transition probabilities. The transition probabilities depend on the current time within the season. The states are not directly observable, but the remote sensing observations give data describing the snow conditions, which are related to the snow states. A Viterbi algorithm is used to find the most likely snow cover sequence throughout the hydrological year at each grid cell. The HMM solution represents not only a multi-sensor model but also a multi-temporal model.

The advancement from binary to fractional snow cover has followed two main paths: First, we introduced more HMM states to be able to classify the snow cover into 10% FSC intervals. Experiments show that this is a viable and reasonable solution to obtain higher precision than the binary variable gives. However, introducing 100 states to obtain 1% FSC intervals would not give a stable model. For obtaining higher precision, we have interpolated between HMM states using a secondary Viterbi sequence. We estimate the FSC for a given grid cell by taking two

states into account – the state of highest probability and the state of second-highest probability. The two probabilities are used as weights to estimate the FSC.

The algorithm has been implemented to run on a supercomputer as three components. The optical and passive microwave radiometer (PMR) data are processed in two processing chains giving the probability of snow from each type of data, respectively. The probabilities are calculated from Bayesian models combining data features (numerical combinations of bands) conditioned by ancillary data (like land cover). The probabilities are applied in the HMM multi-sensor/multi-temporal model generating the fractional snow cover map. The map also includes a per-grid-cell estimate of the FSC uncertainty.

When this work is completed in summer 2022, a new 38-year time series of daily, global products will be freely available to the climate community.

Keywords Snow cover, climate monitoring, cryosphere

References

- Solberg, R., M. Killie, L. M. Andreassen and M. König, 2014. CryoClim: A new system and service for climate monitoring of the cryosphere. *IOP Conf. Series: Earth and Environmental Science*, 17, 012008. doi:10.1088/1755-1315/17/1/012008
- Rudjord, Ø., A.-B. Salberg and R. Solberg, 2015. Global snow cover mapping using a multi-temporal multi-sensor approach. In *Proceedings of the 2015 8th International Workshop on the Analysis of Multitemporal Remote Sensing Images (Multi-Temp)*. doi:10.1109/Multi-Temp.2015.7245775

Acknowledgements We acknowledge EUMETSAT for providing fundamental climate data records (FCDRs) for daily global observations from AVHRR GAC, SMMR, SSM/I and SSMIS.

The development and application of a UAS and photogrammetry routine in support of Alaska's department of transportation effort to elucidate snow height for avalanche risk assessment in Atigun Pass

Eyal Saiset¹, Billy Connor², Michael Lilly³, Gordon Scott⁴, Ryan Marlow⁵

¹Alaska Center for UAS Integration, Geophysical Institute, University of Alaska Fairbanks, Fairbanks, Alaska, USA. ²Arctic infrastructure Development Center, Institute of Northern Engineering, University of Alaska Fairbanks, Fairbanks, Alaska, USA. ³Geo-Watersheds Scientific, Fairbanks, Alaska, USA. ⁴Northern Region, Department of Transportation and Public Facilities, Alaska, USA. ⁵Central Region, Department of Transportation and Public Facilities, Alaska, USA.

Abstract

Avalanches in Atigun Pass (Brooks Range, Alaska) are a consequence of its unique geographic setting and are often not a result of significant snowfall, as typically the case elsewhere in Alaska. In South-East and South-Central Alaska, snow of several feet in depth is common, whereas in Atigun Pass, significant snow is measured in inches. Thus, heavy snow precipitation is not the dominant reason for heightened avalanche risks. Instead, a few inches of new snow precipitation or even older accumulation are blown off of ridges and add to the snow loads of cornices and gullies. Thus, even a few inches of snow across the landscape from earlier storms can be sufficient to trigger large avalanches that can obstruct the Dalton-Highway and engulf large tractor-trailer vehicles.

A key to an accurate assessment of avalanche risk at Atigun Pass is measuring snow height at areas of high risk and determining the amount of snow transported to those sites during strong wind events. Remote sensing is key to accomplish this task.

In this project, we showcase the application of Unmanned Aircraft System (UAS) to determine snow depth on a routine basis, using photogrammetry and custom-built change-detection software to automatically inform DOT&PF personnel of critical snow accumulation values in avalanche-prone gullies. Despite the success we have had in recent years, with DOT&PF staff flying UAS and automatically generating photogrammetry data products (as seen in Figure 1), the UAS is only an effective tool on bluebird days (ideally with direct sun on the surveyed slopes).

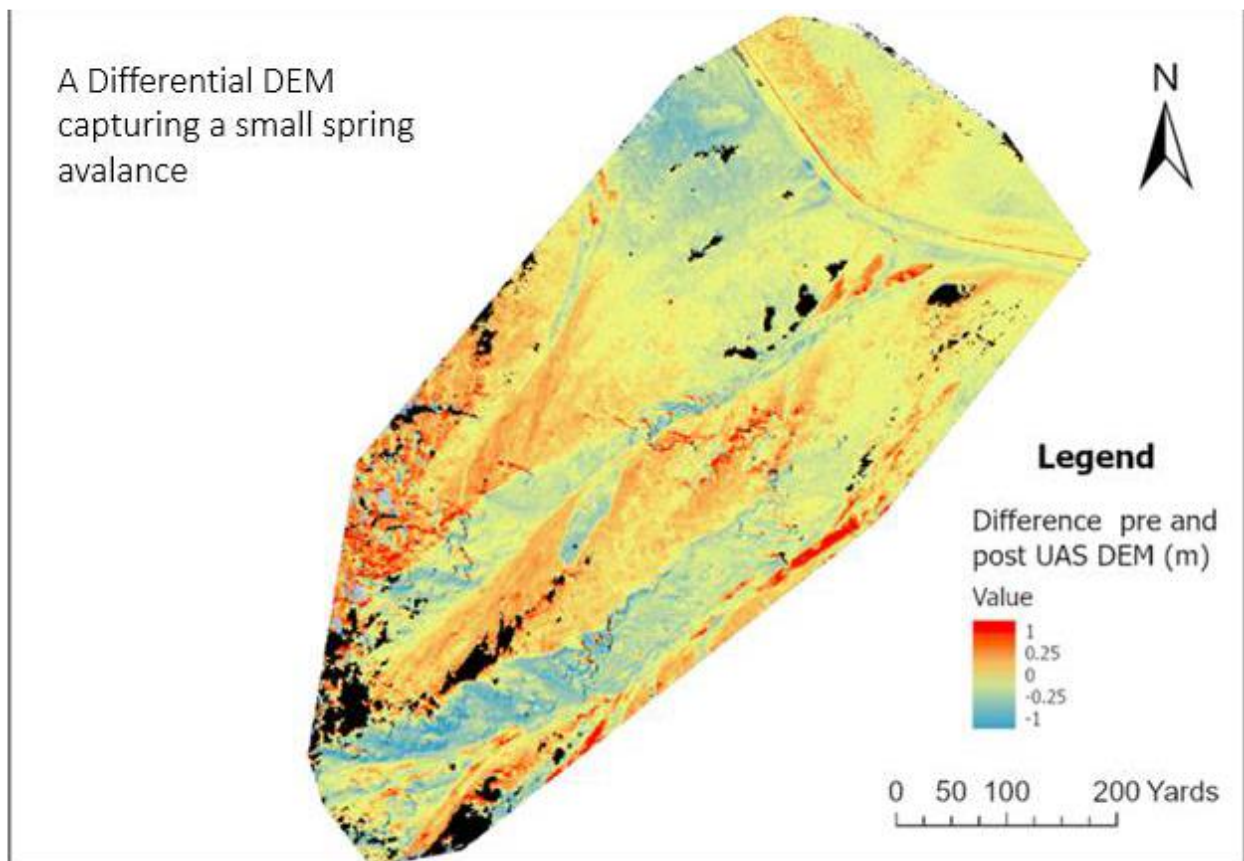
Yet, a significant fraction of avalanches in Atigun Pass occur during intense wind events- unsafe for the UAS. Over this past year, we installed a new weather station on the southside of Atigun Pass. The station measures wind, snow height as well blowing snow flux. The current effort is to make the change-detection software use the weather station in concert with snow-height measurements derived from the photogrammetry. In practice, the aim is to use the snow-height measurements from the photogrammetry before a storm as a set of initial conditions. With the parametrization of blowing snow at different sites, and ongoing snow flux

measurements at the station, we plan to develop regression and non-linear models to be able to highlight areas of higher avalanche risk and perhaps suggest when to apply avalanche control. Example outcomes can help improve strategies and limit the use of expensive howitzer ammunition for avalanche control.

This project also demonstrates fruitful work between the Geophysical Institute (GI), private business; Geo-Watershed Scientific (GWS), and DOT&PF. The project demonstrates how technology and scientific understanding of processes can be applied operationally, resulting in the reduction of significant and life-threatening hazards. DOT&PF personnel routinely and independently operate the UAS successfully and retrieve high-quality information (imagery with survey-grade localization) to yield repeatedly superb raster quality products. This is in conjunction with the Winter-Hazards Station that reports storm conditions during periods when the UAS cannot operate. The process from imagery to high-detail avalanche assessment is completely done through an inhouse software development.

We think this type of collaboration between the GI and DOT&PF can yield many more successful partnerships with the warming climate and its threat to infrastructure.

Keywords (UAS, Infrastructure, Change Detection)



Session 1.1 : Observing Permafrost I

Deep Learning for mapping retrogressive thaw slumps across the Arctic

I. Nitze¹, K. Heidler^{2,3}, S. Barth^{1,4}, G. Grosse^{1,4}

1 Alfred Wegener Institute Helmholtz Centre for Polar and Marine Research, 14473 Potsdam, Germany

2 Remote Sensing Technology Institute (IMF), German Aerospace Center (DLR), 82234 Weßling, Germany

3 Data Science in Earth Observation, Technical University of Munich (TUM), 80333 Munich, Germany

4 Institute of Geosciences, University of Potsdam, 14476 Potsdam, Germany

Abstract

Retrogressive thaw slumps (RTS) are typical landscape processes of thawing and degrading very ice-rich permafrost in hillslope terrain and along the Arctic coast. To this point, their distribution and dynamics are almost completely undocumented across many regions in the permafrost domain. This is mostly due to the lack of high resolution data for these vast regions and insufficient techniques for monitoring and processing such large areas in the past. We are tackling this shortcoming by creating a deep learning (DL) based semantic segmentation framework to detect RTS, using multi-spectral PlanetScope imagery, high-resolution topographic (ArcticDEM), and multi-temporal Landsat trend data. We created a highly automated processing pipeline, which is designed to create reproducible results and to be flexible for multiple input features (Nitze et al., 2021).

We tested our DL based model in six different regions of 100 to 300 km² size across Canada (Banks Island, Tuktoyaktuk Peninsula, Horton River, Herschel Island), and Siberia (Kolguev Island, Lena River). We performed a regional cross-validation (5 regions training, 1 region validation) to test the spatial robustness and transferability of the algorithm. Furthermore, we tested different architectures to identify the best performing and most robust parameter sets. For training the models we created a training database of manually digitized and validated RTS polygons.

The resulting model performance varied strongly between different regions. This emphasizes the need for sufficiently large training data, which is representative for the massive variety of RTS. However, the creation of good training data proved to be challenging due to the fuzzy definition and delineation of RTS, particularly on the lower part of the slump floor and outlets.

We have recently expanded our analysis to several RTS-rich regions across the Arctic (Fig.1) for the year 2021 and annual analysis (2018-2021) for hot-spots of RTS occurrence, such as Banks Island, Peel Plateau and other areas. First model inference runs are promising for detecting RTS, but are still strongly overestimating the number and area of RTS. Model performance however, varies strongly between regions. Due to the strong variability of landscapes with RTS, we expect training datasets. The community driven formation of the IPA Action Group RTSInTrain, which aims to create standardized RTS digitization protocols and training datasets for deep/machine-learning purposes will be a great boost for this purpose.

Our standardized processing pipeline allows us to add more features based on user requirements and data availability. We tested our workflow for surface water and pingos, producing encouraging results and showed that the designed workflow is transferable beyond the segmentation of RTS only.

In the near future, we are aiming to integrate the community-based training data and further gradually improve our training database. Within the framework of the ML4Earth project, we will create a temporal and pan-arctic monitoring system for RTS based on our highly automated processing chain. This will enable us to better understand pan-arctic RTS dynamics, their influencing factors, and consequences.

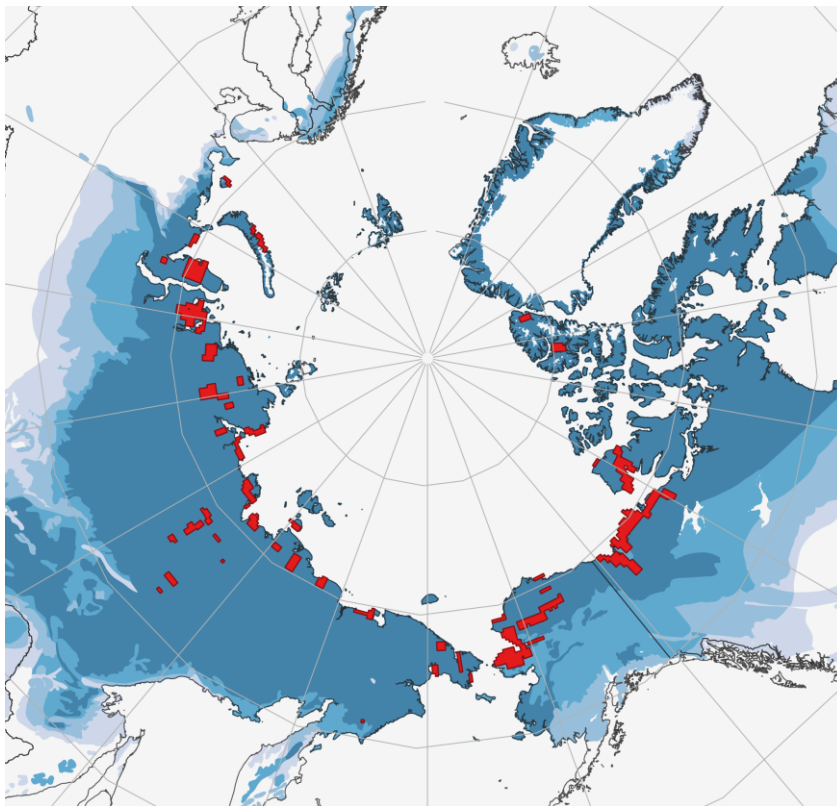


Figure 1. Current processing domain for mapping RTS and further permafrost related landscape

features.

Keywords: Deep learning, retrogressive thaw slumps, permafrost disturbance

References

Nitze, I., Heidler, K., Barth, S., & Grosse, G. (2021). Developing and Testing a Deep Learning Approach for Mapping Retrogressive Thaw Slumps. *Remote Sensing*, 13(21).

<https://doi.org/10.3390/rs13214294>

Acknowledgements

We thank the organizers of the ICRSS for having an invited talk and covering the conference fees. We further acknowledge the HGF AI-CORE project, NSF Discovery Gateway project and ESA CCI+ Permafrost project for funding this work. This work is part of the "RTSInTrain" action group funded by the IPA.

Circum-Arctic distribution of topographic asymmetry

*S. Zwieback*¹

¹ Geophysical Institute, University of Alaska Fairbanks, Fairbanks, AK, 99775 USA

Abstract

For centuries, it has been noted that in some Arctic landscapes the steepness of hillslopes varies systematically with direction. The north-facing slopes are often steeper. They are also colder because they receive less sunlight. The warmer south-facing hillslopes are thought to be gentler because deeper thaw promotes soil transport. By studying topographic asymmetry, we can gain insights into the formation and fate of Arctic landscapes. However, we do not know how widespread such asymmetry is across the Arctic.

In this contribution, the circum-Arctic distribution of north–south asymmetric is estimated from the ArcticDEM. The maps of asymmetry add nuance to the notion that periglacial conditions promote steeper north-facing slopes. Across the Arctic landmass, only 20% of the area shows elevated north–south asymmetry. Elevated asymmetry predominantly occurs in rugged terrain. Across all moderate-relief landscapes, there is a bell-shaped trend with temperature. Steeper south-facing slopes are common in very cold (around -15° mean annual temperature) and cool (around 0°) regions. In between, steeper north-facing slopes predominate. Despite multiple caveats, the bell-shaped trend with temperature suggests controls that vary with climatic factors, including permafrost conditions.

The bell-shaped trend and observations of permafrost degradation further indicate that certain asymmetric transition-zone landscapes are predisposed to enhanced geomorphic activity in a warming climate. I will show examples of terrain instability and reorganization from the Taymyr Peninsula in the transition zone between very cold and cold temperatures, where a recent acceleration of thaw slumping is largely restricted to the steeper south-facing slopes. In the cold-to-cool transition zone, examples from the Alaskan Interior show (steeper) north-facing slopes undergoing increased erosion and mass wasting as previously frozen soil thaws. In summary, enhanced geomorphic activity in the transition zones suggests certain asymmetric landscapes are on the cusp of change, with attendant geohazards and ecological consequences.

Keywords Asymmetric valleys, topographic asymmetry, periglacial geomorphology

References

Bronhofer, M. (1957). Field investigations on Southampton Island and around Wagner Bay, Northwest territories. CanadaRand Corporation.

French, H. M. (1971). Slope asymmetry of the Beaufort Plain, northwest Banks Island, NWT, Canada. *Canadian Journal of Earth Sciences*, 8(7), 717– 731. <https://doi.org/10.1139/e71-070>

Hopkins, D., & Taber, B. (1962). Asymmetrical valleys in central Alaska (p. 116). Geological Society of America Special Paper.

Kennedy, B., & Melton, M. (1972). Valley asymmetry and slope forms of a permafrost area in the Northwest Territories, Canada. *Polar geomorphology*, 4, 107– 121.

Zwieback, S. (2021). Topographic asymmetry across the Arctic. *Geophysical Research Letters*, 48, e2021GL094895. <https://doi.org/10.1029/2021GL094895>

Acknowledgements: ArcticDEM DEMs provided by the Polar Geospatial Center under NSF-OPP awards 1043681, 1559691, and 1542736.

Session 2 (11:00-12:20): Observing Permafrost II

Permafrost thaw drives surface water drainage across the pan-Arctic

Elizabeth E. Webb^{1}, Anna K. Lijedahl², Jada A. Cordeiro³, Michael M. Lorant⁴, Chandi Witharana⁵, and Jeremy W. Lichstein³*

¹School of Natural Resources and Environment, University of Florida, Gainesville, FL, USA

²Woodwell Climate Research Center, Falmouth, MA, USA

³Department of Biology, University of Florida, Gainesville, FL, USA

⁴Colgate University, Hamilton, NY, USA

⁵Department of Natural Resources and the Environment, University of Connecticut, Storrs, CT, USA

Abstract

Lakes constitute 20-40% of Arctic lowlands, the largest area fraction occupied by water bodies in any terrestrial biome. These lakes provide crucial habitat for fish and migrating bird species, support human subsistence fisheries, and provide a source of water for remote Arctic communities. Recent evidence suggests that climate change could be shifting these dynamic systems across an ecological threshold, towards long-term landscape-scale wetting (lake formation) or drying (lake drainage). The net direction of and mechanisms underlying these shifts, however, are not well understood. Here we present evidence for large-scale drying across the pan-Arctic over the past 21 years (2000-2021), a trend that is correlated with increases in annual air temperature and fall rain. Given that increasing air temperatures and fall rain are known to promote permafrost thaw, our results suggest that permafrost thaw is leading to lake drainage and increasing surface water infiltration across the region.

Keywords: surface water, permafrost thaw

Acknowledgements: This work was supported by NASA FINESST Award 80NSSC19K134, and NSF awards 2051888, 2052107, 1927872, [1722572](#), and [1927723](#), OPP-170812, and OPP-1708322.

Change detection of permafrost-thaw triggered slope instabilities in coastal south-central Alaska using aerial lidar

Katreen Wikstrom Jones¹, Gabriel Wolken^{1,2}, Ronald Daanen¹, De Anne Stevens¹

¹Division of Geological & Geophysical Surveys, Alaska Department of Natural Resources, Fairbanks, Alaska

²Alaska Climate Adaptation Science Center, University of Alaska, Fairbanks, Alaska

Abstract Rapid changes in the cryosphere (e.g., permafrost degradation and glacier mass loss) are thought to be responsible for the increased frequency of mass movements in subarctic high-elevation areas. Fjords in south-central Alaska are geologically young and dynamic settings, where freeze-thaw cycles, heavy precipitation, and slope debutting due to retreating glaciers are common triggers of rockfalls, rock avalanches, and landslides. Beyond the hillslope hazard itself, landslide-generated tsunamis can threaten people and boat traffic, cause significant material and ecological damage, and are a concern for many coastal communities. At the Alaska Division of Geological & Geophysical Surveys (DGGS), we use field-based observations, remote sensing, and geospatial analysis to study changes in these dynamic landscapes.

Though slope failures frequently occur at remote locations all over Alaska and can remain undetected for years, we focus our efforts on sites where potential slope failures could have devastating effects on communities, resources, and infrastructure. As one of the partners in an interagency team studying landslide hazards in Prince William Sound, south-central Alaska, we participate in monitoring and research efforts at the deep-seated Barry Arm landslide, located 30 miles (50 kilometers) northeast of Whittier. Like other periglacial mass wasting events in Alaska, e.g., the catastrophic rock slope failure at Lamplugh Glacier in 2016 (Dufresne et al., 2019) and the tsunamigenic landslide in Taan Fjord in 2015 (Higman et al., 2018), we believe that thawing permafrost plays a critical role in destabilizing rock masses in alpine areas surrounding Barry Arm. Since our baseline campaign of June 26, 2020, which included both lidar acquisition from a fixed-wing platform and a UAS-based photogrammetric survey, we have conducted three airborne lidar acquisitions (including one near-peak snow height survey) to provide high accuracy (< 10 cm) terrain models of the landslide and the upper Barry Arm fjord. We use these high-resolution elevation datasets to map landslide structures and kinematic elements (Coe et al., 2021) to calculate material volume loss and gain (transport) on the slope surface. Based on elevation data acquired on October 16, 2020, we were able to estimate the height (50 m) and volume (over 600,00 m³) of an isolated rockfall that had released from the Barry Arm slide mass earlier in the month (fig. 1), generating a strong signal that was picked up by in-situ seismic sensors. The rockfall and other activity that we detected in the lidar data

agreed with larger-scale downslope movement that showed in interferometric radar data between October 9 and 24, 2020 (Schaefer et al., 2020). The need to collect extensive ground control points to calibrate the point cloud (commonly required for photogrammetrically derived products) can be reduced for these lidar acquisitions thanks to our system's integrated GPS unit and the internal consistency of the Inertial Measurement Unit. As ground access is both difficult and dangerous at Barry Arm landslide, the site is a good example of how aerial lidar is a useful method for producing high quality elevation data on an interannual and interseasonal basis.

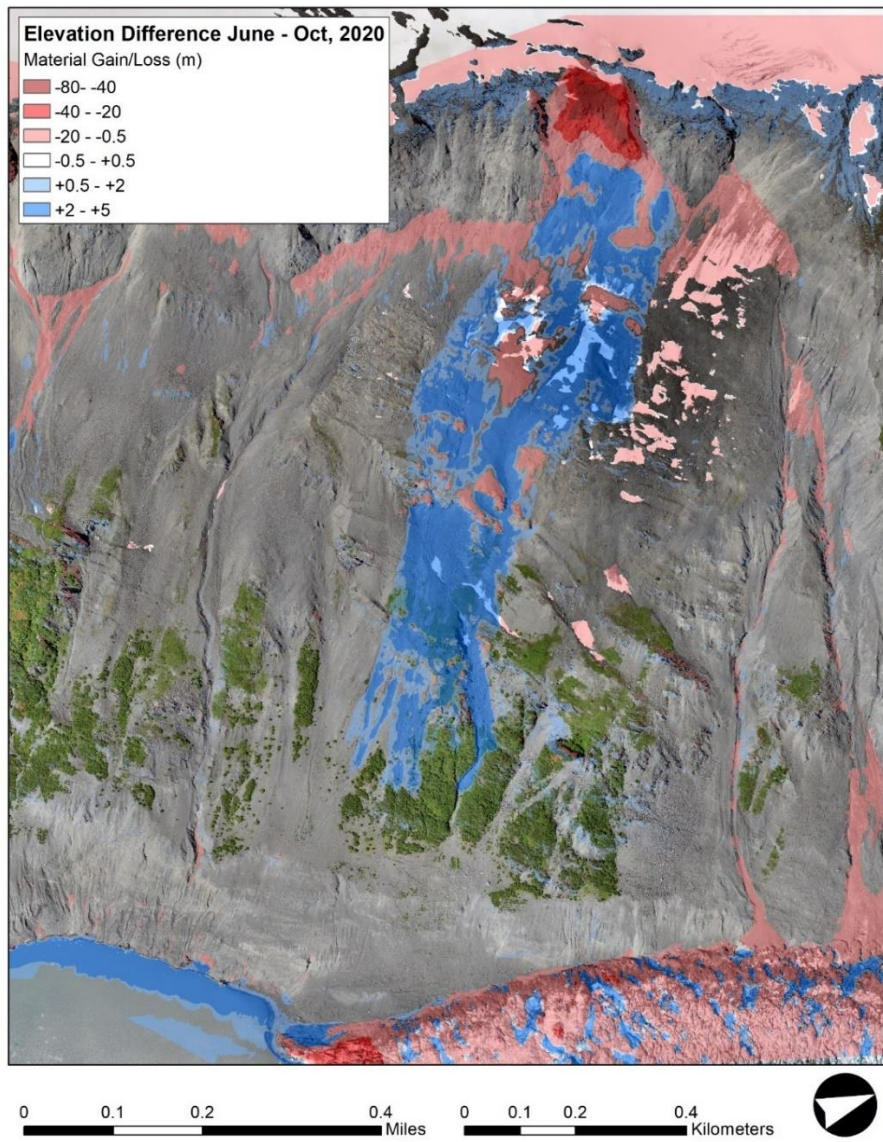


Figure 1. Material gain and loss on a section of Barry Arm landslide from 06/26/2020 to 10/16/2020 based on lidar-derived elevation data.

Keywords: Landslide, Rockfall, Slope Failure, Permafrost Thaw, Barry Arm

References

- Coe, J.A., Wolken, G.J., Daanen, R.P., and Schmitt, R.G., 2021, Map of landslide structures and kinematic elements at Barry Arm, Alaska in the summer of 2020: U.S. Geological Survey data release, <https://doi.org/10.5066/P9EUCGJQ>.
- Dufresne, A., Wolken, G., Hibert, C., Bessette-Kirton, E., Coe, J., Geertsema, M., and Ekström, G.. 2019, Emplacement dynamics of supraglacial rock avalanches: details from the 2016 Lamplugh event, Alaska, EGU General Assembly 2020, Online, 4–8 May 2020, EGU2020-391, <https://doi.org/10.5194/egusphere-egu2020-391>, 2019
- Higman, B., Shugar, D. H., Stark, C.P., Ekström, G., Koppes, M. N., Lynett, P., Dufresne, A., Haeussler, P. J., Geertsema, M., Gulick, S., Mattox, A., Venditti, J. G., Walton, M. A. L., McCall, N., Mckittrick, E., MacInnes, B., Bilderback, E. L., Tang, H., Willis, M. J., Richmond, B., Reece, R. S., Larsen, C., Olson, B., Capra, J., Ayca, A., Bloom, C., Williams, H., Bonno, D., Weiss, R., Keen, A., Skanavis, V., and Loso, M., 2018, The 2015 landslide and tsunami in Taan Fiord, Alaska, *Scientific Reports*, 2018, 8:12993, <https://doi.org/10.1038/s41598-018-30475-w>
- Schaefer, L.N., Coe, J.A., Godt, J.W., and Wolken, G.J., 2020, Interferometric synthetic aperture radar data from 2020 for landslides at Barry Arm Fjord, Alaska (ver. 1.4, November 2020): U.S. Geological Survey data release, <https://doi.org/10.5066/P9Z04LNKx>

Acknowledgement

We would like to thank our partners at U.S. Geological Survey (USGS), Alaska Earthquake Center, University of Alaska, and everyone else involved in the Prince William Sound Landslide Hazards group. Thank you to Clearwater Air, Alpine Air, Egli Air Haul, Lazy Otter Charters and Epic Charters for assisting our work at Barry Arm. We thank Alaska Climate Adaptation Science Center and USGS for funding our attendance at the ICRSS 2022.

Multiscale analysis of remotely sensed imagery to quantify spatial and temporal patterns of river bank erosion in floodplains with permafrost

J. Rowland¹, J. Schwenk¹, J. Muss², E. Shelef³, J. Stachelek¹, S. Stauffer¹, D. Ahrens⁴, M. Douglas⁵, A. Chadwick⁵, M. Lamb⁵, A. Piliouras⁶

¹ Earth and Environmental Science Division, Los Alamos National Lab, Los Alamos, NM.

²Commonwealth Computer Research, Inc., Charlottesville, VA.

³Department of Geology and Environmental Science, University of Pittsburgh, Pittsburgh, PA.

⁴University of California, Berkeley, CA.

⁵ Division of Geological and Planetary Sciences, California Institute of Technology, Pasadena, CA.

⁶Department of Geosciences, Pennsylvania State University, State College, PA.

Abstract

Bank erosion controls the rate at which rivers shift locations within their floodplains. The rates and patterns of this movement may directly impact communities by damaging built infrastructure. It also can impact water quality, fish habitat, and the navigability of rivers due to sediment input and changing river planforms. In addition to sediment, bank erosion also releases carbon, nutrients, and metals from floodplain deposits into rivers affecting carbon and biogeochemical cycling in rivers and coastal waters. In high latitude regions, permafrost is present within many river floodplains. The effect of permafrost on the rates and patterns of river bank erosion has not been systematically assessed to date. As such, how projected Arctic temperature and hydrological changes may alter the erosional dynamics of rivers remains highly speculative.

Here we present results of a study that coupled remotely-sensed change detection analysis of river with focused field investigations to examine the role of permafrost on controlling both the rates and patterns of river bank erosion. We measured bank erosion rates on over 5,500 km of channel along 14 sections of 13 Arctic and sub-Arctic rivers with permafrost extent ranging from isolated to continuous in order to quantify river bank erosion rates across the northern high latitudes. The analyzed rivers range in drainage area from 1,300 (Selawik) to 2.5×10^6 (Yenisei) km², and in width from 50 (Selawik) to 6,500 m (Lena). River planform morphologies vary from predominantly single-threaded meandering to multi-threaded braided and anastomosing. All river sections analyzed were bounded by alluvial floodplains. We produced a pixel-level resolution of bank erosion rates (> 1.6 million individual measurements) via analysis of remotely sensed aerial photographs, Landsat, and high-resolution satellite imagery. We also used focused analysis of high-resolution aerial photographs and satellite imagery to examine erosion rates along reaches of rivers where we collected data on permafrost extent, bank ice content, and monitored bank temperature changes during active erosion.

Our pan-arctic analysis shows that despite large spatial and temporal variations in erosion rates, high-latitude rivers have systematically lower erosion rates compared to temperate and tropical systems. Our combined remote-sensing and field observations indicate that even on small river systems with very episodic erosion, the magnitude of the infrequent but largest erosion events are constrained by the presence of frozen bank materials. Along a reach of the Koyukuk River, we found a decrease in bend-scale erosion rates with increasing ice content of the bank sediments. Across both large spatial and temporal scales, we find that a consistent result emerges from both the pan-Arctic and local analyses: permafrost appears to limit maximum riverbank erosion rates.

Keywords Change detection, permafrost, river bank erosion, satellite imagery

Acknowledgements This research was supported by a DOE Early Career Award to Joel Rowland. The Interdisciplinary Research for Arctic Coastal Environments (InterFACE) project funded by the Regional and Global Model Analysis program with in the Earth & Environmental Systems Sciences Division of the DOE Biological & Environmental Research Program. Additional support was provided by the Laboratory Directed Research and Development program at Los Alamos National Laboratory.

Permafrost vulnerability – deriving a vulnerability index from ESA CCI EO-datasets

A. Runge¹, B. Juhls¹, A. Bartsch², S. Westermann³ G. Grosse^{1,4}

¹Permafrost Research, Alfred Wegener Institute Helmholtz Centre for Polar and Marine Research, 14473 Potsdam, Germany

²b.geos GmbH, 2100 Korneuburg, Austria

³Department of Geosciences, University of Oslo, 0371 Oslo, Norway

⁴Institute of Geosciences, University of Potsdam, 14476 Potsdam, Germany

Abstract

Permafrost is a key indicator of global climate change and hence considered an Essential Climate Variable. Current studies show a warming trend of permafrost globally, which induces widespread permafrost thaw, leading to near-surface permafrost loss at local to regional scales and impacting ecosystems, hydrological systems, greenhouse gas emissions, and infrastructure stability. Permafrost thaw can unfold slowly from gradual top-down thawing and deepening of the active layer but also rapidly from abrupt thawing of ice-rich permafrost, involving processes such as thermokarst formation, lake drainage, retrogressive thaw slumps and coastal erosion. Many of these processes impact landscapes irreversibly, while posing a particular threat to infrastructure and livelihoods of people in the Arctic.

Permafrost is defined as the thermal state of the subsurface, hence Earth Observation methods have limitations in assessing permafrost directly. However, the state of the subsurface is strongly connected to surface conditions and influenced by changes in the atmosphere, biosphere, geosphere, and cryosphere. Therefore, examining changes in the surface state will help identify local to regional trends and impacts on the thermal state of permafrost. Hence, the aim of this study in progress is to investigate changes in the surface state by assessing potential positive and negative trends in variables impacting permafrost and thus identifying areas that are vulnerable to permafrost thaw by developing a permafrost vulnerability framework using a comparative index.

EO-based datasets provide relevant variables impacting the surface state and obtain trends and changes from homogenised long-term datasets. These globally available datasets include land surface temperature, land cover, snow cover, fire, albedo, soil moisture, and information on the freeze/thaw state, which are ECVs too. Furthermore, a modelled permafrost_cci product is available from the ESA CCI+ Permafrost project, which reveals changes and trends in ground temperature and active layer thickness for the last two decades and serves as link between modelled and EO-based permafrost thaw assessments. So far, a combined assessment of all these permafrost-relevant products to better understand, quantify, and project permafrost thaw and its potential trajectories is still missing.

We conducted spatiotemporal variability and decadal trend analyses of all the individual ECVs for the panarctic permafrost region and identified statistically significant positive and negative feedbacks. The first individual results show interesting spatially different trends in the panarctic, for example that the snow water equivalent increased in eastern Yakutia and Chukotka in Russia and in the same time period decreased in most parts of Alaska. In a next step, we will combine the positive and negative feedbacks in a vulnerability framework, reflecting the impact they pose on permafrost. This will help to identify prevailing regional trends in the surface state not only from individual variables but their coupled feedback on the thermal state of the permafrost. Our EO-based assessment of permafrost vulnerability uses existing and available datasets to further improve our understanding on permafrost thaw in the near future. It will build a foundation for a wide range of studies focusing on permafrost-thaw and its impacts, such as hydrological change, infrastructure stability, ecosystem change, or greenhouse gas emissions.

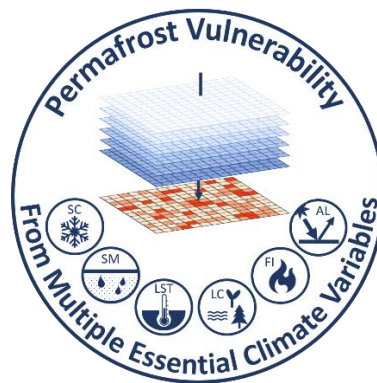


Figure 1. Permafrost vulnerability from multiple essential climate variables project logo indicating the variables assessed for permafrost vulnerability.

Keywords: spatiotemporal trends, vulnerability index, time series analysis

References

- Grosse, G., Romanovsky, V. E., Jorgenson, T., Walter Anthony, K., Brown, J., & Overduin, P. P. (2011). Vulnerability and Feedbacks of Permafrost to Climate Change. *Eos, Transactions American Geophysical Union*, 92(9), 73–80. <https://doi.org/10.1002/ppp.689>.
- Jorgenson, M. T., Romanovsky, V., Harden, J., Shur, Y., Donnell, J. O., Schuur, E. A. G., Kanevskiy, M., & Marchenko, S. (2010). Resilience and vulnerability of permafrost to climate change. *Canadian Journal of Forest Research*, 40(7).
- Park, H., Kim, Y., & Kimball, J. S. (2016). Widespread permafrost vulnerability and soil active layer increases over the high northern latitudes inferred from satellite remote sensing and process model assessments. *Remote Sensing of Environment*, 175, 349–358. <https://doi.org/10.1016/j.rse.2015.12.046>
- Trofaier, A. M., Westermann, S., & Bartsch, A. (2017). Progress in space-borne studies of permafrost for climate science: Towards a multi-ECV approach. *Remote Sensing of*

Environment, 203, 55–70. <https://doi.org/10.1016/j.rse.2017.05.021>

Acknowledgements

I would like to thank the Potsdam Graduate School of the University of Potsdam (Germany) for contributing financially to the travel expenses.

Session 3: Observing Permafrost III

Mapping drained lake basins on a circumpolar scale

Helena Bergstedt¹, Benjamin M. Jones², Guido Grosse³, Alexandra Veremeeva⁴, Amy Breen⁵, Anna Liljedahl⁶, Annett Bartsch¹, Benjamin Gaglioti², Frédéric Bouchard⁷, Gustaf Hugelius⁸, Ingmar Nitze³, Juliane Wolter^{3,13}, Kenneth Hinkel⁹, Louise Farquharson¹⁰, Matthias Fuchs³, Mikhail Kanevskyi², Pascale Roy-Leveille¹¹, and Trevor Lantz¹²

¹bgeos, Korneuburg, Austria (helena.bergstedt@bgeos.com)

²Institute of Northern Engineering, University of Alaska Fairbanks

³Permafrost Research Section, Alfred Wegener Institute for Polar and Marine Research Potsdam

⁴Laboratory of Soil Cryology, Institute of Physicochemical and Biological Problems in Soil Science, Russian Academy of Sciences

⁵International Arctic Research Center, University of Alaska Fairbanks

⁶Woodwell Climate Research Centre

⁷Géosciences Paris Sud (GEOPS), Université Paris Saclay, France

⁸Department of Physical Geography, Stockholm University

⁹Michigan Technological University

¹⁰Geophysical Institute Permafrost Laboratory University of Alaska Fairbanks

¹¹Department of Geography, Université Laval

¹²University of Victoria

¹³Institute of Biochemistry and Biology, University of Potsdam

Abstract

Lakes and drained lake basins (DLB) are ubiquitous landforms in permafrost lowland regions. The long-term dynamics of lake formation and drainage is evident in the abundance of DLBs covering 50% to 75% of permafrost lowlands in parts of Alaska, Siberia, and Canada. Over time as the DLBs age, ground ice enrichment occurs, the surface heaves and soils and vegetation communities evolve. DLBs of different age are exhibiting spectral and texture patterns indicative of these changing conditions that can be observed with remote sensing techniques. The mosaic of vegetative and geomorphic succession and the distinct differences between DLBs and surrounding areas can be discriminated and used to derive a landscape-scale classification employing various indices derived from multispectral remote sensing imagery that, when combined with field sampling and peat initiation timing, can be used to scale across spatial and temporal domains. Previously published local and regional studies have demonstrated the importance of DLBs regarding carbon storage, greenhouse gas and nutrient fluxes, hydrology, geomorphology, and habitat availability. A coordinated pan-Arctic scale effort is needed to better understand the importance of DLBs in circumpolar permafrost-regions.

Here we present an update of ongoing work within the International Permafrost Association (IPA) Action Group on DLBs, an effort by the science community that includes developing a first pan-Arctic drained lake basin data product. A prototype of this data product covering the North Slope of Alaska published in Bergstedt et al. (2021) demonstrated the methodological basis of this large-scale mapping effort. The methodology developed here is a novel and scalable remote sensing-based approach to identifying DLBs in lowland permafrost regions. Our approach uses Landsat-8 multispectral imagery and high-resolution topographic information to derive a pixel-by-pixel statistical assessment of likelihood of DLB occurrence in sub-regions with different permafrost and periglacial landscape conditions, as well as to quantify aerial coverage of DLBs.

We present first results of a DLB dataset covering pan-Arctic permafrost lowlands. Utilizing remote sensing imagery (Landsat-8) and freely available DEM data sets (e.g., ArcticDEM, Copernicus DEM) allows us to implement our mapping approach on a circumpolar scale. Comprehensive mapping of DLBs areas across the circumpolar permafrost landscape will allow for future utilization of these data in pan-Arctic models and greatly enhance our understanding of DLBs in the context of permafrost landscapes. Better resolution of the spatial distribution of DLBs in lowland permafrost regions will improve quantitative studies on landscape diversity, wildlife habitat, permafrost, hydrology, geotechnical conditions, and high-latitude carbon cycling.

Keywords

Permafrost, DLB, Lakes

References

Bergstedt, H.; Jones, B.M.; Hinkel, K.; Farquharson, L.; Gaglioti, B.V.; Parsekian, A.D.; Kanevskiy, M.; Ohara, N.; Breen, A.L.; Rangel, R.C.; Grosse, G.; Nitze, I. Remote Sensing-Based Statistical Approach for Defining Drained Lake Basins in a Continuous Permafrost Region, North Slope of Alaska. *Remote Sens.* **2021**, *13*, 2539. <https://doi.org/10.3390/rs13132539>

Acknowledgements

This research was funded by the US National Science Foundation under grant numbers OPP-1806213, 1806287, and 1806202. Further support was received by European Research Council project No. 951288 (Q-Arctic) and the European Union's Horizon 2020 Research and Innovation Programme under Grant Agreement No. 869471 (CHARTER). This work is part of the Action Group 'Development of a pan-Arctic drained lake basin product' funded by the International Permafrost Association (IPA).

The spatio-temporal variability of frost blisters in a perennial frozen lake along the Antarctic coast as indicator of the groundwater supply

Stefano Ponti¹, Riccardo Scipinotti², Samuele Pierattini³, Mauro Guglielmin¹

¹Department of Theoretical and Applied Sciences, Insubria University, 21100 Varese, Italy

²Technical Antarctic Unit, Energy and Sustainable Economic Development, National Agency for New Technologies, 40129 Bologna, Italy

³Computer Systems and ICT Development, National Agency for New Technologies, Energy and Sustainable Economic Development, 50019 Sesto Fiorentino, Italy

Abstract

Remote sensing, and unmanned aerial vehicles (UAVs) in particular, can be a valid tool for assessing the dynamics of cryotic features and to monitor the deriving surface changes. As an example, frost blisters and the sublimation rates on perennially frozen lakes can affect the topography of polar areas that host important ecosystems. In this paper, through the use of remote sensing techniques, we aim to understand the type of groundwater supply of an Antarctic perennially frozen lake that encompasses two frost blisters (M1 and M2) through the temporal analysis of the features' elevation changes (frost blisters and lake ice level). The perennially frozen lake is located at Boulder Clay (Northern Victoria Land, Antarctica), close to the Italian Antarctic Station "Mario Zucchelli". We relied on several photogrammetric 3D models, past satellite images and ground-based images to assess the surface changes through differencing of digital elevation models, areal variations and pixel counting. In addition, in situ measurements of the ice sublimation or snow accumulation were carried out according to previous experiments (Guglielmin et al., 2009). The two frost blisters showed different elevation trends with M1 higher in the past (1996–2004) than recently (2014–2019), while M2 showed an opposite trend, similarly to the ice level. Indeed, the linear regression between M2 elevation changes and the ice level variation was statistically significant, as well as with the annual thawing degree days, while M1 did not show significant results. From these findings we can infer that the groundwater supply of M1 can be related to a sublake open talik (hydraulic system) (Dugan et al., 2013; Wellman et al., 2013) as confirmed also by pressurized brines found below M1, during a drilling in summer 2019. For M2 the groundwater flow is still not completely clear although the hydrostatic system seems the easiest explanation (French and Guglielmin, 2000) as well as for the uplift of the lake ice.

Keywords: frost mounds; frozen lakes; structure from motion

References:

Dugan, H.A.; Obryk, M.K.; Doran, P.T. Lake ice ablation rates from permanently ice-covered Antarctic lakes. *J. Glaciol.* 2013, *59*, doi:10.3189/2013JoG12J080

French, H.M.; Guglielmin, M. Frozen ground phenomena in the vicinity of the Terra Nova bay, Northern Victoria land, Antarctica: A preliminary report. *Geogr. Ann. Ser. A Phys. Geogr.* 2000, *82*, doi:10.1111/j.0435-3676.2000.00138.x

Guglielmin, M.; Lewkowicz, A.G.; French, H.M.; Strini, A. Lake-ice blisters, terra nova bay area, Northern Victoria Land, Antarctica. *Geogr. Ann. Ser. A Phys. Geogr.* 2009, *91*, doi:10.1111/j.1468-0459.2009.00357.x

Wellman, T.P.; Voss, C.I.; Walvoord, M.A. Impacts of climate, lake size, and supra- and sub-permafrost groundwater flow on lake-talik evolution, Yukon Flats, Alaska (USA). *Hydrogeol. J.* 2013, *21*, doi:10.1007/s10040-012-0941-4

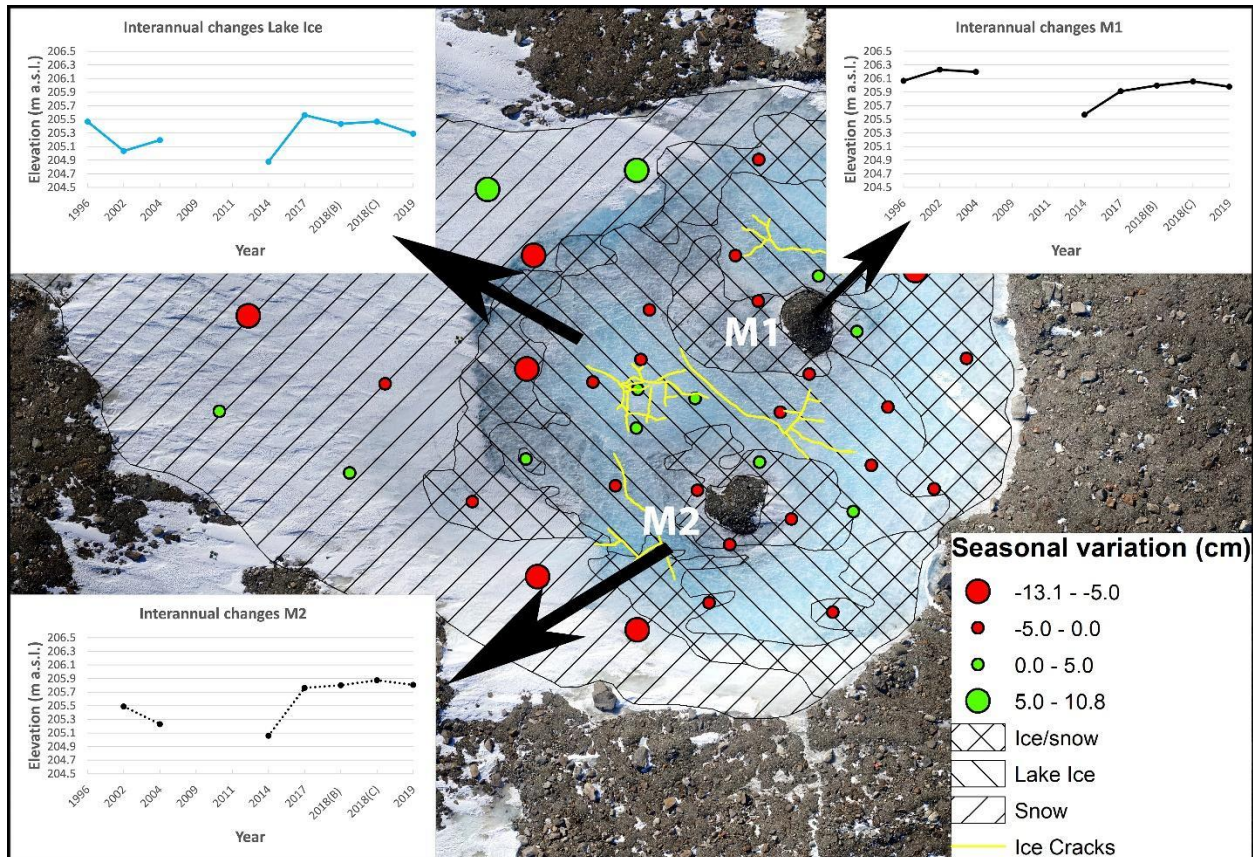


Figure 1. Temporal variation of the perennially frozen lake's features: multi-temporal variation of the lake ice and the inter-annual variation of the frost blisters (M1 and M2).

Acknowledgements: We want to thank the ENEA logistical support in the frame of PNRA and in particular the Projects "PNRA 2013/AZ1.05 "Permafrost ecology in Victoria Land"; 274 PNRA16_00194-A1 "Climate Change and Permafrost Ecosystems in Continental Antarctica"; 275 PNRA18_00186-E" Interactions between permafrost and ecosystems in Continental Antarctica that allowed this research.

Mapping retrogressive thaw slumps in High Arctic Canada using high-spatial resolution satellite imagery and deep learning

Mahendara R. Udawalpola¹, Chandi Witharana¹, Amit Hasan^{1}, Anna Liljedahl², Melissa Ward-Jones³, Benjamin Jones³*

¹Department of Natural Resources and Environment, University of Connecticut, Connecticut, USA

² Woodwell Climate Research Center, Falmouth, MA, USA

³ University of Alaska Fairbanks, AK, USA

*presenter

Abstract

The accelerated warming conditions of the high Arctic have intensified the extensive thawing of permafrost. Retrogressive thaw slumps (RTSs) are considered as the most active landforms in the Arctic permafrost. An increase in RTSs has been observed in the Arctic in recent decades. Continuous monitoring of RTSs is important to understand climate change-driven disturbances in the region. Manual detection of these features is extremely difficult as they occur over exceptionally large areas. Only very few studies have explored the utility of very-high spatial resolution (VHSR) commercial satellite imagery in the automated mapping of RTSs. We have developed a deep learning (DL) convolution neural net (CNN) based workflow to automatically detect RTSs from VHSR satellite imagery acquired over the Canadian High Arctic. This study systematically compared the performance of different DL-CNN model architectures and varying backbones. Our candidate CNN models include: DeepLabV3+, UNet, UNet++, Multi-scale Attention Net (MA-Net), and Pyramid Attention Network (PAN) with ResNet50, ResNet101 and ResNet152 backbones. The RTS modelling experiment was conducted in Banks Island and Ellesmere Island in Canada. The UNet++ model demonstrated the highest accuracy (F1 score 87%) with the ResNet101 backbone at the expense of training and inferencing time. PAN, DeepLabV3, MaNet and UNet, models reported mediocre F1 scores of 72%, 75%, 80%, and 81% respectively. Our findings unravel the performances of different DL-CNNs in imagery-enabled RTS mapping and provide useful insights on operationalizing the mapping application over large areas.

Keywords Deep Learning, Remote Sensing, Retrogressive thaw slumps

Acknowledgements

This research was supported by the US National Science Foundation grants 1720875, 1722572, 1927872, 1927723, and 1927729. Supercomputing resources were provided by the Extreme Science and Engineering Discovery Environment (award DPP 190001) and Texas Advanced Computing Center (award DPP20001). The authors would like to thank the Polar Geospatial Center at the University of Minnesota for imagery support.

An approach to inventorying retrogressive thaw slumps on a continental scale

Lingcao Huang¹, Guiye Li², Michael Willis³, Kevin Schaefer⁴, Guofeng Cao², Kristy Tiampo³

¹Earth Science and Observation Center, Cooperative Institute for Research in Environmental Sciences (CIRES), University of Colorado Boulder, Boulder, CO, USA

²Department of Geography, University of Colorado Boulder, Boulder, CO, USA

³Geological Sciences and CIRES, University of Colorado Boulder, Boulder, CO, USA

³National Snow and Ice Data Center, CIRES, University of Colorado Boulder, Boulder, CO, USA

Abstract

Ongoing permafrost warming results in shrinking in permafrost areas, an increase in thaw depth, and abrupt thaw. A retrogressive thaw slump (RTS) is a type of abrupt permafrost thaw that has been reported in many local areas in the Arctic. RTS consists of an ice-rich exposure or headwall that advances toward uphill during each thawing season. RTS also removes materials frozen in permafrost and further affects the local and global environment. However, the spatial distribution and thawing rate of RTS in many permafrost regions are still unknown due to the challenges in mapping their location and extent.

We propose an approach by integrating an automated data processing system for high-resolution satellite data, deep learning algorithms, and a web-based validation system, aiming to overcome the mapping challenges and provide RTS inventories on a continental scale, even pan-Arctic. The automated system divides a large area into many grids (20 km by 20 km), processes ArcticDEM at a 2-m resolution grid by grid using workstations and a supercomputer, and produces composited images showing RTS-related features including regions of terrain reduction and annual headwall lines on hillshades. We use YOLOv4, a super-efficient object detection algorithm based on convolutional neural networks, to locate RTS from the composited images. The web-based, crowd-sourcing system integrates Google Maps (www.google.com/maps), Wayback imagery (livingatlas.arcgis.com/wayback), and a form showing RTS possibility into one interactive interface, allowing users to validate the automated mapping results and facilitating the mapping pipeline.

We applied this approach to Alaska as a case study. With one TB of ArcticDEM, we identified around 100 RTSs. We found that (1) relocating ArcticDEM from Polar Geospatial Center was time-consuming and processing time on the super-computers varied due to job loads on the shared computing resource; (2) many false positives were output by YOLOv4 on the composited images and many of them were likely over ponding or lake regions, although no accurate maps of surface water were available; (3) artifacts on ArcticDEM also contributed to false positives; and (4) the web-based system facilitated manual validation but needed to be improved for large numbers of concurrent users.

Keywords

Permafrost, deep learning, automated mapping.

References

Huang, L.; Liu, L.; Jiang, L.; Zhang, T. Automatic Mapping of Thermokarst Landforms From Remote Sensing Images Using Deep Learning: A Case Study in the Northeastern Tibetan Plateau. *Remote Sensing* 2018, 10, 2067.

Huang, L., Luo, J., Lin, Z., Niu, F. and Liu, L., 2020. Using deep learning to map retrogressive thaw slumps in the Beiluhe region (Tibetan Plateau) from CubeSat images. *Remote Sensing of Environment*, 237, p.111534.

Porter, C.; Morin, P.; Howat, I.; Noh, M.J.; Bates, B.; Peterman, K.; Keeseey, S.; Schlenk, M.; Gardiner, J.; Tomko, K.; et al. *ArcticDEM* 569 2018. Accessed on December 15, 2021, doi:10.7910/DVN/OHHUKH.

Bochkovskiy, Alexey, Chien-Yao Wang, and Hong-Yuan Mark Liao. "Yolov4: Optimal speed and accuracy of object detection." *arXiv preprint arXiv:2004.10934* (2020).

Acknowledgements

Lingcao Huang was supported by the CIRES Visiting Fellows Program and the NOAA Cooperative Agreement with CIRES, NA17OAR4320101. This work utilized resources from the University of Colorado Boulder Research Computing Group, which is supported by the National Science Foundation (awards ACI-1532235 and ACI-1532236), the University of Colorado Boulder, and Colorado State University.

Session 4 : Floating Ice

Sea ice from the ground up using distributed acoustic sensing

Robert E. Abbott¹, Michael G. Baker¹, Leiph Preston¹, Madison M. Smith, Jim Thomson²

¹Geophysics Department, Sandia National Laboratories, Albuquerque, New Mexico, USA

²Applied Physics Laboratory, University of Washington, Seattle, Washington, USA

Abstract

We present results from an ongoing multiyear effort to acquire Distributed Acoustic Sensing (DAS) data on a submarine telecommunications optical fiber in the Beaufort Sea. The approximately 38-km long fiber section we interrogated leaves land at Oliktok Point, Alaska, and extends northward into the Beaufort Sea. We have completed five of eight planned week-long dataset acquisitions. The timing of these datasets centers around informal sea ice “seasons” (i.e., ice bound, ice free, ice formation, and ice breakup). A wide range of interesting sea-ice phenomena have been observed. These include, but are not limited to, icequakes, ice grounding events, ice flexural gravity waves, and rapid freezing events. During periods of partial sea ice coverage, the geographical boundary of ice vs. open water is readily apparent in the data in both the time domain and frequency domain. The ice/water boundary derived from DAS measurements may be at odds with the boundary derived from other measurement techniques such as satellite imagery and synthetic aperture radar. This is most likely due to DAS measuring some aspect of ice material properties (e.g., thickness, rigidity, and interconnectivity), while other methods rely on properties such as albedo and surface roughness. We will also show that DAS measurements are promising for reproducing ocean-wave parameters traditionally measured by buoys or seafloor moorings. Significant wave height and peak wave period track well with results from a regional wave model and a nearly co-incident buoy deployment, suggesting a transfer function between sea floor strain-rate and surface wave signal is within reach. These preliminary results suggest seafloor cables may provide unprecedented temporal and spatial (2 m) resolution of geophysical parameters that are typically difficult to measure in polar regions.

Keywords

Distributed Acoustic Sensing, Sea Ice, Beaufort Sea

References

Baker, M.G., and R.E. Abbott, 2021, Distributed Acoustic Sensing of Seasonal Wavefields in the Coastal Polar Waters of the Beaufort Sea, Alaska, *FastTIMES*, Vol 23,3
Icequakes and Rogue Waves: Geoscientists and Musicians Interpret the Sounds of the Sea, 2021, *Physics World Weekly Podcast*, <https://physicsworld.com/a/icequakes-and-rogue-waves-geoscientists-capture-the-sounds-of-the-sea/>

Acknowledgements

This work was supported by the Laboratory Directed Research and Development program at Sandia National Laboratories, a multimission laboratory managed and operated by National Technology and Engineering Solutions of Sandia LLC, a wholly owned subsidiary of Honeywell International Inc. for the U.S. Department of Energy's National Nuclear Security Administration under contract DE-NA0003525. We thank our partners at Quintillion, LLC, and Silixa, LLC for their contributions.

Physiographic controls on landfast ice variability from 20 years of maximum extents across the Northwest Canadian Arctic

*Eleanor E. Wratten*¹, *Sarah W. Cooley*², *Paul J. Mann*³, *Dustin Whalen*⁴, *Paul Fraser*⁵ and *Michael Lim*^{6*}

^{1*} Department of Geography and Environmental Sciences, Northumbria University

² Department of Geography, University of Oregon

³ Department of Geography and Environmental Sciences, Northumbria University

⁴ Geological Survey of Canada (Atlantic), Natural Resources Canada

⁵ Geological Survey of Canada (Atlantic), Natural Resources Canada

^{6*} Department of Mechanical and Construction Engineering, Northumbria University

Abstract

Landfast ice is a defining feature among Arctic coasts, providing a critical transport route for communities and exerting control over the exposure of Arctic coasts to marine erosion processes. Despite its significance, there remains a paucity of data on the spatial variability of landfast ice and limited understanding of the environmental processes controlling its variability. We pre-sent a new high spatiotemporal record (2000 - 2019) across the Northwest Canadian Arctic using MODIS Terra satellite imagery to determine maximum landfast ice extent (MLIE) at the start of each melt season.

Average MLIE across the Northwest Canadian Arctic declined by 73% in a direct comparison between the first and last year of the study period, but this was highly variable across regional to community scales, ranging from 14% around North Banks Island to 81% in the Amundsen Gulf. The variability was largely a reflection of 5 – 8 year cycles between landfast ice rich and poor periods with no discernible trend in MLIE. Interannual variability over the 20 year record of MLIE extent was more constrained across open, relatively uniform and shallower sloping coastlines such as West Banks Island, in contrast with a more varied pattern across the numerous bays, headlands and straits enclosed within the deep Amundsen Gulf. Comparing MLIE change across regional sites in relation to static (topography and bathymetry) and dynamic (storm duration, mean air temperature, freezing and thawing degree day occurrence) controls, we found an observable static control but no clear dynamic control that could explain MLIE variability. For example, despite an exponential increase in storm duration from 2014 - 2019 (from 30 hrs to 140 hrs or a 350% increase) across the Mackenzie Delta, MLIE extents remained relatively consistent. Mean air temperatures, freezing and thawing degree day occurrences (over 1, 3 and 12-month periods) also reflected progressive northwards warming influences over the last two decades, but none showed a statistically significant relationship with MLIE interannual variability.

These results indicate inferences of landfast ice variations commonly taken from wider sea ice trends may misrepresent more complex and variable sensitivity to process controls. The influences of different physiographic coastal settings need to be considered at process level scales to adequately account for community impacts and decision making or coastal erosion exposure.

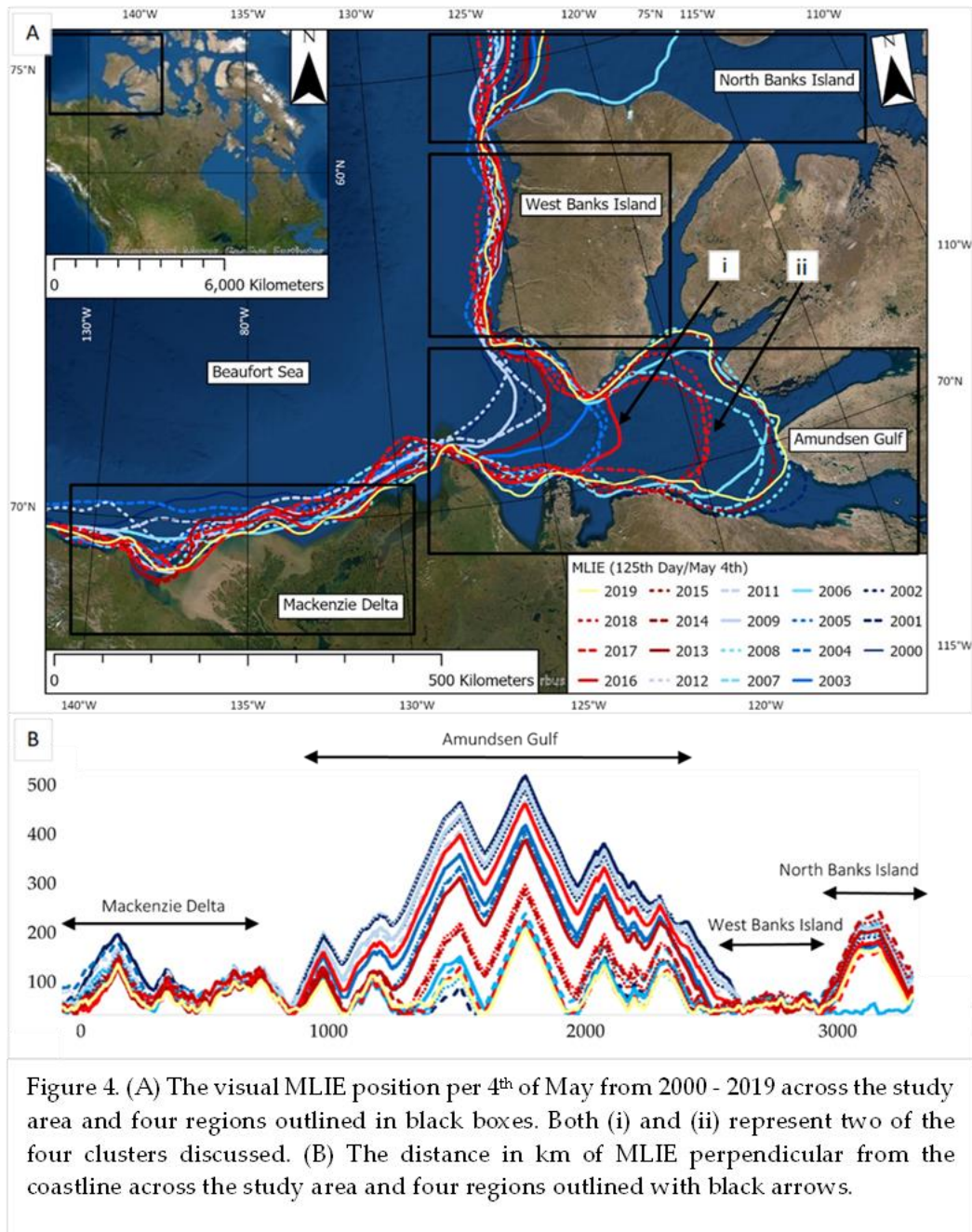


Figure 4. (A) The visual MLIE position per 4th of May from 2000 - 2019 across the study area and four regions outlined in black boxes. Both (i) and (ii) represent two of the four clusters discussed. (B) The distance in km of MLIE perpendicular from the coastline across the study area and four regions outlined with black arrows.

Keywords: Landfast Ice Extent; Scale; Topographic Setting

References

Li, Z.; Zhao, J.; Su, J.; Li, C.; Cheng, B.; Hui, F.; Yang, Q.; Shi, L. Spatial and Temporal Variations in the Extent and Thickness of Arctic Landfast Ice. *Remote Sens.* 2020, Vol. 12, Page 64 2020, 12, 64, doi:10.3390/RS12010064.

Mahoney, A.R.; Eicken, H.; Gaylord, A.G.; Gens, R. Landfast sea ice extent in the Chukchi and Beaufort Seas: The annual cycle and decadal variability. *Cold Reg. Sci. Technol.* 2014, 103, 41–56, doi:10.1016/J.COLDREGIONS.2014.03.003.

Cooley, S.W.; Ryan, J.C.; Smith, L.C.; Horvat, C.; Pearson, B.; Dale, B.; Lynch, A.H. Coldest Canadian Arctic communities face greatest reductions in shorefast sea ice. *Nat. Clim. Chang.* 2020 106 2020, 10, 533–538, doi:10.1038/s41558-020-0757-5.

Lim, M.; Whalen, D.; Martin, J.; Mann, P.J.; Hayes, S.; Fraser, P.; Berry, H.B.; Ouellette, D. Massive Ice Control on Permafrost Coast Erosion and Sensitivity. *Geophys. Res. Lett.* 2020, 47, e2020GL087917, doi:10.1029/2020GL087917.

Divine, L.M.; Pearce, T.; Ford, J.; Solovyev, B.; Galappaththi, E.K.; Bluhm, B.; Kaiser, B.A. Protecting the future Arctic. *One Earth* 2021, 4, 1649–1651, doi:10.1016/j.oneear.2021.11.021.

Acknowledgements: We gratefully acknowledge the NERC UK-Canada Bursary funding scheme and the NERC ONE Planet project (OP20241) that funded this research. S.C. gratefully acknowledges funding from NSF Navigating the New Arctic (NNA) grant #1836573 managed by R. Delgado.

The work is currently under review with Remote Sensing Journal Special Issue of Sea Ice and Icebergs

A neural network-based method for satellite mapping of sediment-laden sea ice in the Arctic

Hisatomo Waga^{1,2}, Hajo Eicken¹, Bonnie Light³, Yasushi Fukamachi²

¹International Arctic Research Center, University of Alaska Fairbanks, Fairbanks, Alaska, USA

²Arctic Research Center, Hokkaido University, Sapporo, Hokkaido, Japan

³Applied Physics Laboratory, University of Washington, Seattle, Washington, USA

Abstract

Sediment-laden sea ice is a ubiquitous phenomenon in the Arctic Ocean and its marginal seas (Tucker et al., 1999). This study presents a satellite-based approach at quantifying the distribution of sediment-laden ice that allows for more extensive observations in both time and space to monitor spatiotemporal variations in sediment-laden ice. A structural-optical model coupled with a four-stream multilayer discrete ordinates method radiative transfer model was used to examine surface spectral albedo for four surface types (Light et al., 1998): clean ice, sediment-laden ice with 15 different sediment loadings from 25 to 1000 g m⁻³, ponded ice, and ice-free open water.

Based on the fact that the spectral characteristics of sediment-laden ice differ from those other surface types, fractions of sediment-laden ice were estimated from the remotely-sensed surface reflectance by a spectral unmixing algorithm using a least square method (Tschudi et al., 2008). Sensitivity analyses demonstrated that a combination of sediment loads of 50 and 500 g m⁻³ effectively represents the areal fraction of sediment-laden ice with a wide range of sediment loads. The estimated fractions of each surface type and corresponding remotely-sensed surface reflectances were used to train an artificial neural network to speed up processing relative to the least squares method (Rösel et al., 2012). Comparing the fractions of sediment-laden ice derived from these two approaches yielded good agreements for areal fractions of sediment-laden ice, highlighting the superior performance of the neural network for processing large datasets.

Although our approach contains potential uncertainties associated with methodological limitations, spatiotemporal variations in sediment-laden ice exhibited reasonable agreement with spatial patterns and seasonal variations reported in the literature on in situ observations of sediment-laden ice. Systematic satellite-based monitoring of sediment-laden ice distribution can provide extensive, sustained, and cost-effective observations to foster our understanding of the role of sediment-laden ice in a wide variety of research fields including sediment transport

and biogeochemical cycling. This study was published recently in *Remote Sensing of Environment* (Waga et al., 2022).

Keywords

Sediment-laden sea ice; Spectral unmixing algorithm; Artificial neural network

References

- Light, B., Eicken, H., Maykut, G.A., Grenfell, T.C., 1998. The effect of included particulates on the spectral albedo of sea ice. *J Geophys Res Oceans* 103, 27739–27752. <https://doi.org/10.1029/98jc02587>
- Rösel, A., Kaleschke, L., Birnbaum, G., 2012. Melt ponds on Arctic sea ice determined from MODIS satellite data using an artificial neural network. *The Cryosphere* 6, 431–446. <https://doi.org/10.5194/tc-6-431-2012>
- Tschudi, M.A., Maslanik, J.A., Perovich, D.K., 2008. Derivation of melt pond coverage on Arctic sea ice using MODIS observations. *Remote Sensing of Environment* 112, 2605–2614. <https://doi.org/10.1016/j.rse.2007.12.009>
- Tucker, W.B., Gow, A.J., Meese, D.A., Bosworth, H.W., Reimnitz, E., 1999. Physical characteristics of summer sea ice across the Arctic Ocean. *J Geophys Res Oceans* 104, 1489–1504. <https://doi.org/10.1029/98jc02607>
- Waga, H., Eicken, H., Light, B., Fukamachi, Y., 2022. A neural network-based method for satellite-based mapping of sediment-laden sea ice in the Arctic. *Remote Sens Environ* 270, 112861. <https://doi.org/10.1016/j.rse.2021.112861>

Acknowledgements

This work was supported by the Ministry of Education, Culture, Sports, Science, and Technology of Japan (MEXT), and the Grant-in-Aids for JSPS Overseas Research Fellowships, Early-Career Scientists 21K14894, and Scientific Research (B) 19H01961. This work was also supported by the Arctic Challenges for Sustainability (ArCS) Program for Overseas Visit by Young Researchers. This research was partly funded by the Interdisciplinary Research for Arctic Coastal Environments (InterFACE) project through the U.S. Department of Energy, Office of Science, Biological and Environmental Research RGMA program. We gratefully acknowledge support from NSF Office of Polar Programs grant OPP-1724467.

Identifying spatial patterns of river ice formation and hazardous open water zones with Synthetic Aperture Radar (SAR)

Dana Brown¹, Chris Arp², Allen Bondurant², Todd Brinkman³, Barbara Cellarius⁴, Melanie Engram², Mark Miller⁴, Cristina Ornelas², Carol Simmons⁵, Katie Spellman¹, Lindsay Sturm⁵

¹International Arctic Research Center, University of Alaska Fairbanks, USA

²Water and Environmental Research Center, University of Alaska Fairbanks, USA

³Institute of Arctic Biology and Department of Biology and Wildlife, University of Alaska Fairbanks, USA

⁴Wrangell-St. Elias National Park and Preserve, Copper Center, Alaska, USA

⁵McGrath School, McGrath, Alaska, USA

Abstract

River ice is an important component of the arctic environment that is sensitive to climate change. People living at high-latitudes use ice-covered rivers for inter-village travel, access to subsistence resources, and recreation. In remote villages off of the road system, rivers serve as the primary travel corridors. Climate-driven changes in ice regimes such as shorter winters, thinner ice, and persistent open water present new challenges and safety hazards to river users. Here, we aim to help improve public safety and better understand the dynamics of dangerous ice conditions in Alaskan rivers with satellite remote sensing and community science. We monitor and map seasonal ice cover expansion and open water leads throughout winter with Sentinel-1 Synthetic Aperture Radar (SAR), and validate and contextualize our remote sensing products with the help of georeferenced photo observations from citizen scientists and a network of fixed cameras. We use support vector machine (SVM) algorithms for image classification of VV and VH bands implemented within Google Earth Engine's cloud-computing platform. We analyze multiple years of imagery to identify recurring spatial patterns of hazardous open areas versus contiguous ice cover to aid in decision-making regarding local river ice use.

Keywords: River ice, SAR, citizen science

Acknowledgements

We thank the Fresh Eyes on Ice community-based monitoring teams and citizen scientists for contributing their observations. Funding for this research is provided by the Department of Interior, National Park Service (#P20AC00031), National Science Foundation's Arctic Observing Network (#1836523) and the National Aeronautics and Space Administration's Citizen Science for Earth Systems Program (#180NSSC21K0858).

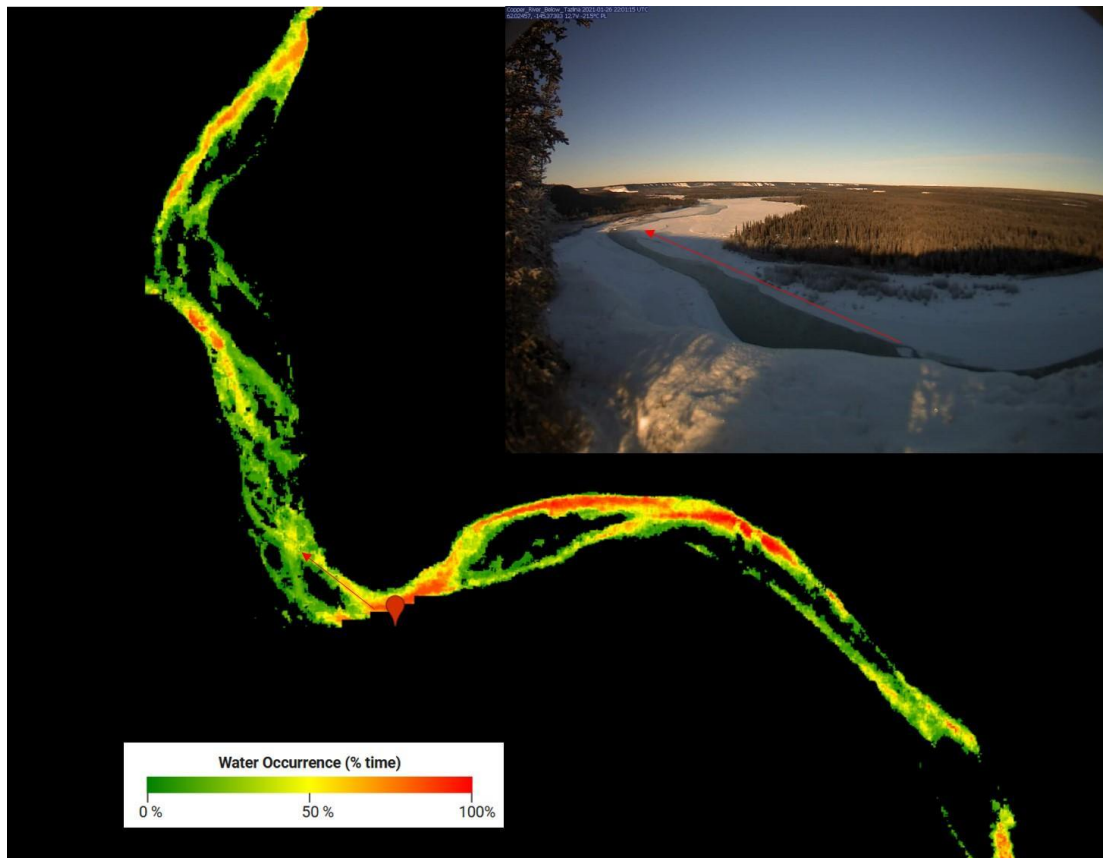


Figure 1. Example of derived product from Sentinel-1 SAR imagery showing average water occurrence over four winter seasons on the Copper River (Dec-Feb, 2017-2021), highlighting hazardous areas with persistent open water (red). Photos from fixed cameras (upper right) and community observers help us interpret the satellite imagery and validate our classifications. The location of the camera (red marker) and pictured open lead (red arrow) are notated on the map.

Session 1 : Microwave Remote Sensing

Potential monitoring of surface organic soil properties in arctic tundra using microwave remote sensing data

Yonghong Yi^{1,2}

¹Center for Spatial Information Science and Sustainable Development Applications, Tongji University, Shanghai, China

²College of Surveying and Geo-Informatics, Tongji University, Shanghai, China.

Contact: yonghong_yi@tongji.edu.cn

Abstract

Surface organic carbon content and soil moisture (SM) represent first-order controls on pan-Arctic permafrost thaw and vulnerability, yet remain challenging to map accurately. In this study, we explored the linkage between tundra SM dynamics and organic soil properties in the Alaska North Slope using multi-frequency microwave remote sensing data.

The rate at which SM drydown occurs is a measure of SM “memory”, and has been shown closely related to soil physical properties. Here we first derived the soil drydown characteristics using in-situ SM data and L-band (1.41 GHz) polarization ratio (PR) observations from the SMAP mission, and then examined its sensitivity to soil carbon properties. Our analysis indicated that more rapid drydown was generally observed in areas with high SOC concentration (SOCC) or low bulk density. At regional scale, the drydown time scale derived from the SMAP polarization ratio (PR) was significantly correlated with SoilGrids surface (0-5 cm) SOCC data ($R=-0.54\sim-0.68$, $p<0.01$).

However, we have not found a strong correlation between longwave radar backscatter changes with soil organic carbon properties. Our analysis showed that the surface soil drydown time constant in areas with high SOCC is in the range of a few days to ~10 days, which is generally shorter than the revisit period of current satellite or airborne radar sensors. This makes it challenging to use those data to characterize the SM dynamics.

We finally used a coupled permafrost hydrology and emission model to clarify the sensitivity of L-band PR to tundra SM changes and surface organic soil properties. The model sensitivity runs showed larger L-band PR decreases during the early thaw season in soils with higher SOCC, consistent with the above analysis, whereby highly organic soils (SOCC>34.8%) drain water more easily with a larger amount of water discharged or lost (through evapotranspiration). Similar analysis will be conducted for the L/P band radar backscatter.

Our findings indicated potential new capabilities for satellite-based monitoring of pan-Arctic soil conditions using microwave remote sensing. However, multi-temporal observations with enhanced temporal coverage are desired. A more promising approach would be combining the active and passive microwave sensors with similar frequency to obtain quality retrievals of pan-Arctic SM and carbon properties.

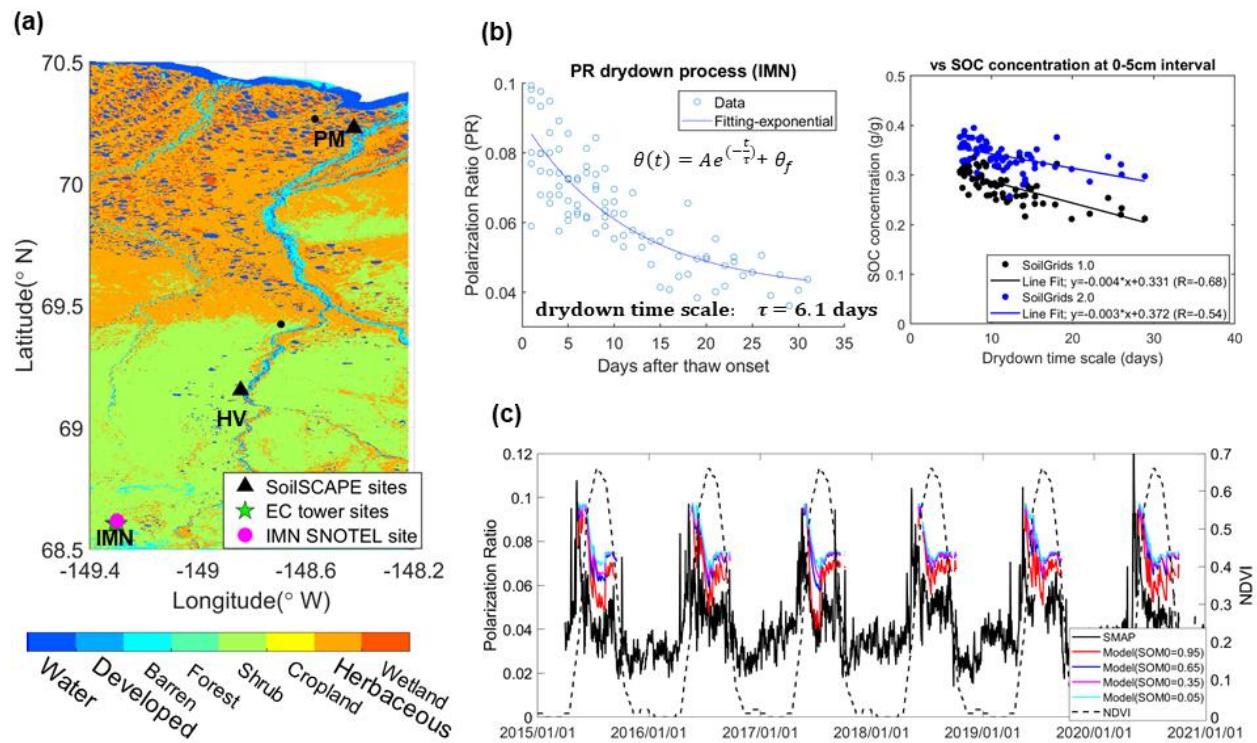


Figure 1. Linkage between SM drydown characteristics and surface SOC properties: (a) the study area - Alaska North Slope; (b) SM drydown curve indicated by L-band polarization ratio and correlation between the drydown constant derived and surface SOC concentration; (c) more rapid soil moisture drydown during the early thaw season for soils with high SOC (SOM) concentration, indicated by both modeled and observed L-band polarization ratio time series.

Keywords: soil moisture dynamics, soil organic carbon content, microwave remote sensing

References

Yi, Y., Chen, R.H., Kimball, J.S., et al. (2022) Potential Satellite Monitoring of Surface Organic Soil Properties in Arctic Tundra from SMAP. *Water Resources Research*, in press.

Acknowledgements:

Part of the work was supported by NASA ABOVE (80NSSC19M0114) and Terrestrial Hydrology program (80NSSC21K1340). The work is also supported by the Fundamental Research Funds for the Central Universities, China.

Fine-scale ground truth of ground displacement in the Anaktuvuk River Fire (ARF) for satellite and airborne L-band SAR

Go Iwahana^{1}, Robert Busey¹, Reginald Muskett¹, Simon Zwieback², Franz Meyer², Hiroshi Ohno³, Masao Uchida⁴, Kazuyuki Saito⁵*

1. International Arctic Research Center, University of Alaska Fairbanks, Fairbanks 99775, USA
 2. Geophysical Institute, University of Alaska Fairbanks, Fairbanks 99775, USA
 3. Kitami Institute of Technology, Kitami 090-8507, Japan
 4. National Institute for Environment Studies, Tsukuba 305-0053, Japan
 5. Japan Agency for Marine-Earth Science and Technology, Yokohama 236-0001, Japan
- *Corresponding author. E-mail: giwahana@alaska.edu (Go Iwahana)

Abstract

Spatial variations in inter-annual and seasonal ground displacements are essential information to estimate the rate of permafrost degradation. The differential SAR interferometry (DInSAR) has been deployed in permafrost regions to evaluate freeze/thaw-related ground surface displacement. However, the interpretation of the DInSAR results over permafrost terrains was often performed without detailed knowledge about ground surface conditions. To better understand the nature of DInSAR signals over changing permafrost lands, we investigated surface displacement caused by frozen ground dynamics and thermokarst development triggered by a tundra wildfire in Alaska. The Anaktuvuk River Fire (ARF) combusted surface vegetation and organic mat of the tundra region underlain by variously ice-rich permafrost in 2002. High-precision GNSS survey, thaw depth, and surface moisture were measured along 60 – 200 m transects at three representative sites in ARF during snow-free seasons in 2017 – 2019. The three sites were located in the northernmost fire boundary, the central area, and the southernmost of the ARF burn scar underlain by differently ice-rich permafrost. High-resolution (~1 m) DInSAR signals by UAVSAR depicted enhanced seasonal thaw settlement not only in the burned area but also a linear pattern development of larger subsidence in unburned areas, which coincides with slightly concaved linear micro-topography at Site N. Significant thermokarst subsidence and seasonal thaw settlement were measured along a Yedoma hill slope both by ground survey and DInSAR at Site M. The intensive permafrost degradation on the slopes was also confirmed by frozen ground coring and optical image analysis. The ground measurements of surface displacement were aligned well with DInSAR displacement using UAVSAR and ALOS2 data except for the anomaly subsidence along the troughs of ice-wedge polygons at earlier thermokarst stages. Less intensive ground surface displacement was observed at Site S, underlain by less ice-rich permafrost. Our results indicate that seasonal thaw settlement was governed mainly by spatial variation in soil frost-susceptibility and thermokarst subsidence by ground ice distribution.

Keywords

InSAR, thermokarst, Anaktuvuk River Fire

Acknowledgements

This study was performed under the projects NASA ABoVE (Arctic Boreal and Vulnerability Experiment (grant no. NNX17AC57A)) and the Environment Research and Technology Development Fund (2-1605). The Toolik Field Station GIS and Remote Sensing Department, University of Alaska Fairbanks was funded by NSF Grant #: 1623461.

Monitoring soil water and organic carbon storage patterns in the active layer of the Arctic Foothills using spaceborne InSAR surface deformation data

Yue Wu^{1,2}, Jingyi Chen^{1,2,3}, Michael O'Connor³, Stephen Ferencz³, George Kling⁴, M. Bayani Cardenas³

¹Aerospace Engineering & Engineering Mechanics, University of Texas at Austin, Austin, TX

²Center of Space Research, University of Texas at Austin, Austin, TX

³Jackson School of Geoscience, University of Texas at Austin, Austin, TX

⁴Ecology and Evolutionary Biology, University of Michigan, Ann Arbor, MI

Abstract

The carbon-rich permafrost soil stores more carbon found in the atmosphere. Groundwater flows through the topmost portion of the permafrost soil, known as the active layer, and transports the land carbon to the ocean and the atmosphere. As the permafrost continues to degrade and the active layer deepens, it becomes increasingly important to characterize the groundwater flow and to quantify carbon storage in the active layer. Because the Arctic covers continent-sized areas that are mostly inaccessible, remote-sensing has become a critical tool for observing the continuous permafrost. Particularly, the density difference between liquid water and ice causes seasonal ground surface deformation that can be detected over large spatial scales using InSAR.

Here we jointly analyzed L-band ALOS PALSAR data and more than 200 soil samples to determine soil properties that control the seasonal freeze-thaw process of the active layer. We demonstrate that the magnitude of the seasonal freeze-thaw deformation correlates with land vegetation cover types. This is because the seasonal deformation is a measure of the active layer soil water content, and the amount of water in the soil limits the type of vegetation that can grow. Furthermore, we found that surface vegetation types influence the soil carbon storage, and thus soils that contain more carbon in the active layer also tend to produce larger seasonal deformation. Our results suggest that InSAR can be used to monitor changes in hydrological and ecological characteristics in soils above continuous permafrost and for estimating large-scale soil moisture.

Keywords

InSAR, soil water estimates, soil carbon storage estimates

References

- Chen, J., Wu, Y., O'Connor, M., Cardenas, M. B., Schaefer, K., Michaelides, R., & Kling, G. (2020). Active layer freeze-thaw and water storage dynamics in permafrost environments inferred from insar. *Remote Sensing of Environment*, 248, 112007. Retrieved from <https://www.sciencedirect.com/science/article/pii/S0034425720303771> doi: <https://doi.org/10.1016/j.rse.2020.112007>
- O'Connor, M. T., Cardenas, M. B., Ferencz, S. B., Wu, Y., Neilson, B. T., Chen, J., & Kling, G. W. (2020). Empirical models for predicting water and heat flow properties of permafrost soils. *Geophysical Research Letters*, 47 (11), e2020GL087646. Retrieved from <https://agupubs.onlinelibrary.wiley.com/doi/abs/10.1029/2020GL087646> (e2020GL087646 2020GL087646) doi: <https://doi.org/10.1029/2020GL087646>

Acknowledgments

This study is funded by the NASA FINESST program, grant 80NSSC20K1622.

This research was funded, in part, by a grant to J. Chen, M. B. Cardenas, and G. Kling from the NASA Terrestrial Hydrology Program, grant 80NSSC18K0983.

Session 2 : Microwave Remote Sensing II

Synthetic Aperture Radar (SAR) detects large gas seep in lake

Melanie Engram¹, Katey Walter Anthony¹

¹Water and Environmental Research Center, Institute of Northern Engineering, University of Alaska Fairbanks, Fairbanks, Alaska, USA

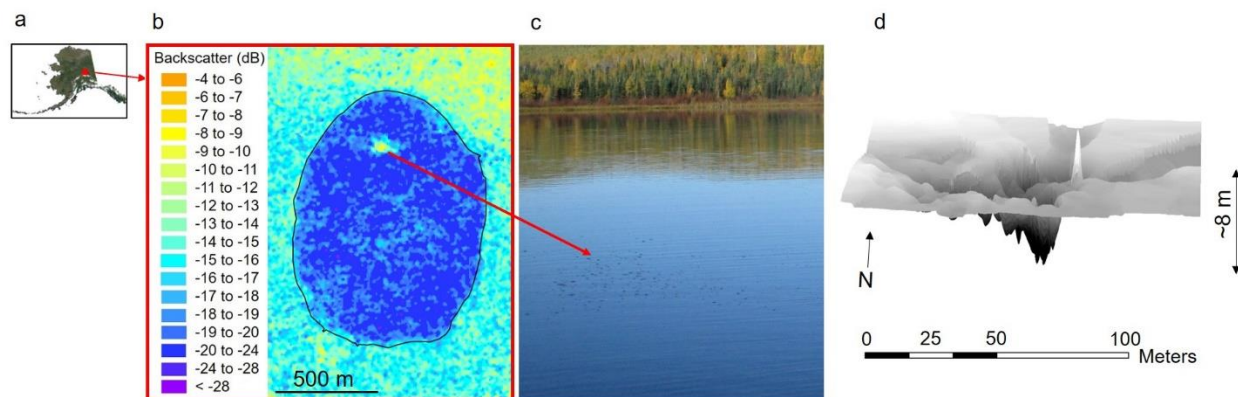


Figure 1. Located in the Tanana River floodplain south of Fairbanks, Alaska (a), North Blair lake exhibits a perennial high-backscatter anomaly as shown in Dec. 12, 2007 L-band SAR image (b). September fieldwork revealed a large bubbling methane seep (c) and bathymetric measurements indicate a pock-mark below the seep (d). Note vertical scale in (d) is ten times horizontal scale. SAR imagery (b) is from the PALSAR instrument on the ALOS-1 satellite (© JAXA/METI 2007).

Abstract

Arctic permafrost caps a large pool of ^{14}C -depleted methane (CH_4) (Isaksen et al., 2011). Natural emissions of this methane are not included in earth system models because little is known about the magnitude and timing of release. There is evidence that permafrost thaw, potentially enhanced by groundwater hydrology, creates conduits (open taliks) through which ^{14}C -depleted methane can escape to the atmosphere (Sullivan et al., 2021). An acceleration of sub-permafrost methane emission may be important to future climate; however, a baseline knowledge of current emissions is needed.

Synthetic aperture radar (SAR) remote sensing was used to quantify methane bubbling from ecologic sources based on the bubble-induced rough ice/water interface in lakes, to which SAR is sensitive (Engram et al., 2013). A remote sensing (RS) method to detect large gas seeps released from permafrost through taliks or geologic faults would be useful. Pointer and Barscsh (2020) ascribed low C-band SAR backscatter anomalies on Lake Neyto in Western Siberia to possible open-hole methane seeps. However, no field work was conducted to confirm this hypothesis.

In interior Alaska, we observed high SAR L-band backscatter (σ^0) from a spot (~80 m by ~100 m) on a frozen lake, North Blair Lake (Fig. 1a, b). The feature occurred perennially in the same place on the frozen lake in every available L-band SAR scene from 1992 to 2011. Optical multispectral RS imagery showed an open hole in shoulder-season ice at the same location as the high SAR σ^0 anomaly.

December 2020 field work indicated ice and snow across the lake, but penetration of the ice with a spear at the suspected seep location released pressurized gas. In September 2021 field work, we mapped a large (70 m x 90 m) field of bubbles rising through the open water column (Fig. 1c). Ebullition, measured with a dynamic floating chamber system, was $1,661 \pm 174 \text{ mg CH}_4 \text{ m}^{-2} \text{ d}^{-1}$, which was ~45 times higher than background diffusive methane emissions in the lake. Water depth ranged from ~1 to 4 m across the lake except for a deep (~4 to 8 m) complex pock mark found below the gas seep (Fig. 1d).

Bubbles had a relatively low methane concentration (6.6%), indicating potential groundwater association. Bubble diameter < 1 cm was smaller than the 1-2 cm diameter bubbles observed among ecologic methane seeps. The $^{14}\text{C}_{\text{CH}_4}$ age ($18,470 \pm 50$ years BP) could result from a methane substrate of 18,470 years or it could be a mixture of older/fossil methane with a younger source. Stable isotope $\delta^{13}\text{C}_{\text{CH}_4}$ of $-44.5 \pm 0.1 \text{ ‰}$ suggests a potential thermogenic origin. A geologic fault has been mapped approximately 4.3 km N of the seep field: Blair Lakes Fault (Gedney and VanWormer, 1974). Our study indicates the potential for RS to be used as a tool to quantify large, sub-permafrost gas seeps in Arctic and sub-Arctic lakes. We explore single and dual-polarized C-band SAR and polarimetric L-band SAR decompositions to determine optimal SAR imaging parameters to detect large methane seeps in frozen lakes.

Keywords: SAR, lake, methane, ebullition, geologic seep

References

- Engram, M., Anthony, K.W., Meyer, F.J., & Grosse, G. (2013). Characterization of L-band synthetic aperture radar (SAR) backscatter from floating and grounded thermokarst lake ice in Arctic Alaska. *The Cryosphere*, 7, (6) 1741-1752, 10.5194/tc-7-1741-2013
- Gedney, L.D., & VanWormer, J.D. (1974). Evaluation of Feasibility of Mapping Seismically Active Faults in Alaska. *NASA-CR-138679 Technical Report*: National Aeronautics and Space Administration, Goddard Space Flight Center/ Geophysical Institute, University of Alaska Fairbanks
- Isaksen, I.S.A., Gauss, M., Myhre, G., Walter Anthony, K.M., & Ruppel, C. (2011). Strong atmospheric chemistry feedback to climate warming from Arctic methane emissions. *Global Biogeochemical Cycles*, 25, (2) <https://doi.org/10.1029/2010GB003845>
- Pointner, G., & Bartsch, A. (2020). Interannual Variability of Lake Ice Backscatter Anomalies on Lake Neyto, Yamal, Russia. *GI_Forum*, 8, (1) 47-62, 10.1553/giscience2020_01_s47

Sullivan, T.D., Parsekian, A.D., Sharp, J., Hanke, P.J., Thalasso, F., Shapley, M., Engram, M., & Walter Anthony, K. (2021). Influence of permafrost thaw on an extreme geologic methane seep. *Permafrost and Periglacial Processes*, <https://doi.org/10.1002/ppp.2114>

Acknowledgements: We thank A. Bondurant, P. Hanke, and P. Anthony for field work. We acknowledge and thank the Alaska Satellite Facility for access to SAR data and MapReady tool suite.

SAR data, on-demand processing and analysis tools, and other user support services available at the Alaska Satellite Facility

Alex Lewandowski¹, Heidi Kristenson¹, Franz J. Meyer^{1,2}, Joseph H. Kennedy¹

¹Alaska Satellite Facility, University of Alaska Fairbanks, Fairbanks, AK

²Geophysical Institute, University of Alaska Fairbanks, Fairbanks, AK

Abstract

Synthetic Aperture Radar (SAR) has great potential for use in applications such as change detection and monitoring of landscape dynamics. Modern spaceborne sensors, such as Sentinel-1 and the upcoming NASA-ISRO SAR mission NISAR, provide global coverage with a resampling rate of 12 days or less. The regular acquisition schedule and ability to image the Earth's surface through clouds and smoke make Sentinel-1 and NISAR excellent resources for monitoring dynamic processes on the earth surface.

SAR is still a data set that is difficult for many geoscientists to use. While it has demonstrated benefits for a range of applications in polar environments, it can be difficult to process and interpret. The Alaska Satellite Facility (ASF), which hosts the global Sentinel-1 and NISAR archive on behalf of NASA, has developed a range of tools and resources to help users access and analyze SAR datasets.

ASF offers On-Demand processing services that generate analysis-ready data products from Sentinel-1 imagery. These services are available directly through ASF's Vertex Data Search portal (<https://search.asf.alaska.edu/>), and use ASF's Hybrid Pluggable Processing Pipeline (HyP3; <https://asf.alaska.edu/information/general/custom-processing/>) cloud computing platform to quickly and efficiently process Level 1 Sentinel-1 data to higher-level products. Users can submit scenes for Radiometric Terrain Correction (RTC) or Interferometric SAR (InSAR) processing, and download the products within about an hour. Services to generate surface movement vectors via feature tracking are also available.

In addition to the Vertex interface, HyP3 provides a RESTful API and a Python software development kit (SDK) so that HyP3 can be built into research and application workflows. In combination with the `asf_search` Python package, a user can programmatically search Sentinel-1 holdings for desired input scenes, submit them for On-Demand processing, and download the data for use in analysis or existing workflows.

For users interested in analyzing SAR data end-to-end in the cloud, ASF also offers OpenSARlab, a cloud-based SAR data analysis platform. OpenSARlab uses a Jupyter Lab interface, with managed computing environments that provide users easy access to a wide range of open-source SAR software such as ISCE2 and MintPy. Users have access to a library of ASF-developed Jupyter notebooks for amplitude and InSAR analysis, and can also develop their own Python-based workflows.

In combination, ASF's HyP3 and OpenSARlab services allow experienced SAR users to skip the time, effort, and cost involved in processing Level-1 Sentinel-1 data, and move directly to time series analysis or other advanced workflows. It also makes it easy for users who are new to SAR to experiment with the dataset.

This presentation provides an overview of the tools and resources available from ASF that make it easier for new and seasoned users to integrate SAR datasets into their analysis of landscape dynamics.

Keywords SAR, RTC, InSAR

A potential SAR-based approach to remote sensing methane superseeps in Arctic lakes

Natalie Tyler¹, Melanie Engram¹, Hilary Nyström¹, Guido Grosse^{2,3}, Katey Walter Anthony¹

¹Water and Environmental Research Center, University of Alaska Fairbanks, Fairbanks, AK, USA

²Alfred Wegener Institute Helmholtz Centre for Polar and Marine Research, Permafrost Research Section, Potsdam, Germany

³University of Potsdam, Institute of Geosciences, Potsdam, Germany

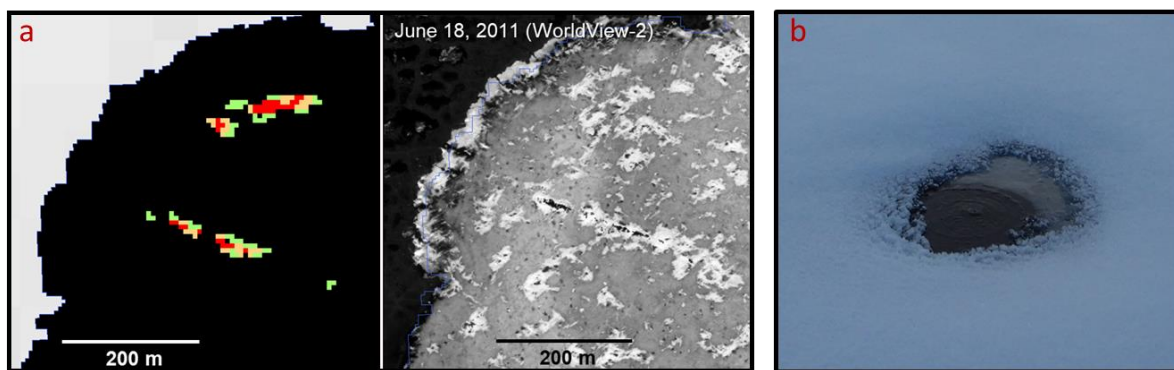


Figure 2. Example of a SAR-detected superseep (a, left) feature compared to the linear seep visible in very high-resolution optical imagery (a, right) (WorldView-2; Imagery © 2010, 2011 DigitalGlobe, Inc.) at a known seep site within Sukok Lake (Utqiagvik region). In the same lake, an open hole is visible (b) in thick winter lake ice at a separate superseep site (Photo credit: Natalie Tyler, November 18, 2019).

Abstract

Ebullition (bubbling) is often the dominant pathway for methane (CH_4) emission in Arctic lakes. Understanding the dynamics of CH_4 ebullition in these lakes is important to the global atmospheric CH_4 budget and climate models. Lake CH_4 ebullition bubbles generally originate from either ecologic or geologic sources. Ecologic CH_4 is produced through anaerobic microbial decomposition of organic matter within lake sediments and the underlying talik. Emissions from these seeps have been quantified and scaled based on existing field-based and remote-sensing methods. Space-borne synthetic aperture radar (SAR), a powerful tool for remote sensing ebullition, was used to quantify ecologic ebullition in Alaskan lakes (Engram et al., 2020). Specifically, L-band (~ 24 cm wavelength) backscatter correlates with roughness caused by stratigraphically-layered ecologic CH_4 bubbles trapped during lake freeze-up: the stronger the ebullition, the higher the backscatter signal (Engram et al, 2013).

While thought to be a far rarer occurrence, geologic CH₄ ebullition has not been as well quantified as ecologic CH₄. Geologic CH₄, unlike ecologic CH₄, is often fossil (¹⁴C-free) and originates from microbial, thermogenic, or a combination of both processes altering buried organics in ancient sedimentary basins. Ebullition rates from these “superseeps” are much higher than ecologic ebullition and are often strong enough to maintain holes in thick (>1 m) lake ice. Overall, quantification and upscaling of geologic CH₄ seepage is challenging because CH₄ accumulations are distributed beneath complex, site-specific geologic and cryospheric settings.

Engram et al. (unpublished data) observed very high perennial backscatter features in L- and P-band (~ 70 cm wavelength) SAR imagery at the locations of known superseeps. From this correlation, we developed an intensity-threshold method for locating potential superseeps on a landscape-scale using 11 previously ground-truthed superseeps. Using L-band ALOS-1 PALSAR data acquired in HH polarization from late 2006 to early 2011, we identified 513 high-confidence SAR-detected superseep sites (defined as lakes with superseep features) across three Arctic Alaska regions. Our site density in northern Alaska was >10 times greater than previous estimates, indicating there may be more superseeps in the Arctic than previously thought.

Keywords methane; ebullition; SAR

References

Engram M, Anthony K W, Meyer F J, and Grosse G 2013 Synthetic aperture radar (SAR) backscatter response from methane ebullition bubbles trapped by thermokarst lake ice. *Canadian Journal of Remote Sensing*, 38(6), 667–682. <https://doi.org/10.5589/m12-054>
Engram M, Walter Anthony K M, Sachs T, Kohnert K, Serafimovich A, Grosse G and Meyer F J 2020 Remote sensing northern lake methane ebullition *Nat. Clim. Chang.* 10 511–7 Online: <https://doi.org/10.1038/s41558-020-0762-8>

Acknowledgements

We thank Allen Bondurant, Philip Hanke, Janelle Sharp, Fred Thalasso and Peter Anthony for assistance with field work. Prajna Lindgren, John Wagner and Elisa Johnson assisted with seep identification in optical satellite imagery. The Ukpeaġvik Iñupiat Corporation granted permission to conduct research on native land and provided logistical support for field work. CH2M Hill Polar Services provided logistical support to field work. SAR data were provided by the Alaska Satellite Facility. Geospatial support was provided by the Polar Geospatial Center under NSF-OPP awards 1043681 and 1559691. This study was part of the Arctic-Boreal Vulnerability Experiment (NASA NNN12AA01C and NNH18ZDA001N-TE).

Posters Abstracts

Baldwin: Utilizing multispectral imagery to assess historic maximum flood heights in remote Alaskan communities and improve flood mitigation strategies

*Harper Baldwin*¹

¹Arctic Coastal Geoscience Lab, Geophysical Institute, Fairbanks, AK

Abstract

There is a dearth of geoscientific data to inform mitigation strategies in remote and historically underfunded Alaskan coastal communities. These communities face increasing coastal hazards, such as erosion and flooding, as a result of projected climate changes. Currently, flood modeling in many communities is based on bathtub models that only consider elevation above a geodetic tidal gauge and utilize single point data on historic flood heights. This modeling is insufficient to describe potential flood impacts, as it does not consider hydrologic flow patterns. Improving these models is necessary to create sufficient mitigation strategies, but up-to-date bathymetric and real-time oceanographic data necessary to create storm surge models is unavailable, and imagery depicting areal extents of historical flood events is lacking due to cloud cover. Consideration of the areal extent of historic flooding based on vegetation characteristics is one approach to assessing the accuracy current bathtub models. The objectives of this research are (1) to assess the feasibility of utilizing multispectral image analysis for delineating historic maximum flood height based on the spectral characteristics of inundated vegetation, and (2) to utilize resultant flooding areal extents to evaluate the accuracy of bathtub flood models in remote, coastal communities in Bristol Bay, AK.

This project uses Maxar multispectral imagery to compare historic trends in NDVI (normalized difference vegetation index) at Goodnews Bay, AK. Estimates of vegetation health from NDVI are compared to a longitudinal series of data based on a large flooding event in 2011 in Goodnews Bay. Vegetation health is assessed at peak growth in 2002, and then in subsequent peak growth imagery in 2012, 2016, and 2021, for a temporal assessment of the effects of flooding on vegetation health. The difference of NDVI values is taken between 2002 and all subsequent years of analysis to highlight areas where vegetation was damaged from flood impacts. The areal extent of flooding in the 2011 storm is extrapolated from vegetation health differences between 2002 and 2012 and is compared to the bathtub model for the 2011 storm. This comparison is a novel application of a well-documented relationship between flood extent and vegetation health characteristics that yields insights into the accuracy of the bathtub model in Goodnews Bay and indicates potential improvements to current flood mitigation strategies.

Keywords: Remote sensing, flooding, hazard mitigation

References

Buzard, Richard M., Christopher V. Maio, David Verbyla, Nicole E.M. Kinsman, and Jacquelyn R. Overbeck. "Measuring Historical Flooding and Erosion in Goodnews Bay Using Datasets Commonly Available to Alaska Communities." *Shore & Beach* 88(3), (Summer 2020): 3–13.

<http://doi.org/10.34237/1008831>

Kearney, Michael, David Stutzer, Kevin Turpie, and John Stevenson. "The Effects of Tidal Inundation on the Reflectance Characteristics of Coastal Marsh Vegetation." *Journal of Coastal Research* 25 (November 1, 2009): 1177–86. <https://doi.org/10.2112/08-1080.1>.

Rodgers, John, Adam Murrah, and William Cooke. "The Impact of Hurricane Katrina on the Coastal Vegetation of the Weeks Bay Reserve, Alabama from NDVI Data." *Estuaries and Coasts* 32 (May 1, 2009): 496–507. <https://doi.org/10.1007/s12237-009-9138-z>.

Tahsin, Subrina, Stephen C. Medeiros, and Arvind Singh. "Assessing the Resilience of Coastal Wetlands to Extreme Hydrologic Events Using Vegetation Indices: A Review." *Remote Sensing* 10, no. 9 (September 2018): 1390. <https://doi.org/10.3390/rs10091390>.

Acknowledgements

This project is funded by NSF grant 1848542. Geospatial support for this work provided by the Polar Geospatial Center under NSF-OPP awards 1043681 and 1559691.

Barth: Earth observation-based time series analysis of retrogressive thaw slump dynamics in the Russian High Arctic

Sophia Barth^{1,2}, Ingmar Nitze¹, Alexandra Runge¹, Guido Grosse^{1,2}

¹Permafrost Research, Alfred Wegener Institute Helmholtz Centre for Polar and Marine Research, 14473 Potsdam, Germany

²Institute of Geosciences, University of Potsdam, 14476 Potsdam, Germany

Abstract

Since climate change is directly impacting the Arctic, landscapes underlain by permafrost experience increased thaw and degradation. Retrogressive Thaw Slumps (RTS) are dynamic thermokarst features which result from slope failure after ice-rich permafrost thaws. While they are small-scale features, they can reach considerable annual growth rates. Thousands of RTS have been inventoried in detail, mostly in northwestern Canada and Alaska, where thaw slumping substantially modified terrain morphology, altered the discharge into aquatic systems, and led to infrastructure hazards (Kokelj et al. 2013, Kokelj et al. 2015, Swanson & Nolan 2018). Furthermore, recent studies revealed increased temporal thaw dynamics of RTS in northern high latitudes and projected that abrupt thermokarst disturbances contribute significant amounts of greenhouse gas emissions (Knoblauch et al. 2021).

As observed in Arctic regions, RTS have been developing in the Russian High Arctic as well. Recently, Runge et al. (2022) analyzed RTS dynamics in large parts of Siberia using Landsat/Sentinel-2, but detailed high-resolution observations exist so far only for a few regions in West Siberia, where industrial development required mapping of potential landscape hazards. In most other regions of the Russian High Arctic, RTS occurrence and distribution is poorly investigated so far. The objective of this study is to better understand growth patterns and development rates of RTS at high temporal resolution in the Russian High Arctic between 2011 and 2020.

We here investigated five sites with different permafrost types that are affected by strong RTS development. The mapped area totals more than 600 km² located on Novaya Zemlya, Kolguev Island, Bolshoy Lyakhovsky Island and eastern and western Taymyr Peninsula. Some of the sites are characterized by buried glacial ice while others are characterized by thick syngenetic Yedoma permafrost. To quantify changes in active RTS occurrences and their extent, a GIS-based inventory of manually mapped RTS was created. The inventory is derived from high temporal and spatial resolution, multispectral imagery, obtained between 2011 and 2020 by satellite sensors including PlanetScope, RapidEye, Pleiades and Spot. Additional datasets such as the ArcticDEM, ESRI satellite basemap, and Tasseled Cap Landsat Trends were used to support the mapping process.

First results show that active thaw slumps have increased significantly in size in recent years. The surface area covered by active RTS at the sites on Novaya Zemlya and Taymyr Peninsula more than doubled in 2020 in comparison to 2011 and 2013, respectively. At Kolguev we retrieved headwall and bluff base erosion rates along two sections of the west coast between 2013 and 2020. The slumps located further north revealed average thermal abrasion rates at the base of 1.4 m/yr and

average thermal denudation rates at the headwall of 3.9 m/yr. We discovered that the RTS located further south showed average thermal abrasion rates of 5.2 m/yr and average thermal denudation rates of 2.9 m/yr. Our approach gives a first insight on the variability and magnitude of thaw slumping observed in the Russian High Arctic and will further contribute substantially to our understanding of local and regional permafrost thaw dynamics in this region.

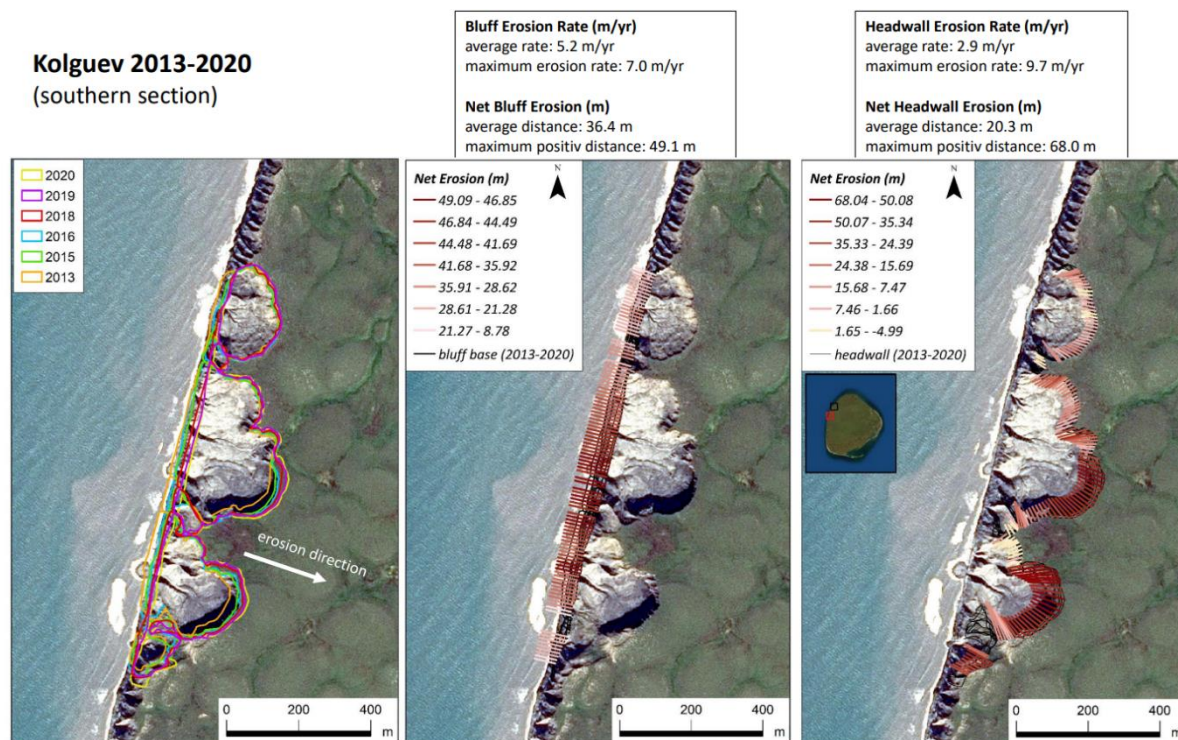


Figure 1: Bluff base and headwall erosion rates in meters of Retrogressive Thaw Slumps along the western coast of Kolguev Island. The three maps show the southern section of the study site. Left: Individual slump outlines between 2013 and 2020. Middle: Net erosion at the bluff base (thermal abrasion). Right: Net headwall erosion (thermal denudation). High erosion values represented with darker colored and low erosion values with brighter colored transects.

Keywords: Retrogressive Thaw Slumps, Russian High Arctic, Time series

References

Knoblauch, C., Beer, C., Schuett, A., Sauerland, L., Liebner, S., Steinhof, A., ... & Pfeiffer, E. M. (2021). Carbon dioxide and methane release following abrupt thaw of Pleistocene permafrost deposits in Arctic Siberia. *Journal of Geophysical Research: Biogeosciences*, 126(11), e2021JG006543.

Kokelj, S. V., Lacelle, D., Lantz, T. C., Tunnicliffe, J., Malone, L., Clark, I. D., & Chin, K. S. (2013). Thawing of massive ground ice in mega slumps drives increases in stream sediment and solute flux across a range of watershed scales. *Journal of Geophysical Research: Earth Surface*, 118(2), 681-692.

Kokelj, S. V., Tunnicliffe, J., Lacelle, D., Lantz, T. C., Chin, K. S., & Fraser, R. (2015). Increased precipitation drives mega slump development and destabilization of ice-rich permafrost terrain, northwestern Canada. *Global and Planetary Change*, 129, 56-68.

Runge, A., Nitze, I., & Grosse, G. (2022). Remote sensing annual dynamics of rapid permafrost thaw disturbances with LandTrendr. *Remote Sensing of Environment*, 268, 112752.

Swanson, D. K., & Nolan, M. (2018). Growth of retrogressive thaw slumps in the Noatak Valley, Alaska, 2010–2016, measured by airborne photogrammetry. *Remote Sensing*, 10(7), 983.

Acknowledgements

The NSF Permafrost Discovery Gateway project (subaward contract to AWI) supported participation in this conference. I would also like to thank the University of Potsdam, which further contributed to the financing of the travel costs. Imagery for the analysis was provided through the ESA Third Party Mission proposal **TPM4-ID-54054**, HGF AI-CORE project, and AWI.

Bogardus: Integrating iVR into education and community planning in rural Alaska; a case study from Drew Point, Alaska

Reyce Bogardus¹, Matthew Balazs¹, Benjamin Jones², Melissa Jones²

¹Arctic Coastal Geoscience Lab, Geophysical Institute, Fairbanks, AK, USA

²Institute of Northern Engineering, University of Alaska Fairbanks, Fairbanks, AK, USA

Abstract

The number of 3D elevation datasets collected by governments, researchers, industry, and hobbyists has increased over the last decade. These digital elevation models (DEMs) are useful for analyzing the spatial and temporal scales of geomorphic change as well as associated driving mechanisms. Displaying these data has historically been limited to 2D representations on a computer screen, limiting the efficacy of such products in communicating, training, and teaching place-based geoscience concepts to local decision makers and students in Alaska. Recently, the number of tools and software used to conduct analyses and planning exercises using such data within a virtual 3D environment are growing and most are compatible with consumer-grade virtual reality (VR) headsets.

This project capitalizes on these recent advancements by comparing multi-temporal 3D models of an actively eroding ice-rich permafrost bluff near Drew Point, Alaska, within a virtual environment. Point clouds of the site were derived via UAV-borne structure-from-motion data using photogrammetry software from which high-resolution 3D meshes and textures were produced (Fig 1.). The resulting models were exported as geometry definition files and are now being used in novel immersive virtual reality (iVR) programs for research, outreach, and educational purposes. These models complement ongoing efforts by the Arctic Coastal Geoscience Lab (ACGL) to develop a curriculum of class and lab exercises that use VR headsets to study and map geomorphological features in various sub-Arctic and Arctic communities. The models produced by this project allow researchers, decision makers, and students alike to explore and quantify wave-cut niches, thermoerosional gullies, collapsed ice blocks, ice wedge polygons, as well as thaw mechanics from unique angles, scales, and perspectives. In this manner, this project advances the integration of iVR into collegiate and K-12 education as well as community planning in rural Alaska.

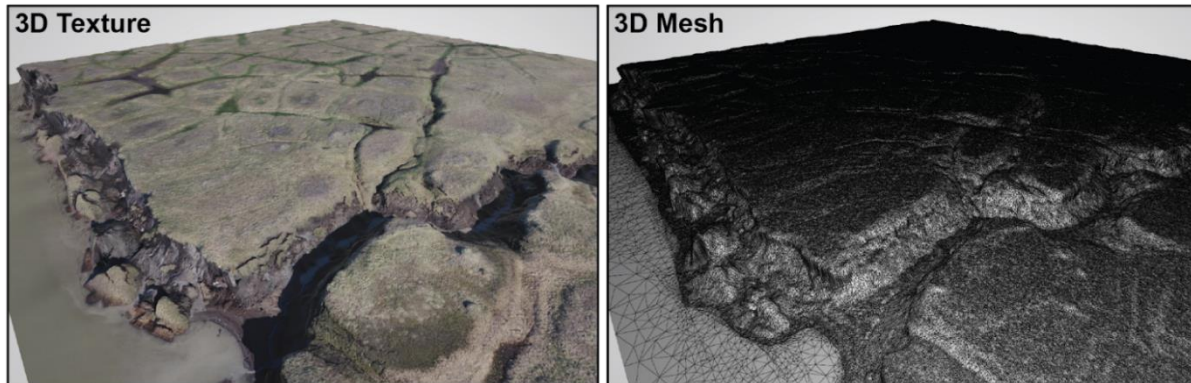


Figure 1. 3D texture (left) and mesh (right) of a portion of coastline near Drew Point, AK.

Keywords: Immersive-virtual-reality, Structure-from-Motion, Novel-education

References

- Balazs, M., Bogardus, R., Phillips, C., Darrow, M., Meyer, F., Wolken, G., Prakash, A. Improving Surficial Geology and Mass Wasting Hazard Mapping with Virtual Reality Remote Sensing (to be submitted).
- Bonali F.L., Tibaldi A., Russo E., Pasquaré Mariotto F., Marchese F., Fallati L., Savini A., Vitello F., Becciani U., Sciacca E., (2019). Immersive virtual reality for studying volcano-tectonic features: A case study from the northern active rift zone of Iceland. *Geophysical Research Abstracts*, Vol. 21, EGU2019-1159, EGU General Assembly 2019.
- Mesa-Mingorance, J. L., & Ariza-López, F. J. (2020). Accuracy assessment of digital elevation models (DEMs): A critical review of practices of the past three decades. *Remote Sensing*, 12(16), 2630. <https://doi.org/10.3390/rs12162630>
- Tibaldi, A., Bonali, F. L., Vitello, F., Delage, E., Nomikou, P., Antoniou, V. Whitworth, M. (2020). Real world-based immersive Virtual Reality for research, teaching and communication in volcanology. *Bulletin of Volcanology*, 82(5). <https://doi.org/10.1007/s00445-020-01376-6>
- Zhao, J., Wallgrün, J. O., LaFemina, P. C., Normandeau, J., & Klippel, A. (2019). Harnessing the power of immersive virtual reality-visualization and analysis of 3D earth science data sets. *Geospatial Information Science*, 22(4), 237-250. <https://doi.org/10.1080/10095020.2019.1621544>

Acknowledgements

Funding for this project was provided by PerCS-Net NSF-OISE 1927553 and NSF Career grant 1848542.

Bondurant: Aufeis growth detection on the Sagavanirktok and Dietrich Rivers using unmanned aerial systems and optical photogrammetry

Allen Bondurant¹, Horacio Toniolo¹, John Keech¹, Eric LaMesjerant¹, Alexandre Lai²

¹ Water & Environmental Research Center, University of Alaska Fairbanks, Fairbanks, Alaska, USA

² Alyeska Pipeline Service Company, Fairbanks, Alaska, USA

Abstract

We are exploring the use of low-cost Unmanned Aerial Systems (UAS) and optical photogrammetry technique to make repeat digital surface models (DSM) of aufeis field growth and development on the Sagavanirktok River in northern Alaska near the Dalton Highway, Alyeska Pipeline, and Prudhoe Bay. In year 1, we used the onboard GPS of a DJI Mavic 2 Pro with limited ground control and manual georeferencing to map aufeis extent in May of 2020, but were unable to resolve elevation with any degree of certainty. In year 2, we used the same DJI Mavic 2 Pro with extensive ground control to map larger sections of the river in both March and April of 2021 in an effort to show changes in ice elevation during this dynamic river ice season, but due to the limits of our technique and a perceived low aufeis accumulation year, for most of the mapped area the change in ice elevation was within the tolerance of our technique. One area of interest, however, saw aufeis development of >0.5m within the one-month interval between surveys, and was accurately detected using this technique. Finally, for year 3, we upgraded our system to a DJI Phantom 4 RTK. The greater accuracy of the GPS system combined with the mechanical shutter of the Phantom has led to increased survey accuracy and resolution. Using this system we mapped areas on the Sagavanirktok River, as well as the Dietrich River north of Coldfoot, AK, in early March and mid-April of 2022. Aufeis growth this year has been moderate on the Sagavanirktok but extreme on the Dietrich, which is why it was added to the observation surveys. For all years, we compared the vertical aufeis accumulation to an areal aufeis extent derived from Landsat NIR scenes.

Sagavanirktok River Aufeis near Franklin Bluffs, Spring 2021

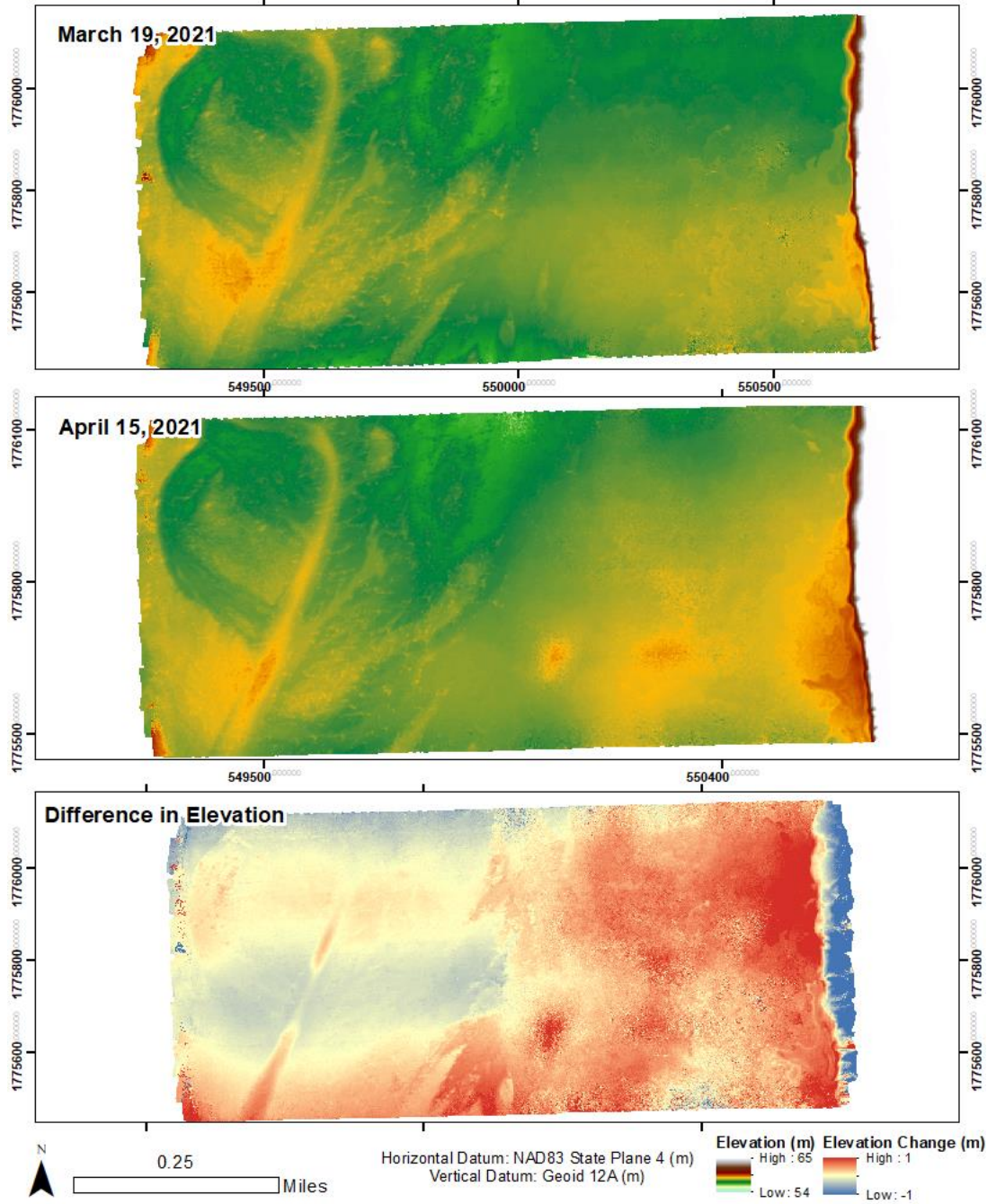


Figure 1. River ice surface elevation in an active aufeis field on the Sagavanirktok River near Franklin Bluffs in spring of 2021. Scenes show March 19, 2021, April 15, 2021, and the difference in elevation between each of these surveys.

Keywords Aufeis, UAS, Photogrammetry

Brown: Identifying spatial patterns of river ice formation and hazardous open water zones with Synthetic Aperture Radar (SAR)

Dana Brown¹, Chris Arp², Allen Bondurant², Todd Brinkman³, Barbara Cellarius⁴, Melanie Engram², Mark Miller⁴, Cristina Ornelas², Carol Simmons⁵, Katie Spellman¹, Lindsay Sturm⁵

¹International Arctic Research Center, University of Alaska Fairbanks, USA

²Water and Environmental Research Center, University of Alaska Fairbanks, USA

³Institute of Arctic Biology and Department of Biology and Wildlife, University of Alaska Fairbanks, USA

⁴Wrangell-St. Elias National Park and Preserve, Copper Center, Alaska, USA

⁵McGrath School, McGrath, Alaska, USA

See Abstract above under Floating Ice session

Bryant: Integrating ICESat-2 and optical imagery to measure coastal erosion rates and bluff morphology along the Alaskan Beaufort Sea Coast

Marnie Bryant¹, Adrian Borsa¹, Roger Michaelides², Matthew Siegfried²

¹ Institute of Geophysics and Planetary Physics, Scripps Institution of Oceanography, University of California San Diego, La Jolla, CA USA

² Department of Geophysics, Colorado School of Mines, Golden, CO, USA

Abstract

The Arctic coastline is retreating at high rates due to the combination of declining sea ice extent, increasing storm frequency and intensity, and increasing air temperatures. This coastal retreat threatens infrastructure, cultural sites and practices, and habitability of coastal communities. Coastal erosion also leads to the release of carbon, methane, and other compounds into the ocean and atmosphere, with potential impacts on ecosystems and carbon cycling (Irrgang et al, 2022). The response of coastlines to environmental forcings is both dependent on and affects coastal morphology. While previous research has sought to characterize variations in coastal morphology and erosion rates on regional (e.g. Farquharson et al, 2018) and circumpolar scales (e.g Lantuit et al, 2012) using in-situ data, airborne remote sensing data, and commercial satellite imagery, these methods are limited in their ability spatially and temporally to monitor seasonal and multi-annual changes. Recent advances in satellite remote sensing provide improved capability for monitoring short-term coastal changes. Recent advances in satellite remote sensing provide improved capability for monitoring short-term coastal changes. With a 91-day repeat time, dense along-track spacing and high vertical precision (Brunt et al, 2021), the satellite laser altimeter ICESat-2 has the potential to provide high-resolution elevation profiles across the coastline. Furthermore, the frequent revisit times of both moderate-resolution government-funded optical satellites and high-resolution commercial CubeSats facilitates the estimation of year-to-year and potentially sub-annual erosion rates in regions with high rates of retreat. This study seeks to assess the utility of integrating ICESat-2 with optical satellites and previous elevation measurements to better constrain seasonal to multi-year changes in coastal bluff height, position, and morphology. We will consider several near-coincident ICESat-2 profiles spanning 2019-2021 along with available satellite optical imagery and digital elevation models to estimate short-term erosion rates, elevation change, and morphological changes for a case study on the Alaskan Beaufort Sea Coast, where documented erosion rates are high and variable (Jones et al, 2018). We will compare erosion rates between areas with differing bluff geometry to assess the interdependency between morphology and vulnerability to erosion. This multi-sensor approach can help capture short-term coastal processes where limited in-situ data is available and improve our understanding of how these processes influence coastal responses to environmental forcings.

Keywords: ICESat-2, Erosion

References

K. M. Brunt, B. E. Smith, T. C. Sutterley, N. T. Kurtz, and T. A. Neumann. Comparisons of Satellite and Airborne Altimetry With Ground-Based Data From the Interior of the Antarctic Ice Sheet. *Geophysical Research Letters*, 48(2), January 2021. ISSN 0094-8276, 1944-8007. doi: 10.1029/2020GL090572.

L.M. Farquharson, D.H. Mann, D.K. Swanson, B.M. Jones, R.M. Buzard, and J.W. Jordan. Temporal and spatial variability in coastline response to declining sea-ice in northwest Alaska. *Marine Geology*, 404:71–83, October 2018. ISSN 00253227. Doi: 10.1016/j.margeo.2018.07.007.

Anna M. Irrgang, Mette Bendixen, Louise M. Farquharson, Alisa V. Baranskaya, Li H. Erikson, Ann E. Gibbs, Stanislav A. Ogorodov, Pier Paul Overduin, Hugues Lantuit, Mikhail N. Grigoriev, and Benjamin M. Jones. Drivers, dynamics and impacts of changing Arctic coasts. *Nature Reviews Earth & Environment*, 3(1):39–54, January 2022. ISSN 2662-138X. doi: 10.1038/s43017-021-00232-1.

Benjamin M Jones, Louise M Farquharson, Carson A Baughman, Richard M Buzard, Christopher D Arp, Guido Grosse, Diana L Bull, Frank G unther, Ingmar Nitze, Frank Urban, Jeremy L Kasper, Jennifer M Frederick, Matthew Thomas, Craig Jones, Alejandro Mota, Scott Dallimore, Craig Tweedie, Christopher Maio, Daniel H Mann, Bruce Richmond, Ann Gibbs, Ming Xiao, Torsten Sachs, Go Iwahana, Mikhail Kanevskiy, and Vladimir E Romanovsky. A decade of remotely sensed observations highlight complex processes linked to coastal permafrost bluff erosion in the Arctic. *Environmental Research Letters*, 13(11):115001, October 2018. ISSN 1748-9326. doi: 10.1088/1748-9326/aae471.

Hugues Lantuit, Pier Paul Overduin, Nicole Couture, Sebastian Wetterich, Felix Are, David Atkinson, Jerry Brown, Georgy Cherkashov, Dmitry Drozdov, Donald Lawrence Forbes, Allison Graves-Gaylord, Mikhail Grigoriev, Hans-Wolfgang Hubberten, James Jordan, Torre Jorgenson, Rune Strand deg ard, Stanislav Ogorodov, Wayne H. Pollard, Volker Rachold, Sergey Sedenko, Steve Solomon, Frits Steenhuisen, Irina Streletskaaya, and Alexander Vasiliev. The Arctic Coastal Dynamics Database: A New Classification Scheme and Statistics on Arctic Permafrost Coastlines. *Estuaries and Coasts*, 35(2):383–400, March 2012. ISSN 1559-2723, 155F9-2731. doi: 10.1007/s12237-010-9362-6.

Burrell: Climate change, fire return intervals and the growing risk of permanent forest loss in boreal Eurasia

Arden L. Burrell^{1,2*}, Qiaoqi Sun^{3,4}, Robert Baxter³, Elena A. Kukavskaya⁵, Sergey Zhila⁵, Tatiana Shestakova¹, Brendan M. Rogers¹, Jörg Kaduk², Kirsten Barrett²

1. Woodwell Climate Research Center, Falmouth, MA, United States of America
2. Centre for Landscape and Climate Research, School of Geography, Geology and Environment, University of Leicester, University Road, LE1 7RH, UK
3. Department of Biosciences, University of Durham, Upper Mountjoy, South Road, Durham, DH1 3LE, United Kingdom.
4. College of Wildlife and Protected Area, Northeast Forestry University, 26 Hexing Road, Harbin 150040, China
5. V.N. Sukachev Institute of Forest of the Siberian Branch of the Russian Academy of Sciences - separate subdivision of the FRC KSC SB RAS, 660036 Russian Federation, Krasnoyarsk, Akademgorodok 50/28. Author¹, Author², Author³, etc.

Abstract

Climate change has driven an increase in the frequency and severity of fires in Eurasian boreal forests. A growing number of field studies have linked the change in fire regime to post-fire recruitment failure and permanent forest loss. In this study we used four burned area and two forest loss datasets to calculate the landscape-scale fire return interval (FRI) and associated risk of permanent forest loss. We then used machine learning to predict how the FRI will change under a high emissions scenario (SSP3-7.0) by the end of the century. We found that there are currently 133 000 km² forest at high, or extreme, risk of fire-induced forest loss, with a further 3 M km² at risk by the end of the century. This has the potential to degrade or destroy some of the largest remaining intact forests in the world, negatively impact the health and economic wellbeing of people living in the region, as well as accelerate global climate change.

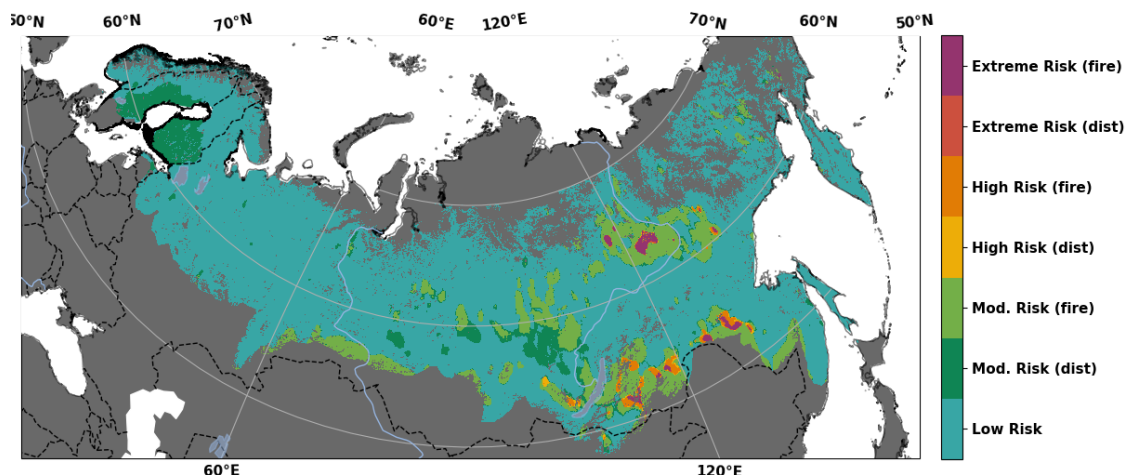


Figure 1 Current Risk of Forest Loss. The risk of permanent forest loss using FRI, FRI_{SR} and DRI over the period 2001 to 2018. Criteria are shown in Table 2.

Keywords

Wildfire, Post fire recruitment failure, Boreal forest

References

This work was recently published as <https://doi.org/10.1016/j.scitotenv.2022.154885>

Acknowledgements

This work was supported by (i) the UK Natural Environment Research Council [grant number NE/N009495/1] awarded to KB, RB and JK and (ii) the National Aeronautics and Space Administration (NASA) Arctic Boreal Vulnerability Experiment (ABOVE) grant 80NSSC19M0112. EK and SZ

Czarnecki: The use of remote sensing methods and the capabilities of UAV in polar research – examples of transformation of the shoreline in Kaffiøyra Plain (Svalbard)

Kamil Czarnecki, Ireneusz Sobota, Justyna Łukaszewska

Department of Hydrology and Water Management, Faculty of Earth Sciences and Spatial Management
Polar Research Center, Nicolaus Copernicus University in Toruń, Poland

Abstract

In recent years, we have seen rapid and chaotic warming on the globe. This is confirmed by the increased average air temperature or precipitation in measurements. The available data clearly show that the polar regions are the most sensitive areas of climate change. In the Arctic, it is estimated that the average air temperature increases three times faster than the global average.

As a result, there is a global recession of glaciers, sea level rise, and coastal changes. The shoreline transform include research into the Kaffiøyra, which is a coastal plain located in northwestern Spitsbergen (Oscar II Land). Kaffiøyra is a closed ecosystem surrounded by tidewater glaciers and the Forlandsundet Strait. The shape of the lowland coast is dichotomous: in the north the coastal strip of the plain is low and aggradational, whereas its southern part is predominantly cliffy.

This study uses remote sensing methods of data acquisition and conducts field research. The analysis was based on an area of nearly 44 ha, divided into 3 zones of influence: the mouth of the Waldemar River, the primary coast and the quasi bay in Hornbæk. Initially UAVs were used where a number of routes were planned. The data was processed into a point cloud using specialized software. In order to improve the accuracy of the results, measurements were made with geodesic equipment - a GNSS receiver. A string of coastal changes in the space are noticeable in the remote sensing dimension. Over 50 years, the zones of accumulation and erosion are clearly visible. The image allowed to define the dynamics of changes, the formation of new sandy bank or sand spit. This study was carried out as part of the project "Changes of north-western Spitsbergen glaciers as the indicator of contemporary transformations occurring in the cryosphere" (2017/25/B/ST10/00540) funded by the National Science Centre, Poland.

Keywords shoreline changes, Kaffiøyra, UAV measurements, remote sensing

Czarnecki: Evaluation of the usefulness of Landsat 8 imagery in 2013-2020 on the example of the Aavatsmarkbreen (NW Spitsbergen, Svalbard)

Kamil Czarnecki, Marcin Nowak

Department of Hydrology and Water Management, Faculty of Earth Sciences and Spatial Management
Polar Research Center, Nicolaus Copernicus University in Toruń, Poland

Abstract

In polar researches, remote data acquisition methods are increasingly used. Hard-to-reach places for scientists generate high logistics and transport costs, and on the example of the SARS-CoV-2 pandemic, they partially disqualify any scientific expeditions. Since the start of the Landsat program, many scientists have been using satellite imagery for environmental analysis and to complement fieldwork. However, everything is fraught with the risk of cloudiness over a given area, which absolutely eliminates the data to further processing. What if cloud cover becomes the main subject of research? What is the scale of cloudiness in the polar regions?

The main purpose of the presented work was to evaluate Landsat 8 imagery in terms of cloud cover over the terminal zone of the Aavatsmarkbreen (Kaffiøyra, NW Spitsbergen). The work applied all Landsat 8 imagery available for download at earthexplorer.usgs.gov services which were acquired from the beginning of the mission (early 2013) to the end of 2020 and also covered the entire area of interest (AOI). In total, the data included 868 satellite imagery. AOI visibility on each image was calculated using Quality Assessment Band (QA) which constitute an integral part of the Landsat 8 dataset. QA consisted of several pixels with values containing information about their content and thus also possible cloudiness. The data was reclassified, grouped into visibility classes and presented on the basis of GIS software, calculation and statistical methods. Of all the Landsat 8 images, only 176 (approx. 20%) contained the area fully visible, thus was suitable for further use. As much as 60% of the images were covered with clouds in over 95%. This study was carried out as part of the project "Changes of north-western Spitsbergen glaciers as the indicator of contemporary transformations occurring in the cryosphere" (2017/25/B/ST10/00540) funded by the National Science Centre, Poland.

Keywords cloud cover, Kaffiøyra polar region, remote sensing data acquisition

Sobota: Hydrological analysis of Kaffiøyra Plain: Change in areas, coastline and amount of glacial lakes in the light of remote sensing imagery and UAV measurements, Elisebreen sample

Ireneusz Sobota, Kamil Czarnecki, Krzysztof M. Róžański

Department of Hydrology and Water Management, Faculty of Earth Sciences and Spatial Management
Polar Research Center, Nicolaus Copernicus University in Toruń, Poland

Abstract

The recession of glaciers is one of the main topics of the climate change conference. In the common understanding of words, it becomes mainly a negative symbol of the global problems of humanity. Landscape changes in the polar regions including transformations of the coastline, changes in the range of glaciers and their foregrounds. In the cause-and-effect relationship, the recession of the valley glaciers contributes to the increased outflow of meltwater, but also creates new surface forms such as frontal moraines and glaciers lakes.

Kaffiøyra is a coastal plain located in northwestern Spitsbergen (Oscar II Land) – the largest island of the Svalbard archipelago. On the Kaffiøyra Plain, lakes occur in the marginal zones of all glaciers, as well as in the coastal zone and marine terraces. In general, they are small water bodies. Such ephemeral bodies are numerous in the marginal zones of Waldemarbreen, Oliverbreen and Irenebreen. The largest lakes are on the foreland of Elisebreen and Andreasbreen. The marginal zone of Elisebreen has the highest number of lakes.

Remote sensing methods and field observations documented the creation of a new glacial lake in the foreground of the Elisebreen. The main source of data were images of the Sentinel and Landsat program. Based on the spectral bands of the satellite and their combinations, the materials was digitized and preliminary surface calculations were carried out. The area was determined on the basis of the NDWI index, considered by the authors to be the most appropriate in these measurements. In the UAV imagery, currently used in the form of a research reconnaissance, there is a marked change in the mass balance of the glacier and the nature of the lake in its foreground. This study was carried out as part of the project “Changes of north-western Spitsbergen glaciers as the indicator of contemporary transformations occurring in the cryosphere” (2017/25/B/ST10/00540) funded by the National Science Centre, Poland.

Keywords Kaffiøyra glaciers region, Elisebreen’s foreground lakes, remote sensing and UAV

Dann: Identification of secondary factors controlling Synthetic Aperture Radar (SAR) -derived root-zone soil moisture over the Seward Peninsula using random forest modelling

Julian Dann¹, Katrina Bennett², Cathy Wilson², Bob Bolton¹

¹International Arctic Research Center, University of Alaska Fairbanks, Fairbanks, AK, USA

²Earth and Environmental Sciences, Los Alamos National Laboratory, Los Alamos, NM, USA

Abstract

Root-Zone soil moisture exerts a fundamental control on vegetation, energy balance, and the carbon cycle in Arctic ecosystems, but it is still not well understood in vast, remote, and understudied regions of discontinuous permafrost. The root-zone soil moisture product (30m resolution) used in this analysis was derived using a novel time-series three-layer dielectric forward inversion model based on P-Band (280 – 440 MHz) synthetic aperture radar (SAR) backscatter (Aug, 2017 & Oct, 2017). (Chen et al 2020, Tabatabaeenejad et al 2015) While similar approaches have been taken to retrieve surface (0-5cm) soil moisture from L-Band (1.2 Ghz) SAR backscatter, this is one of the first attempts at reaching the root-zone in regions containing permafrost. Here we analyze secondary factors (excluding precipitation) controlling summer (August) soil moisture at a depth of 20cm over a 4500 km² swath on the Seward Peninsula of Alaska. Using a random forest model we quantify the impact of topography, vegetation, and environmental factors at a variety of scales. In developing the model, we explore a variety of feature scales (30, 60, 90, 120, 180, and 240m), tune hyperparameters (primarily the number and depth of trees), and perform the final feature selections using cross-validated recursive feature elimination. Results suggest that root-zone soil moisture on the Seward Peninsula is driven primarily by five factors (in order of decreasing permutation importance) elevation at 180m, radiation at 240m, winter wind at 240m, System for Automated Geoscientific Analyses (SAGA) Wetness Index (SWI) at 120m, and curvature at 240m. This model accounts for ~60% of the variation observed ($R^2 = 0.58$). These results indicate that vegetation does not have a significant effect on August soil moisture at 20cm retrieved from P-Band SAR backscatter.

Keywords: Random forest, soil moisture, SAR

References:

Chen, Richard H., Alireza Tabatabaeenejad, and Mahta Moghaddam. "Retrieval of Permafrost Active Layer Properties Using Time-Series P-Band Radar Observations." *IEEE Transactions on Geoscience and Remote Sensing* 57, no. 8 (August 2019): 6037–54.

<https://doi.org/10.1109/TGRS.2019.2903935>.

Tabatabaeenejad, Alireza, Mariko Burgin, Xueyang Duan, and Mahta Moghaddam. "P-Band Radar Retrieval of Subsurface Soil Moisture Profile as a Second-Order Polynomial: First AirMOSS Results." *IEEE Transactions on Geoscience and Remote Sensing* 53, no. 2 (February 2015): 645–58.

<https://doi.org/10.1109/TGRS.2014.2326839>.

Data can be downloaded from Chen, R.H., A. Tabatabaeenejad, and M. Moghaddam. 2019. ABoVE: Active Layer and Soil Moisture Properties from AirMOSS P-band SAR in Alaska. ORNL DAAC, Oak Ridge, Tennessee, USA. <https://doi.org/10.3334/ORNLDAAC/1657>.

Acknowledgements

I'd like to acknowledge and thank Dr. Richard Chen for allowing me to use his data product and helping me to better understand how he derived soil moisture from the raw SAR backscatter.

Farquharson: Permafrost thaw and talik development drives future coastal inundation in North Slope communities

Louise Farquharson¹, Dmitry Nicolsky¹, Vladimir Romanovsky¹, Bill Tracey², Anna Irrgang³, Benjamin Jones⁴

¹Geophysical Institute, UAF, Fairbanks, Alaska, USA

²Community of Point Lay, North Slope Borough, Alaska, USA

³Helmholtz Centre for Polar and Marine Research, Alfred Wegener Institute, Potsdam, Germany

⁴Institute of Northern Engineering, UAF, Fairbanks, Alaska, USA

Abstract

Permafrost thaw and coastal erosion are expected to cause widespread land loss (Irrgang et al., 2022.; Nielsen et al., 2022), infrastructure damage (Hjort et al., 2018), the re-routing of tundra and snow travel corridors, and the destruction of important cultural sites across many Arctic coastal communities within the next century (Irrgang et al., 2019). While there have been widespread efforts to map rates of coastal erosion and to some degree project future rates of change, little work has been done to explore how permafrost thaw driven subsidence may exacerbate this process. We use a combination of remote sensing, digital elevation analysis, and ground temperature modelling to establish first order estimates of future subsidence and resulting coastal inundation at the communities of Wainwright, Point Lay and Kaktovik on the North Slope of Alaska. Geophysical Institute Permafrost Laboratory modelling results (Nicolsky et al., 2017) suggest that by the year 2100, under RCP8.5, ground temperature could increase by up to 6 - 8°C under natural conditions. As a result, active layer depths and talik development combined could result in an increase in thaw depth of between 5 and 13 m. By 2100, due to the prevalence of ground ice around all three communities, active layer deepening and talik development could lead to subsidence depths of 4 to 10 m in the areas with high ground ice content conditions. We calculate potential subsidence and map associated coastal inundation for all four communities under a range of ground ice conditions (30 %, 50 %, 80 %) for 2050, 2080 and 2100. By 2100 and under ice-rich conditions, significant inundation, infrastructure damage and land loss occur at all sites.

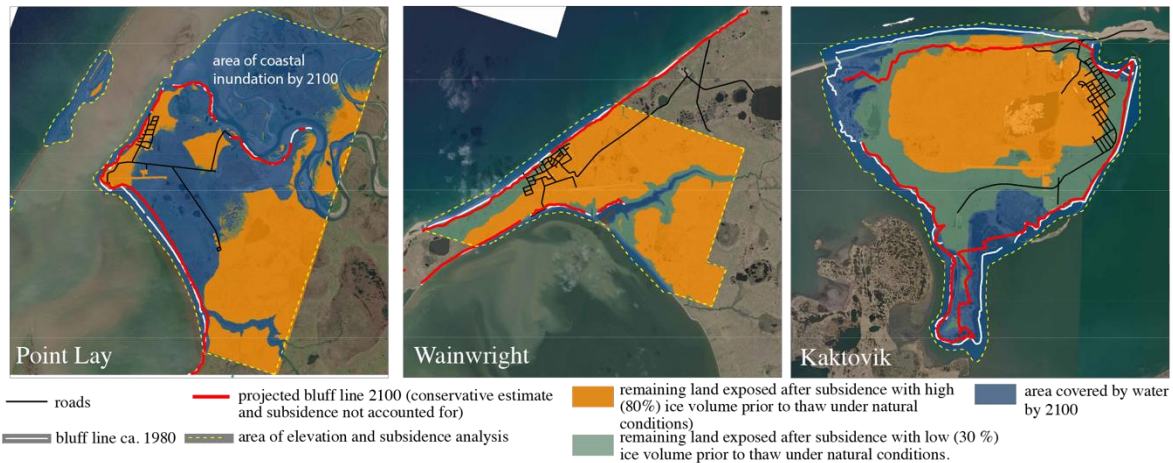


Figure 1. Coastal erosion and potential coastal inundation due to permafrost-thaw driven subsidence by 2100 under high (80%) and low (30%) ground ice conditions for Point Lay, Wainwright, and Kaktovik. Blue shows areas covered by water by 2100, orange shows remaining land under high ground ice conditions, turquoise shows remaining land under low ground ice conditions. Area of subsidence analysis outlined by yellow dotted line. Black lines delineate roads, white line delineates the coastlines in 1980, red line delineates coastline in 2100 without the effects of inundation.

Keywords: Coastal inundation, permafrost modelling, DEM analysis, infrastructure, hazard mapping

References

- Hjort, J., Karjalainen, O., Aalto, J., Westermann, S., Romanovsky, V.E., Nelson, F.E., Etzelmüller, B., Luoto, M., 2018. Degrading permafrost puts Arctic infrastructure at risk by mid-century. *Nature communications* 9, 5147.
- Irrgang, A.M., Bendixen, M., Farquharson, L., Baranskaya, A., Erikson, L., Gibbs, A., Ogorodov, S., Overduin, P.P., Lantuit, H., Grigoriev, M., Jones, B., 2022. Drivers, dynamics and impacts of changing Arctic coasts. *Nature Reviews Earth & Environment*.
- Irrgang, A.M., Lantuit, H., Gordon, R.R., Piskor, A., Manson, G.K., 2019. Impacts of past and future coastal changes on the yukon coast — threats for cultural sites, infrastructure, and travel routes. *Arctic Science*. <https://doi.org/10.1139/as-2017-0041>
- Nicolosky, D.J., Romanovsky, V.E., Panda, S.K., Marchenko, S.S., Muskett, R.R., 2017. Applicability of the ecosystem type approach to model permafrost dynamics across the Alaska North Slope. *Journal of Geophysical Research: Earth Surface*. <https://doi.org/10.1002/2016JF003852>
- Nielsen, D.M., Pieper, P., Barkhordarian, A., Overduin, P., Ilyina, T., Brovkin, V., Baehr, J., Dobrynin, M., 2022. Increase in Arctic coastal erosion and its sensitivity to warming in the twenty-first century. *Nature Climate Change* 1–8.

Acknowledgements This research is funded by National Science Foundation Awards ICER-1927708, OISE-1927553 and ICER-1928237.

Frederick: Space-based observations are critical for validating maps of arctic marine greenhouse gas emissions predicted with numerical models

Jennifer M. Frederick¹, William K. Eymold¹, Michael A. Nole¹, Benjamin Wagman², and Thomas Marchitto³

¹ Center for Energy & Earth Systems, Sandia National Laboratories, Albuquerque, NM, United States ² Center for Climate Change Security, Sandia National Laboratories, Albuquerque, NM, United States ³ Institute of Arctic and Alpine Research, University of Colorado, Boulder, CO, United States

Abstract

Researchers have recently estimated that Arctic submarine permafrost currently traps 60 billion tons of methane and contains 560 billion tons of organic carbon in seafloor sediments and soil (Sayedi et al. 2020), a giant pool of carbon with potentially large feedbacks on the climate system. For comparison, humans have released a total of ~500 billion tons of carbon into the atmosphere since the Industrial Revolution. Unlike terrestrial permafrost, the submarine permafrost system has remained a “known unknown” because of the difficulty in acquiring samples and measurements, and remains a wildcard in the Earth’s climate system.

We will present a work-in-progress which quantifies Arctic methane gas releases from the sediments to the water column, and potentially to the atmosphere, where positive climate feedback may occur, using newly developed modeling capability that allows us to probabilistically map gas distribution and quantity in the seabed by using a hybrid approach of geospatial machine learning and predictive numerical thermodynamic ensemble modeling (Frederick et al. 2021). The novelty in this approach is its ability to produce maps of useful data in regions that are only sparsely sampled, a common challenge in the Arctic, and a major obstacle to progress in the past. By applying this model to the circum-Arctic continental shelves and integrating the flux of free gas from dissociating gas hydrates and thawing submarine permafrost from the sediment column under climate forcing, we are working on providing the most reliable estimate of a time-varying source term for greenhouse gas flux that can be used by global oceanographic circulation and atmospheric climate models (such as DOE’s E3SM).

Space-based observations of atmospheric methane concentrations provide a unique opportunity to validate or constrain model predictions of emission rates from the shallow Arctic Ocean. However, not every satellite can provide useful information. Because of the high latitude, polar or near-polar orbits are required; and because the Arctic is dark in winter, instrumentation methods that do not depend on solar illumination are required for year-round

observations (such as thermal infrared (TIR) sounding). Even under such limitations, recent work presenting analysis of data from three TIR instruments onboard polar orbiting satellites has shown methane emissions from the Arctic Ocean as a whole may be as much as $\sim 2/3$ of the land emission (Yurganov et al. 2021), with significant emissions occurring during the winter months.

This presentation is intended to share our modeling techniques and current estimates of marine methane emissions, with a goal of integrating with the polar remote sensing community for model validation.

Keywords

methane; submarine permafrost; numerical modeling and prediction

References

Frederick, J. M., William K. Eymold, Michael A. Nole, Benjamin J. Phrampus, Taylor R. Lee, Warren T. Wood, David Fukuyama, Olin Carty, Hugh Daigle, Hongkyu Yoon, and Ethan Conley (2021), Forecasting Marine Sediment Properties with Geospatial Machine Learning, SAND2021-10675, Sandia National Laboratories, Albuquerque, NM.

Sayed, S. S., B. Abbott, B. Thornton, J. M. Frederick, J. Vonk, P. Overduin, C. Schadel, E. Schuur, A. Bourbonnais, A. Gavrilov, S. He, G. Hugelius, M. Jakobsson, M. Jones, D. Joung, G. Kraev, R. Macdonald, A. D. McGuire, C. Mu, M. O'Regan, K. Schreiner, C. Stranne, E. Pizhankova, A. Vasiliev, S. Westermann, J. P. Zarnetske, T. Zhang, M. Ghandehari, S. Baeumler, B. Brown, R. Frei, and A. Maslakov (2020), Subsea permafrost carbon stocks and climate change sensitivity estimated by expert assessment, *Environmental Research Letters*, Vol. 15, No. 12, doi:10.1088/1748-9326/abcc29.

Yurganov, L., D. Carroll, A. Pnyushkov, I. Polyakov, and H. Zhang. (2021) Ocean stratification and sea-ice cover in Barents and Kara seas modulate sea-air methane flux: satellite data. *Advances in Polar Science*, Vol. 32, No. 2: 118-140. doi: 10.13679/j.advps.2021.0006.

Acknowledgements

Sandia National Laboratories is a multimission laboratory managed and operated by National Technology and Engineering Solutions of Sandia, LLC., a wholly owned subsidiary of Honeywell International, Inc., for the U.S. Department of Energy's National Nuclear Security Administration under contract DE-NA-0003525. SAND2022-2967 A.

Grosse: A new dynamic land cover classification of the Arctic Lena Delta for scaling methane fluxes

Guido Grosse¹, Alexandra Runge¹, Simeon Lisovski², Birgit Heim², Philipp Jordan¹, Iuliia Shevtsova², Lars Kutzbach³, Ingmar Nitze¹, Christian Knoblauch³, Anne Morgenstern¹, Bennet Juhls¹, Matthias Fuchs¹, Ulrike Herzschuh², Nikolai Lashchinski^{4,5}

¹Permafrost Research Section, Alfred Wegener Institute for Polar and Marine Research, Potsdam, Germany

²Polar Terrestrial Environments Section, Alfred Wegener Institute for Polar and Marine Research, Potsdam, Germany

³Institute for Soil Science, University of Hamburg, Hamburg, Germany

⁴SIB Central Siberian Botanical Garden, Novosibirsk, Russia

⁵Novosibirsk State University, Novosibirsk, Russia

Abstract

Arctic permafrost wetlands are often characterized by overall high methane emissions during summer. However, at the local scale high methane emissions are usually linked to specific land cover (LC) classes while other classes have very low emissions or none at all. Therefore, a detailed characterization of these LC types is necessary to quantify landscape-scale methane fluxes. In addition, climate change may result in either gradual shifts between LC classes or abrupt changes due to disturbances, which is expected to affect the methane budget of Arctic wetlands. We here describe a new approach for methane emission upscaling for the Arctic Lena Delta building on remote sensing-based, dynamic LC classification considering gradual and abrupt LC changes for the period 2000-2020.

So far, a static LC classification exists for the delta based on a 30m-resolution multispectral Landsat-7 ETM+ image mosaic, composed of three images of July 2000 and 2001 (Schneider et al., 2009). New remote sensing resources and processing capabilities now opened the opportunity for an updated and enhanced quantification of LC change and its effects on landscape-scale methane fluxes in the Lena Delta. Our LC classification approach consists of two main steps: First, we performed a static LC classification for the central Lena Delta building an initial classification on training data of Elementary Sampling Units (ESUs). It included 30 x 30 m vegetation plots from field work in summer 2018 and additional ESUs assigned from comprehensive field knowledge from numerous expeditions to the central Lena Delta. This first robust LC training dataset was used to classify a mosaic of 10m resolution Sentinel-2 data from summer 2018 in Google Earth Engine (GEE). The LC classes were optimized to capture characteristics defined by landscape wetness and vegetation types with the goal of upscaling field-observed methane fluxes from these classes. LC classes are also linked to low and high disturbance regimes in different landscape settings in the delta. In total, 13 classes were differentiated (11 vegetated classes, 1 water class, 1 barren sand class) for the static LC map.

Second, based on the static LC classification we further extended the classification scheme to a dynamic model using additional satellite data for 2000 to 2020 (Sentinel-2, Landsat-5, -7 and -8)

to characterize LC changes at 30 m spatial and 5-year temporal resolution (2000-2005, 2006-2010, 2011-2015, 2016-2020). A flexible GEE classification pipeline was used to allow for dynamic classification schemes. Multi-sensor composite medoid mosaics were derived from cloud-free summer (July-August) imagery for the different time periods. Input for the classification were visible, near-, short-wave and mid-infrared multispectral bands, maximum NDVI, and elevation data from the Arctic DEM. Training data was derived from the static 2018 LC classification and then a random forest classifier was applied for the classification.

In addition to the dynamic LC components we applied class stratification to distinguish selected classes important for methane emissions that were spectrally difficult to differentiate with the multispectral input data from Landsat and Sentinel-2 alone. This includes (1) the differentiation of an additional class of wet polygonal tundra in drained thermokarst lake basins that was spectrally similar to wet polygonal tundra on yedoma uplands using elevation information from the ArcticDEM, (2) the differentiation of lakes in different size categories in agreement with the Boreal-Arctic Wetland and Lake Database (Olefeldt et al., 2021), and (3) the differentiation of deep and shallow delta channels according to their water depth as detected by winter Sentinel-1 SAR data (Juhls et al., 2021).

Our 20-year time series indicates a partial reduction in wet polygonal LC classes in the Lena Delta, which is particularly visible in the central Lena Delta on the ground ice-rich yedoma upland surfaces, suggesting enhanced drainage possibly associated with ice wedge degradation or drying due to general warming. Overall, LC trends between the four observation periods from 2000 to 2020 were rather subtle and continuous between neighboring classes. Abrupt changes were identified only at local scales, e.g. when larger lakes drained abruptly or where river shore erosion caused class shifts. In comparison to the overall LC dynamics, abrupt changes played only a minor role in the change of LC class areas so far.

Our dynamic LC remote sensing approach provides a first continuous 20-year observation of LC classes and their shifts in an Arctic delta. Attribution of methane observational data to individual classes and a quantification of changes in methane fluxes is work in progress.

Keywords: Permafrost wetlands, tundra, Google Earth Engine

References

Schneider J, Grosse G, Wagner D (2009): Land cover classification of tundra environments in the Arctic Lena Delta based on Landsat 7 ETM+ data and its application for upscaling of methane emissions. *Remote Sensing of Environment*, 113: 380-391. doi: 10.1016/j.rse.2008.10.013.

Juhls, B., Antonova, S., Angelopoulos, M., Bobrov, N., Langer, M., Maksimov, G., ... & Overduin, P. P. (2021). Serpentine (floating) ice channels and their interaction with riverbed permafrost in the Lena River Delta, Russia. *Frontiers in Earth Science*, 9, <https://doi.org/10.3389/feart.2021.689941>

Olefeldt, D., Hovemyr, M., Kuhn, M. A., Bastviken, D., Bohn, T. J., Connolly, J., Crill, P., Euskirchen, E. S., Finkelstein, S. A., Genet, H., Grosse, G., Harris, L. I., Heffernan, L., Helbig, M., Hugelius, G., Hutchins, R., Juutinen, S., Lara, M. J., Malhotra, A., Manies, K., McGuire, A. D., Natali, S. M., O'Donnell, J. A., Parmentier, F.-J. W., Räsänen, A., Schädel, C., Sonntag, O., Strack, M., Tank, S. E., Treat, C., Varner, R. K., Virtanen, T., Warren, R. K., and Watts, J. D.: The Boreal–Arctic Wetland

and Lake Dataset (BAWLD), Earth Syst. Sci. Data, 13, 5127–5149, <https://doi.org/10.5194/essd-13-5127-2021>, 2021.

Acknowledgements

This research was funded by the BMBF projects KoPF and KoPF Synthesis.

Hanston: Scaling spectral and structural characterizations of vegetation and landscape features along permafrost thaw gradients in Arctic tundra

Wouter Hantson¹, Daniel Hayes^{1*}, Dedi Yang², Shawn Serbin²

¹School of Forest Resources, University of Maine, Orono, ME, USA

²Environmental and Climate Sciences Department, Brookhaven National Laboratory, Upton, NY, USA

* Presenting author

Abstract

The effects of anthropogenic climate change are visible at all scales in the Arctic-Boreal Region (ABR), from locally-degraded ice wedges and thermokarst features in permafrost landscapes, to biome-scale greening/browning trends across the northern high-latitudes. Using remote sensing we can observe landscape disturbances and associated changes in vegetation patterns, such as the distinct tussock–graminoid patterns, that are indicative of underlying ice wedge melting and permafrost degradation. Observing permafrost disturbance in the ABR is challenging due to the spatio-temporal variability of the active layer, the complex interactions between vegetation cover and permafrost (McGuire et al. 2002), and variable ground ice content that results in large heterogeneity across regions. A key research question is: *At what scale do the observed spatial patterns from RS correspond with thaw depth and is there an effect of disturbances?*

Here, we investigate this question across scales - from new collections of high resolution, UAV-based imagery to the medium resolution Landsat historical record - for characterizing local- to landscape vegetation patterns in relation to thaw depth modeling for tundra landscapes on the Seward Peninsula, Alaska. Field-based transects of thaw depth, vegetation status, and hyperspectral scans covering a gradient of thermokarst and other disturbance features are used as training and validation data. Thaw depth is modeled with RandomForest on rescaled UAV imagery and the dominant landscape and vegetation patterns are analyzed at the different scales using wavelet and variograms. The dominant scales are characterized for landscapes that vary from monotone to highly heterogeneous. Observed scales are compared to the thaw feature scale.

The Optimum Feature Scale (OFS) combines the optimum modeling scale and the optimal observation scale. Using the OFS creates synergy between datasets and the features studied and will overcome the spectral- and spatial- scale mismatches as means to understand the vegetation

and underlying permafrost changes for the ABR. OFS is useful for planning field sampling, selecting imagery, and modeling strategies. As a case study, the UAV imagery was collected under the AVIRIS-NG flight lines from ABoVE (Miller et al. 2018). The processed AVIRIS-NG hyperspectral imagery is used to detect small changes in vegetation traits and characteristics (Serbin and Yang 2021) that could be a first indication of thaw-driven changes in active layer, hydrology, or nutrient availability. By selecting the spectral vegetation traits that correlate with the disturbance patterns, we created a Thaw Functional Trait (TFT) spatial data sets for high resolution mapping of the resilience of permafrost to future warming. The different observed disturbance and thaw features from the TFT dataset is compared with the OFS determined from the remote sensing analysis.

Keywords

thermokarst, scaling, Seward Peninsula

References

- McGuire, A. D., C. Wirth, M. Apps, J. Beringer, J. Clein, H. Epstein, D. W. Kicklighter, et al. 2002. "Environmental Variation, Vegetation Distribution, Carbon Dynamics and Water/energy Exchange at High Latitudes." *Journal of Vegetation Science: Official Organ of the International Association for Vegetation Science* 13 (3): 301–14.
- Miller, C. E., P. C. Griffith, S. J. Goetz, D. J. Hodkinson, E. K. Larson, E. S. Kasischke, H. A. Margolis, and E. E. Hoy. 2018. "The Arctic Boreal Vulnerability Experiment (ABoVE) Airborne Campaign."
- Serbin, Shawn, and Dedi Yang. 2021. "Maps of Arctic Vegetation Leaf Nitrogen Concentration, Albedo and Plant Functional Type (PFT) Derived from Imaging Spectroscopy Data, Council Watershed, Seward Peninsula, Alaska, 2019." Next Generation Ecosystems Experiment-Arctic, Oak Ridge National Laboratory. <https://www.osti.gov/biblio/1838174>.
- Yang, D., Morrison, B.D., Hantson, W., Breen, A.L., McMahon, A., Li, Q., Salmon, V.G., Hayes, D.J. and Serbin, S.P. (2021). Landscape-scale characterization of Arctic tundra vegetation composition, structure, and function with a multi-sensor unoccupied aerial system. *Environmental Research Letters*, 16 (8), 085005.

Acknowledgements

This work is supported by the Next-Generation Ecosystem Experiments (NGEE Arctic) project under the Office of Biological and Environmental Research in the United States Department of Energy, Office of Science, with subcontracts to Oak Ridge National Laboratory and Brookhaven National Laboratory.

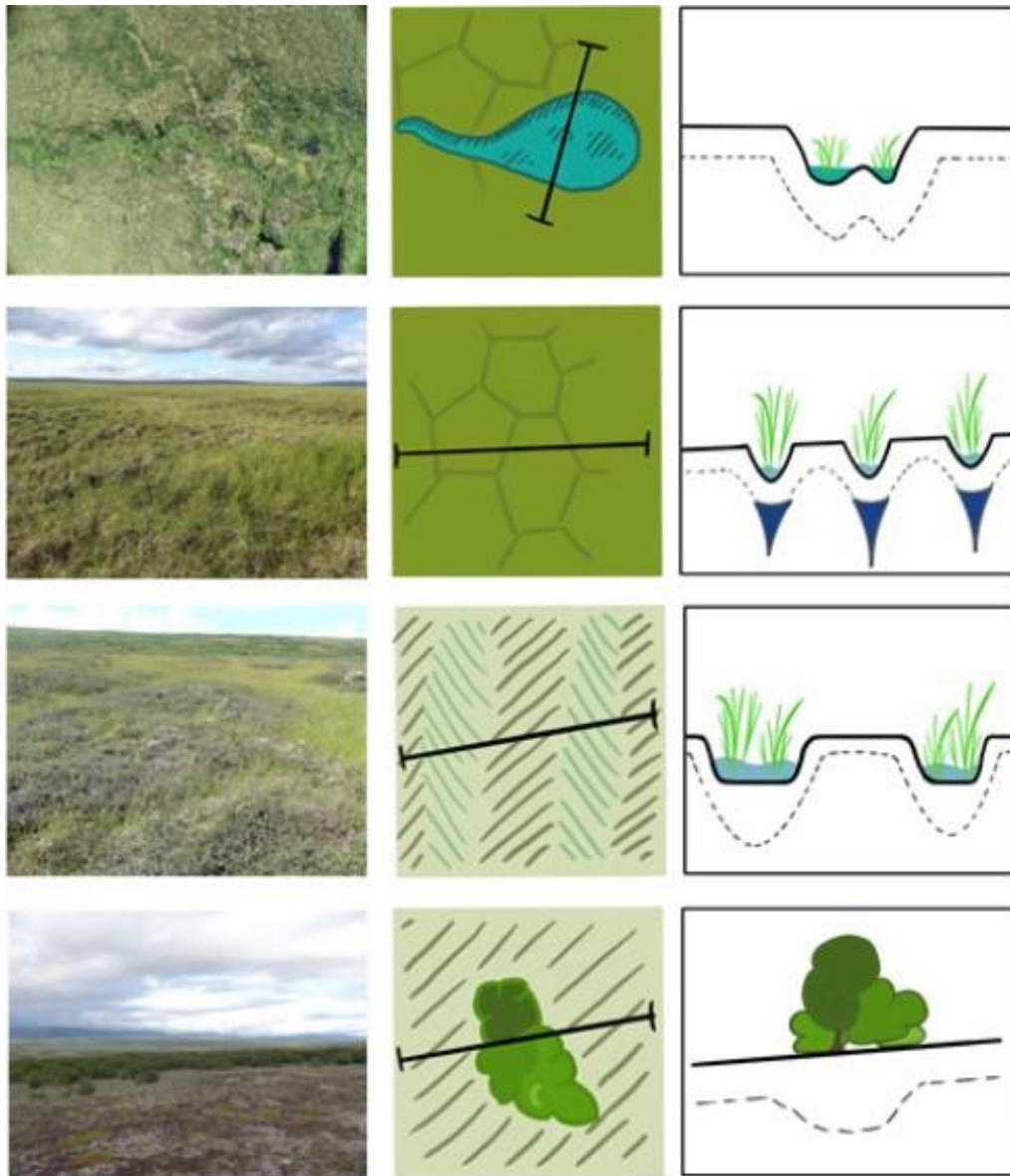


Figure 1. Conceptual overview of the thaw gradients covered in this study. 1. Thaw lakes, sometimes drained, leave small to large depressions in the tundra landscape. Typical vegetation: Dry tussock- and dwarf-shrub tundra shifting to Tussock-sedge, moss tundra in the depressions; 2. Ice wedge polygon tundra with intermediate and complete degraded ice wedges creating depressions above the ice wedge polygon structure, sometimes drained toward a water track leading to deeper channels. Polygon complex of wet graminoid dominated and dry tussock-sedge, dwarf-shrub lichen tundra; 3. Water tracks in a moderate tundra landscape create linear patterns of drier upland dwarf shrub tundra and wetter depressions with more sedge dominated tundra. Linear complex of wet sedges and dwarf shrub lichen tundra; 4. Shrub encroachment in the tundra landscape. Complex of low-shrub tundra and Alder shrubland/tall shrub thickets. Average transect is approximately 50m.

Helder: Exploring the reliability and scalability of automated shoreline detection tools for the Alaskan Arctic

Noelle K. Helder^{1,2}, Heike Merkel², Jeremy Kasper², and Erin Trochim²

¹Alaska Sea Grant, Fairbanks, AK, United States

²University of Alaska Fairbanks, Alaska Center for Energy & Power, Fairbanks, AK, United States

Abstract

Arctic coastlines are changing rapidly in the face of global climate change, which puts coastal communities and infrastructure at risk. Assessing coastal change is challenged by the limited availability of observational data and by the remoteness of Arctic coasts. Remote sensing data products have emerged as a promising solution to help fill these critical data gaps, with a corresponding proliferation of methods and tools to delineate shoreline positions from optical imagery. However, such approaches are often implemented at relatively small (i.e., 10s – 100s of km) spatial scales with optically clear water conditions, and their scalability for region-wide applications in turbid Arctic waters remains largely unexplored. Here, we test the applicability and scalability of a Google Earth Engine-enabled Python toolkit to automatically detect shoreline positions from publicly-available (Landsat-5-8 and Sentinel-2) satellite imagery along Alaska's northern coastline. First, we explore image preprocessing pipelines to better filter for key images that are spatially extensive and temporally representative of true coastal changes. To date, coastline image classification has used images collected on a specific date, rather than aggregating through a time period. Then we applied the CoastSat classification methodology, which begins by automatically detecting shoreline positions from historical imagery and then uses a supervised image classification approach with sub-pixel border segmentation. Our goal is to quantify rates of shoreline change over time and compare our results with previously-published regional data. We also aim to compare these outputs with an emerging capability to detect shorelines using high resolution, near-daily PlanetScope cubesats. Additionally, we identify scaling issues and discuss analytical bottlenecks in the existing shoreline detection pipelines as applied to remote Arctic coastlines. Preliminary results suggest that this approach can efficiently detect shoreline positions from optical imagery, which may open up a largely untapped source of data to better quantify and predict shoreline behavior in the Arctic. With a growing archive of available satellite imagery, automatic shoreline detection tools have enormous potential to serve as a continually-updating monitoring tool in the face of rapid coastal change.

Keywords: Google Earth Engine; shoreline mapping; CoastSat

References

Doherty, Y., Harley, M. D., Vos, K., & Splinter, K. D. (n.d.). A Python toolkit to monitor high-resolution shoreline change using PlanetScope cubesats, 37.

Gibbs, A. E., & Richmond, B. M. (2017). *National Assessment of Shoreline Change—Summary Statistics for Updated Vector Shorelines and Associated Shoreline Change Data for the North Coast of Alaska, U.S.-Canadian Border to Icy Cape* (Open-File Report No. 2017–1107).

Vos, K., Splinter, K. D., Harley, M. D., Simmons, J. A., & Turner, I. L. (2019). CoastSat: A Google Earth Engine-enabled Python toolkit to extract shorelines from publicly available satellite imagery. *Environmental Modelling & Software*, 122, 104528.
<https://doi.org/10.1016/j.envsoft.2019.104528>

Hessilt: Influences of snowmelt timing on arctic-boreal fire season start across North America

Thomas Duchnik Hessilt¹, Brendan M. Rogers², Stefano Potter², Rebecca C. Scholten¹ and Sander Veraverbeke¹

¹Faculty of Science, Vrije Universiteit Amsterdam, Amsterdam, North Holland, The Netherlands

²Woodwell Climate Research Center, Falmouth, MA, USA

Abstract

Snowmelt timing importantly influences arctic-boreal ecosystem functioning through influences on surface hydrology and energy balance. Since the mid-20th century, spring snow cover extent in the Northern Hemisphere has reduced up to 46 % in June with a strong decrease after the mid-1980s. Over the same time period, parts of arctic-boreal North America have experienced increases in fires. An earlier snowmelt may lead to earlier seasonal occurrence of topsoil drying, thereby increasing the likelihood of early fire ignitions. Earlier fires also tend to grow larger as a lengthening fire season extends the likelihood of fire weather conditions favourable for fire spread. Understanding changes in fire season length and the relationship between snowmelt, ignitions and fire size is important to predict the future fire regimes arctic-boreal North America. We evaluated the timing of snowmelt and fire ignition at an ecoregion level across arctic-boreal North America between 1967 to 2019. We thereby also discriminated between lightning and anthropogenic fires.

We found that snowmelt timing has occurred 0.2 ± 0.17 days earlier between 1967 and 2019 in western arctic-boreal North America, whereas snowmelt timing has shifted to a later occurrence with 0.27 ± 0.33 days between 1967 and 2019 in the eastern part of arctic-boreal North America. From 1967 to 2019, the average day of lightning-ignition has continuously occurred 0.61 ± 1.12 days year⁻¹ earlier and 0.3 ± 0.58 days year⁻¹ later for the western and eastern ecoregions, respectively. We observed significant positive relationships ($p < 0.01$) between the timing of snowmelt and ignition for the majority of the ecoregions, suggesting that snowmelt timing exerts a large control on fire season start. In the western ecoregions, we believe earlier snowmelt and ignition are mainly driven by increases in temperature and vapour pressure deficit in spring. We suggest the higher amounts of winter precipitation explains the later snowmelt and fire season start in the eastern ecoregions. Our results show that the fire season start has shifted in response to changing snowmelt timing across arctic-boreal North America.

Jones: High spatial and temporal resolution remote sensing of a collapsing pingo in northern Alaska

Benjamin M. Jones¹, Frank Urban², Aiman Soliman³, Mikhail Z. Kanevskiy¹, Melissa K. Ward Jones¹, Louise Farquharson⁴, Mary Heise⁵, Helena Bergstedt⁶, Amy Breen⁷, Yuri Shur¹, and Kenneth M. Hinkel⁸

¹Institute of Northern Engineering, UAF, Fairbanks, Alaska USA

²U.S. Geological Survey, Denver, CO USA

³National Center for Supercomputing Applications, University of Illinois, Champaign, Illinois USA

⁴Geophysical Institute, UAF, Fairbanks, Alaska USA

⁵Polar Geospatial Center, University of Minnesota, Minneapolis, MN USA

⁶b.geos, Vienna, Austria

⁷International Arctic Research Center, UAF, Fairbanks, Alaska USA

⁸Michigan Tech University, Houghton, MI USA

Abstract

Pingos are ice-cored mounds occurring in permafrost regions that form through processes associated with the injection and subsequent freezing of groundwater (Mackay, 1973). In the continuous permafrost zone of northern Alaska, formation of pingos occurs mainly because of freezing of taliks in basins following lake drainage (Jones et al., 2012). Here, we document the rapid collapse of a 10 m high pingo that developed in a 2,000 year old drained lake basin in northern Alaska using historic aerial photography, high-resolution satellite imagery, Arctic DEM data (Figure 1), and repeat UAV surveys. A small (45 sq. m) thermokarst depression appeared on the pingo summit in 2010. The depression expanded laterally at a rate of 72 sq. m/yr between 2010 and 2016, with a marked increase in expansion (326 sq. m/yr) between 2016 and 2020. Mean thaw subsidence rates fluctuated between 0.06 and 0.36 m/yr between 2013 and 2018, more than doubling (0.83 m/yr) between 2018 and 2020. Pingo degradation was initially limited by slumping of material that protected the ice core at depth. Drainage of the thermokarst pond in 2017, likely through piping in open frost cracks developed on the flank of the pingo, helped facilitate the rapid pingo collapse that ensued. Sub-lateral drainage of the pond caused evacuation of slumped material from the internal walls of the collapsing pingo, exposing the ice core at depth. A brief site visit to the collapsing pingo in May 2021 revealed a complex pattern of near-surface ice-rich deposits with large bodies of massive ground ice (including intrusive ice, wedge ice, and dilation-crack ice) remaining on the western flank of the pingo and a very thin overburden of organic rich sediments at the surface. The rapid collapse of the pingo was likely triggered by climate-driven increases in active layer that affected the top of the pingo ice core, resulting in more than 60 % of its volume being lost through thermokarst processes in less than ten years. Detailed spatial and temporal observations of the collapsing pingo in northern Alaska provide valuable information for training a deep learning algorithm to more broadly track pingo dynamics using ArcticDEM time series data.

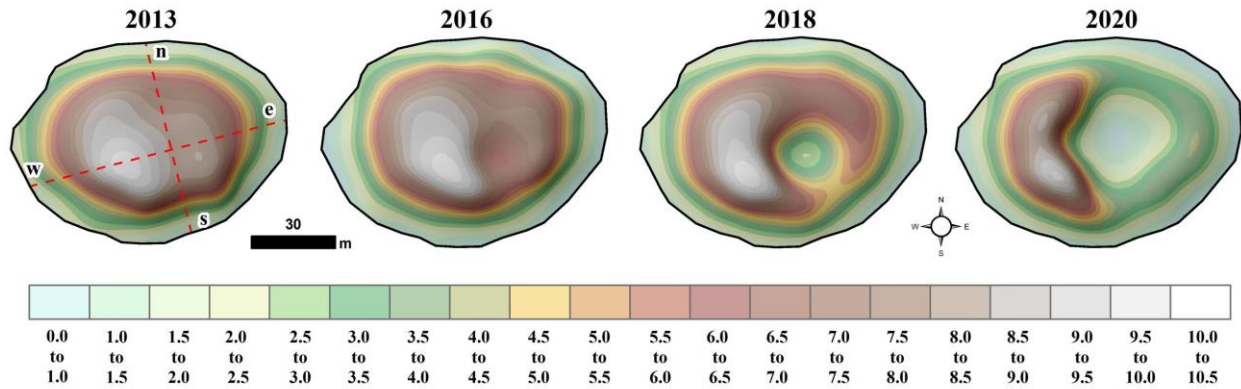


Figure 3. ArcticDEM time series showing collapse of the pingo between 2013 and 2020.

Keywords: Permafrost, pingos, thermokarst

References

- Jones, B.M., Grosse, G., Hinkel, K.M., Arp, C.D., Walker, S., Beck, R.A. and Galloway, J.P., 2012. Assessment of pingo distribution and morphometry using an IfSAR derived digital surface model, western Arctic Coastal Plain, Northern Alaska. *Geomorphology*, 138(1), pp.1-14.
- Mackay, J.R., 1973. The growth of pingos, western Arctic coast, Canada. *Canadian Journal of Earth Sciences*, 10(6), pp.979-1004.

Acknowledgements: Funding for this research provided by National Science Foundation grants OPP 1806213, OPP 1806287, OIA 1929170, and ICER 1927872.

Kelkar: Applying DInSAR for rock glacier inventories

Kaytan Kelkar¹, Louise Farquharson¹, Franz Meyer^{2,3}, Simon Zwieback², Alex Lewandowski³

¹University of Alaska, Fairbanks (Geophysical Institute Permafrost Laboratory, Fairbanks, Alaska, USA)

²University of Alaska, Fairbanks (Geophysical Institute, Fairbanks, Alaska, USA)

³Alaska Satellite Facility (Geophysical Institute, Fairbanks, Alaska, USA)

Abstract

Rock glaciers are striking landforms that consist of a perennially frozen ice/rock matrix, which gradually undergoes slope displacement on permafrost affected slopes (Wahrhaftig and Cox, 1959). These periglacial landforms provide valuable insight into mountain permafrost conditions. Ongoing warming of air and ground surface temperatures is driving a shift in mountain permafrost thermal regimes. As a result, accelerated rock glacier creep and deforming periglacial slopes pose a threat to the built environment in mountain terrain. Thus, monitoring rock glacier kinematics is key to interpreting the role of mountain permafrost in slope instability in better predicting the occurrence of permafrost related geohazards in mountain communities. In the last decade, satellite radar interferometry (InSAR) remote sensing techniques have been widely used to track rock glacier movement rates (Barboux et al., 2014). InSAR is an effective tool capable of locating minute creep to the order of cm/yr. The use of InSAR to develop rock glacier inventories is largely limited to the European Alps, yet there is a growing need to initiate rock glacier inventories in mountain permafrost sites across the world.

We propose to investigate creep rates of the Manissuarsuk rock glacier in Greenland. The Manissuarsuk is a tongue-shaped large rock glacier terminating on the eastern shore of Disko Island (Figure 1). Strozzi et al., 2020 previously created a time series of motion for the Manissuarsuk rock glacier from January 2015 to January 2020. InSAR time series analysis will be conducted using the C-band (wavelength 5.6 cm) Sentinel-1 data for the duration of June 1st 2020 to August 31st 2020. Our workflow will include short temporal baselines to build on Strozzi et al., 2020's work to analyze and examine creep dynamics in the summer months. This proposed study will serve as a framework for future rock glacier kinematic investigations. We aim to further expand this methodology to develop a rock glacier inventory in Denali National Park, Alaska, and the central Alaska Range, which will greatly improve our understanding of spatiotemporal rock glacier dynamics in Alaska (Rick et al., 2015). Results from this effort will also contribute to a better understanding of regional mountain permafrost evolution in permafrost affected mountains within Alaska.



Figure 1. Manissuarsuk is a large rock glacier situated in western Greenland on Disko Island (red rectangle on inset map).

Keywords: Rock glaciers; creep; InSAR

References

Barboux, C., Delaloye, R., and Lambiel, C. (2014). Inventorying slope movement sin an Alpine environment using DInSAR. *Earth Surface Processes and Landforms*, 39, 2087-2099. <https://doi.org/10.1002/esp.3603>

Rick, B., Delaloye, R., Barboux, C., Strozzi, T. (2015). Detecttton and inventorying of slope movements in the Brooks Range, Alaska using DInSARL a test study. *Proceedings of the GEOQuebec (2015)*.

Strozzi, T., Caduff, R., Jones, N., Barboux, C., Delaloye, R., Bodin, X., Kaab, A., Matzler, E., Schrott, L. (2020). Monitoring rock glacier kinematics with Satellite Synthetic Aperture Radar. *Remote Sensing*. 12(3), 559. <https://doi.org/10.3390/rs12030559>

Wahrhaftig, C. and Cox, A. (1959). Rock glaciers in the Alaska Range. *Geological Society of America Bulletin*, 70, 383-436. [https://doi.org/10.1130/0016-7606\(1959\)70\[383:RGITAR\]2.0CO;2](https://doi.org/10.1130/0016-7606(1959)70[383:RGITAR]2.0CO;2)

Acknowledgements We thank Dr. Franz Meyer, Dr. Simon Zweiback, and Alex Lewandowski for their valuable guidance in InSAR data processing.

Kuhle: Quantifying peat carbon mass using ground-penetrating radar (GPR) in high-latitude peatlands of the Kenai Peninsula, Alaska

Cameron Kuhle¹, Eric Klein², Ed Berg³

¹Department of Geological Sciences, University of Alaska Anchorage, Anchorage, AK, USA

²Department of Geological Sciences, University of Alaska Anchorage, Anchorage, AK, USA

³Kenai National Wildlife Refuge, U.S. Fish & Wildlife Service, Soldotna, AK, USA (Retired)

Abstract

In this ongoing project, we estimate carbon mass in peatlands within the Kenai National Wildlife Refuge (KENWR) in southcentral Alaska using ground-penetrating radar (GPR) and soil chemical analyses, with field data collection and analysis occurring through spring and summer 2022. Peat carbon is known to be one of the largest pools of soil carbon globally and is sensitive to environmental and climatic changes. Peatlands in KENWR have been studied for their hydrology, vegetation composition and succession, accumulation, and similar characteristics, but the mass of stored carbon is yet unknown. We expect KENWR peatlands to comprise significant reserves of sequestered carbon and are using a synthesis of soil and wetland surveying techniques to better constrain estimates of regional contributions to global values. A low-frequency (100 MHz) GPR instrument is utilized at sites selected for suitable topography and hydrology to measure peat basal layer depth, and to identify intervening layers where possible. Peat radar velocity is calibrated with manual depth probing to ensure accuracy of measurements, allowing GPR to be used to collect a much greater volume of data points than probing alone. Concurrent GPS data collection enables pairing of GPR depths to available regional LiDAR measurements, from which a geographically-tied model of thickness is derived and interpolated to generate a basin volume estimate. Peat cores are extracted from each site, and sampled at regular intervals for chemical analyses, to be conducted at UAA or partner laboratories. Carbon content by mass percent will inform the primary study objective, while ancillary analyses of carbon isotopes, organic content, nitrogen content, radiocarbon dating, and bulk density will contextualize the data and potentially identify historical trends. The carbon content and bulk density data will enable the calculation of total carbon mass given the basin volume estimate developed from the GPR survey. Understanding the stored carbon mass in peatlands is integral to anticipating the impacts of their responses to climate change, giving them value beyond their known functions with regard to conservation and restoration.

Keywords: Peatland, carbon, GPR

References

Carless, D., Kulesa, B., Booth, A.D., Drocourt, Y., Sinnadurai, P., Alayne Street-Perrott, F., Jansson, P., 2021, An integrated geophysical and GIS based approach improves estimation of peatland carbon stocks: *Geoderma*, v. 402, 115176, doi:10.1016/j.geoderma.2021.115176.

- Comas, X., Slater, L. and Reeve, A., 2004, Geophysical evidence for peat basin morphology and stratigraphic controls on vegetation observed in a Northern Peatland: *Journal of Hydrology*, v. 295(1-4), p. 173-184, doi:10.1016/j.jhydrol.2004.03.008.
- Loisel, J. and Yu, Z., 2013, Recent acceleration of carbon accumulation in a boreal peatland, south central Alaska: *Journal of Geophysical Research: Biogeosciences*, v. 118(1), p. 41-53, doi:10.1002/grl.50744.
- Parsekian, A.D., Slater, L., Ntarlagiannis, D., Nolan, J., Sebesteyen, S.D., Kolka, R.K., Hanson, P.J., 2012, Uncertainty in peat volume and soil carbon estimated using ground-penetrating radar and probing: *Soil Sci. Soc. Am. J.*, v. 76, p. 1911-1918, doi:10.2136/sssaj2012.0040.
- Xu, J., Morris, P.J., Liu, J. and Holden, J., 2018, PEATMAP: Refining estimates of global peatland distribution based on a meta-analysis: *Catena*, v. 160, p. 134-140, doi:10.1016/j.catena.2017.09.010

Acknowledgements

We thank Jens Munk of the University of Alaska Anchorage Electrical Engineering Department for loan of the GPR instrument, and Nolan Vlahovich for field assistance. The data collected by the Homer Drawdown citizen scientists, while not used in these analyses, was instrumental in conceiving the project and testing the GPR. The research was funded in part by the Kenai National Wildlife Refuge.

Lara: Mapping arctic-boreal peatlands in Alaska: implications for historical peatland fire dynamics

Mark J. Lara^{1,2}, Umakant Mishra³, Sarah N. Scott⁴

¹Department of Plant Biology, University of Illinois, Urbana, IL, USA

²Department of Geography, University of Illinois, Urbana, IL, USA

³Computational Bio & Biophysics, Sandia National Laboratories, Livermore, CA, USA

⁴Thermal/Fluids Science and Engineering, Sandia National Laboratories, Livermore, CA, USA

Abstract

Northern peatlands contain between 300 and 600 PgC, representing a globally important pool of carbon and nutrients. During recent summers (i.e., 2019, 2020, and 2021), anomalously warm and dry climatic conditions increased wildfires across the Arctic and Boreal zones (ABZ), likely elevating the prevalence of peatland fires. Though the combustion of peat has direct implications for carbon-climate feedbacks, our fundamental understanding of the spatial distribution of peatlands has been largely limited to coarse spatial scales (≥ 500 m resolutions), thus representing a disconnect between typical heterogeneous patterns of burns and the heterogeneous distribution of peatlands across the ABZ of Alaska. Here we developed a new ABZ high-resolution (10 m resolution) peatland map using a data-fusion of Sentinel-1 (Dual-polarized Synthetic Aperture Radar), Sentinel-2 (Multi-Spectral Imager), and Arctic Digital Elevation Model (Arctic DEM) derivatives. The machine learning classification was guided by over 300 peat cores, ground observations, and sub-meter resolution image interpretation; and spatially constrained by a suitability model developed using a topographic cost-function that determined the terrain suitable for peat accumulation. We used these peatland maps to examine the area and type of peatland impacted by fire across the ABZ of Alaska between 1985 and 2021. Preliminary results indicate (1) high accuracy of ABZ peatland maps and (2) historical wildfire activity disproportionately impacted treed bogs/fens, and wildfire in open bogs/fens increased over time. Such high-resolution peatland maps (e.g., size, location, and extent) will reduce uncertainties in projected carbon-climate feedbacks in response to wildfire disturbance across northern ecosystems.

Keywords peatlands, wildland fires, data-fusion

Acknowledgements This research was supported by the U.S. Department of Energy (DOE, DE-NA0003525 to MJL, UM, and SNS) and the National Science Foundation (NSF, EnvE-1928048 to MJL). Sandia National Laboratories is a multi-mission laboratory managed and operated by national Technology and Engineering Solutions of Sandia, LLC., a wholly owned subsidiary of Honeywell International, Inc. for the DOE National Nuclear Security Administration. Any use of trade, firm, or product names is for descriptive purposes only and does not imply endorsement by the U.S. Government.

Martin: Estimating tall shrub biomass in southcentral Alaska

Kaili Martin¹, Dr. Roman Dial¹, Dr. Erin Larson¹, Hans-Erik Andersen²

¹ Institute of Culture and Environment, Alaska Pacific University, Anchorage, AK

² USDA Forest Service Pacific Northwest Research Station, University of Washington, Seattle, WA

Abstract

One of the many ecosystem consequences of a warming climate is the expansion of shrubs into higher elevations and latitudes. Research has shown that, in Alaska, shrubs are increasing in abundance across Arctic, boreal, and montane ecosystems due to warming. In addition to growing faster, reaching maturity sooner, and dispersing farther than dominant tree genera, shrubs demonstrate rapid community in-filling, leading to increased shrub biomass and shrub dominated landscapes. This encroachment can lead to alterations in carbon cycling, soil nutrient dynamics, albedo, and wildlife habitats. As shrub expansion continues, there will be complex cascading effects on the surrounding ecosystem with ramifications for organisms that inhabit these areas. The increase of shrub biomass also represents a potentially significant change to regional carbon dynamics that is currently unaccounted for in federal survey programs. The addition of shrubs to these survey programs is accompanied by logistic and financial difficulties given the locations and scale of shrub expansion. Having a feasible, robust method to apply shrub biomass estimations at a landscape level would be useful, in particular for calculating their role in carbon sequestration. For this study, we used taxon-specific allometric equations for two common tall shrub taxa, willow (*Salix* spp.) and alder (*Alnus* spp.), to calculate plot-level biomass. Over the summers of 2020 and 2021, we visited a total of 385 plots across 11 sites in the Susitna and Copper River basins in southcentral. Using the calculated plot-level biomass as our response variable, we included metrics from the NASA Goddard's Lidar, Hyperspectral, and Thermal Airborne Imager (G-LiHT; ~3.1 cm pixels) and PRISM temperature and precipitation data (30-year mean, 800 m pixel) as our predictor variables to build shrub probability and biomass models. Preliminary modeling efforts indicate that canopy height (m agl), elevation (m asl), and summer air temperature (°C) are important factors to include when modeling shrub biomass. The best performing shrub probability model was an additive GAM (AUC 0.93, Kappa 0.69) using the square root of mean canopy height (m agl), maximum canopy height (m agl), mean elevation (m asl), and summer air temperature (°C). This model incorporated shrub data from all 385 plots. The best performing shrub biomass model was an additive linear regression using the logged mean canopy height (m agl) and mean elevation (m asl) with a plot-level canopy height cutoff of 6 m agl ($R^2 = 0.74$). This model incorporated a subset

of shrub data from 86 plots, all with canopy height cutoffs of 6 m agl or less. Next steps include investigation and analysis of pixel-level canopy height cutoffs across all sites, incorporating field-collected tree data into modelling, multiplying the best probability and biomass models to give an adjusted shrub biomass estimation, and obtaining a baseline of shrub biomass for the Susitna and Copper River basins. We seek to develop an applicable and accurate shrub biomass model that will aid in future monitoring efforts throughout southcentral Alaska.

Keywords LiDAR; shrub, biomass

References

- Alonzo, M., Dial, R.J., Schulz, B.K., Andersen, H.E., Lewis-Clark, E., Cook, B.D. and Morton, D.C., 2020. Mapping tall shrub biomass in Alaska at landscape scale using structure-from-motion photogrammetry and lidar. *Remote Sensing of Environment*, 245, p.111841.
- Dial, Roman J.; Schulz, Bethany; Lewis-Clark, Eric; Martin, Kaili; Andersen, Hans-Erik. 2021. Using fractal self-similarity to increase precision of shrub biomass estimates. *Ecology and Evolution*. 11(9): 4866-4873.
- Greaves, H.E., Eitel, J.U., Vierling, L.A., Boelman, N.T., Griffin, K.L., Magney, T.S. and Prager, C.M., 2019. 20 cm resolution mapping of tundra vegetation communities provides an ecological baseline for important research areas in a changing Arctic environment. *Environmental Research Communications*, 1(10), p.105004.
- Myers-Smith, I. H. et al. 2011. Shrub expansion in tundra ecosystems: dynamics, impacts and research priorities. *Environ. Res. Lett.* 6: 045509.
- Terskaia, A., Dial, R.J. & Sullivan, P.F. 2020. Pathways of tundra encroachment by trees and tall shrubs in the western Brooks Range of Alaska, *Ecography (Copenhagen)*, vol. 43, no. 5, pp. 769-778.

Acknowledgements

Funding for this research was provided by the United States Forest Service. We thank and acknowledge the field assistance of Amy Wockenfuss, Russell Wong, Madeline Zietlow, Julia Ditto, Toshio Matsuoka, Kinkela Vicich, Scout Donahue, Allen Dahl, Lyreshka Castro-Morales, and Madeline Sadler.

Nole: Predicting permafrost greenhouse gas emissions by linking local and space-based observations through large-scale thermo-hydrologic modeling

Michael Nole¹, Jennifer M. Frederick¹, William K. Eymold¹

¹Center for Energy and Earth Systems, Sandia National Laboratories, Albuquerque, NM, United States

Abstract

Between 2007 and 2016, the top 3 meters of Arctic permafrost warmed an average of 0.4°C (Biskaborn et al., 2019); studies predict a large but uncertain areal extent over which the top permafrost layer could completely thaw by 2100 (0.2-58.8 x10³ km²/year; McGuire et al., 2018). Widespread permafrost thaw is expected to increase microbial activity in previously frozen soils, leading to more rapid degradation of organic matter. Degradation of organic matter generates potent greenhouse gases (GHG's) like CO₂ and CH₄. Currently, Arctic GHG emissions take the form of mostly microbially-mediated CO₂ release because of the predominance of gradual thaws over large regions, which are more often dry-thaw events characterized by aerobic degradation of organic matter (Johnston et al., 2017). However, the composition of Arctic GHG emissions could shift if there is an increase in the prevalence of rapid thaw events (e.g., thermokarst lake development; Figure 1), which can produce anoxic conditions where methanogens convert organic carbon into CH₄. The shift in Arctic GHG emissions toward CH₄ can have devastating climate consequences, as CH₄ has nearly 30 times the warming potential as CO₂ on a 100-year time horizon (IPCC, 2014).

Constraining regional microbially-mediated CO₂ and CH₄ emissions from thawing Arctic permafrost is therefore extremely important in order to understand the potential climate consequences of their release. But this can only be done through a combination of local measurements at ground-level, remote sensing over large regions, and upscaling methods to bridge the gap in scales between these two types of measurements. Regional-scale modeling can be an effective tool for upscaling, but it must consider coupled feedbacks between regionally varying permafrost thaw behavior, heterogeneous carbon distribution, and associated production of GHG's like CO₂ and CH₄. This is inherently a multiphase flow and biogeochemical reactive transport problem which depends heavily on sediment type, organic carbon content, and permafrost thaw behavior.

In this work we demonstrate the early development of our subsurface, massively parallel, multiphase flow and reactive transport simulator, PFLOTRAN, to model large-scale permafrost thawing. We present simple benchmarking case studies illustrating the potential dynamics between thawing permafrost and gas flux from sediments. Then, we demonstrate the capability at a regional scale to model heterogeneous permafrost thawing. Future work will include extension of the framework to capture coupled thermo-hydro-biogeochemical processes to produce estimates of carbon fluxes as a function of thaw behavior. Capturing these coupled phenomena will allow for bridging scales between local

measurements and space-based remote sensing to effectively make forward predictions about the future state of the Arctic under a changing climate. These upscaled results can then ultimately be linked to global climate models through greenhouse gas source terms.

Sandia National Laboratories is a multimission laboratory managed and operated by National Technology and Engineering Solutions of Sandia, LLC., a wholly owned subsidiary of Honeywell International, Inc., for the U.S. Department of Energy's National Nuclear Security Administration under contract DE-NA-0003525. SAND2022-3134 A.

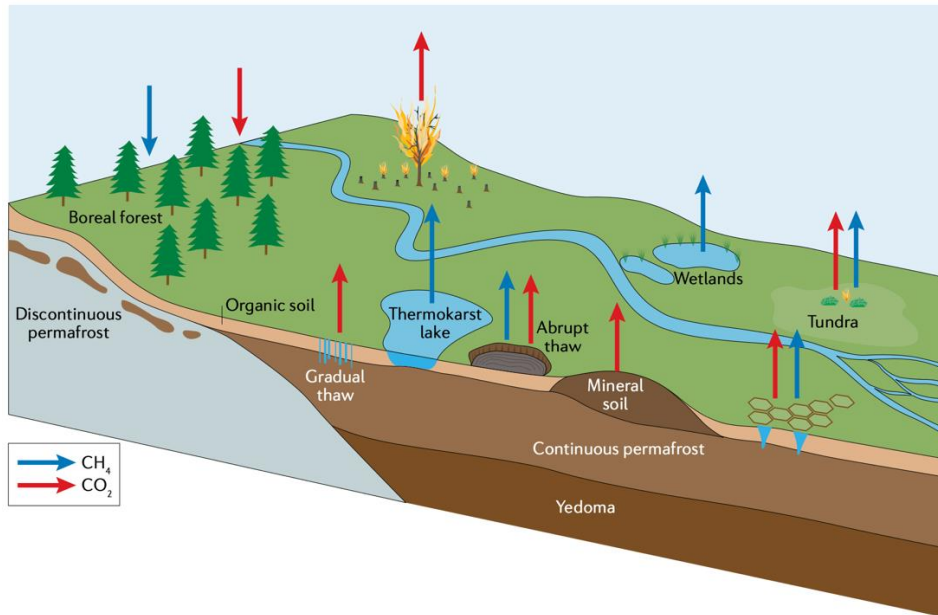


Figure 1. Carbon fluxes in the permafrost (from ACIA, 2004)

Keywords

Numerical modeling; greenhouse gas release; permafrost

References

Arctic Climate Impact Assessment. *Impacts of a Warming Arctic: Arctic Climate Impact Assessment* (Cambridge Univ. Press, 2004).

Biskaborn, B. K. et al. Permafrost is warming at a global scale. *Nat. Commun.* **10**, 264 (2019).

IPCC, 2014: Climate Change 2014: Synthesis Report.

Johnston, E. R. et al. Responses of tundra soil microbial communities to half a decade of experimental warming at two critical depths. *Proc. Natl Acad. Sci. USA* **116**, 15096–15105 (2019).

McGuire, A. D. et al. Dependence of the evolution of carbon dynamics in the northern permafrost region on the trajectory of climate change. *Proc. Natl Acad. Sci. USA* **115**, 3882–3887 (2018).

Raynolds: Vegetation Response to a climate gradient in the eastern Canadian Arctic

Martha Raynolds¹, Helga Bültmann², Shawnee Kasanke³, Jonathan Raberg⁴, Gifford Miller⁴

¹Institute of Arctic Biology, University of Alaska, Fairbanks Alaska USA

²University of Münster, Germany

³Washington State University, Richland Washington USA

⁴INSTAAR, University of Colorado, Boulder Colorado USA

Abstract

The eastern Canadian Arctic encompasses the entire Arctic bioclimate gradient, from treeline to ice caps. We sampled and mapped the vegetation around a series of lakes along this gradient. The maps were based on a suite of remote sensing products, including publicly available satellite imagery, Digital Globe imagery, the Arctic DEM, and locally flown drone imagery. The maps show a 1 km² area around the lakes, and use a consistent legend, so that vegetation units can be compared between lakes. Vegetation plots were sampled around the lakes, and cover values were recorded for lichens, bryophytes and vascular plants. Map units were defined based on dominant plant growth forms.

The four lakes presented include one near Pond Inlet, Baffin Island, Nunavut (next to an ice cap, 72.4 °N), one near Clyde River, one near Iqaluit, and one near Kuujuaq, Nunavik, Quebec (at treeline 58.1°N). The vegetation types range from rocky terrain with lichens at the coldest site (Mean Annual Air Temperature (MAAT) -18.2 °C) to open spruce forest with low shrub and moss understory at the warmest site (MAAT -5.4 °C).

These maps will be used to compare current vegetation with evidence of past vegetation found in lake sediment cores from the lakes, which include times both warmer and colder than present. The differences along the climate gradient will also be used to help predict the response of vegetation to climate warming.

Keywords: Baffin Island, arctic vegetation

Acknowledgements: *Nakurmiik* (Thank you!) to the people of Pond Inlet, Clyde River, Qikiqtarjuaq, Iqaluit, and Kuujuaq in Nunavut and Nunavik who supported this research by allowing access to their lands, and provided housing, transportation, and safety support. This research was funded by NSF OPP #1737750.

Rea: Investigating red snow algae resurfacing and distribution patterns

Madeleine Rea¹, Dr. Roman Dial¹, Dr. Jason Geck¹

¹ Institute of Culture and Environment, Alaska Pacific University, Anchorage, AK

Abstract

Red snow algae (snow algae) –a taxon of green algae containing the red pigment astaxanthin– seasonally reappear on alpine snowpack and glacier surfaces. Snow algae significantly reduce surface albedo, thereby increasing the rates of surrounding snowpack melt, and potentially increasing the rate of global sea level rise, (Lutz et al. 2016). This melt rate is positively correlated with local snow algae abundance (Ganey et al. 2017). However, many of the processes influencing abundance, including the primary mechanism of seasonal reappearance, are currently undocumented. One hypothesis of reappearance is that snow algae act as perennials, lying dormant under annual snowpack accumulation throughout winter, then actively migrate to the surface as spring arrives (Hoham & Remias, 2020). This hypothesis further posits that resurfacing would be limited by access to liquid water and sunlight penetration. Liquid water facilitates upward ‘swimming’ through the interstitial space between snow crystals, while light penetration is thought to allow for phototaxis of germinated cells (Dove et al. 2012). In our pilot study we used Landsat-8 spectral imagery and field validated NDI equations (Ganey et al. 2017) to visualize snow algae presence on the Harding Icefield from 2013 to 2021. These images were combined to create a map of snow algae persistence (Fig. 1). Across the icefield there was an east-west trend of decreasing year after year algae persistence and an edge-center trend of snow algae presence-absence with higher probability of presence around the edges. As noted in previous literature (Takeuchi et al. 2006), these trends may be the result of annual snowpack depth differences across the icefield. Due to the potential limiting effect of annual snowpack deposition on snow algae resurfacing, it is likely that areas which receive larger annual snow loading see less snow algae persistence. In the case of the Harding Icefield, there are larger annual snow loadings on the relative marine or east side of the icefield and at higher elevations near the middle of the icefield. A future project objective aims to experimentally investigate the resurfacing hypothesis and the effect of snow depth on resurfacing. We will introduce physical barriers to prevent seasonal resurfacing on the Harding Icefield in the summer of 2022. In the following summer season, we will monitor the snowpack above these barriers for differences in snow algae concentration, bloom timing, and melt rate.

Keywords: Red snow algae, Albedo, Landsat

Figures

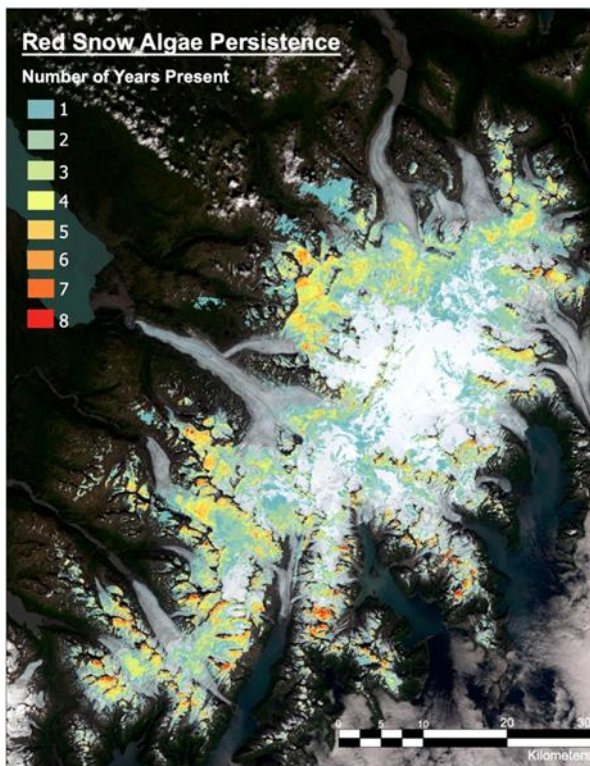


Figure 1. Snow algae persistence on the Harding Icefield 2013-2021. Warmer colors indicate longer observed reoccurrence of snow algae populations.

References

- Dove, A., Heldmann, J., McKay, C., & Toon, O. B. (2012). Physics of a thick seasonal snowpack with possible implications for snow algae. *Arctic, Antarctic, and Alpine Research*, *44*, 36–49.
- Ganey, G. Q., Loso, M. G., Burgess, A. B., & Dial, R. J. (2017). The role of microbes in snowmelt and radiative forcing on an Alaskan icefield. *Nature Geoscience*, *10*, 754–759.
- Hoham, R. W., & Remias, D. (2020). Snow and glacial algae: A review1. *Journal of Phycology*, *56*, 264–282.
- Lutz, S., Anesio, A. M., Raiswell, R., Edwards, A., Newton, R. J., Gill, F., & Benning, L. G. (2016). The biogeography of Red Snow microbiomes and their role in melting Arctic glaciers. *Nature Communications*, *7*.

Takeuchi, N., Dial, R., Kohshima, S., Segawa, T., & Uetake, J. (2006). Spatial distribution and abundance of red snow algae on the Harding Icefield, Alaska derived from a satellite image. *Geophysical Research Letters*, 33.

Acknowledgements

Funding for this research was provided by NASA through the Alaska Space Grant Program.

Rettelbach: The evolution of ice-wedge polygon networks in tundra fire scars

Tabea Rettelbach^{1, 2, 3 *}, Chandi Witharana⁴, Anna K. Liljedahl⁵, Ingmar Nitze¹, Johann-Christoph Freytag³, Guido Grosse^{1, 2}

¹ Alfred Wegener Institute Helmholtz Centre for Polar and Marine Research, 14473 Potsdam, Germany.

² University of Potsdam, Institute for Geosciences, 14476 Potsdam, Germany.

³ Department of Computer Science, Humboldt University of Berlin, 10099 Berlin, Germany.

⁴ Department of Natural Resources and the Environment, University of Connecticut, Storrs, CT 06268, USA.

⁵ Woodwell Climate Research Center, Falmouth, MA 02540

*Corresponding author. E-mail: tabea.rettelbach@awi.de (T. Rettelbach)

Abstract

In response to increasing temperatures and precipitation in the Arctic, ice-rich permafrost landscapes are undergoing rapid changes. In permafrost lowland landscapes, polygonal ice wedges are especially vulnerable, and their melting induces widespread subsidence triggering the transition from low-centered (LCP) to high-centered polygons (HCP) by forming degrading troughs. This process has an important impact on surface hydrology, as the connectivity of such trough networks determines the rate of drainage of an entire landscape (Liljedahl et al., 2016). While scientists have observed this degradation trend throughout large domains in the polygonal patterned Arctic landscape over timescales of multiple decades, it is especially evident in disturbed areas such as fire scars (Jones et al., 2015). Here, wildfires removed the insulating organic soil layer. We can therefore observe the LCP-to-HCP transition within only several years. Until now, studies on quantifying trough connectivity have been limited to local field studies and sparse time series only. With high-resolution Earth observation data, a more comprehensive analysis is possible. However, when considering the vast and ever-growing volumes of data generated, highly automated and scalable methods are needed that allow scientists to extract information on the geomorphic state and on changes over time of ice-wedge trough networks.

In this study, we combine very-high-resolution (VHR) aerial imagery and comprehensive databases of segmented polygons derived from VHR optical satellite imagery (Witharana et al., 2018) to investigate the changing polygonal ground landscapes and their environmental implications in fire scars in Northern and Western Alaska. Leveraging the automated and scalable nature of our recently introduced approach (Rettelbach et al., 2021), we represent the polygon

networks as graphs (a concept from computer science to describe complex networks) and use graph metrics to describe the state of these (hydrological) trough networks. Due to a lack of historical data, we cannot investigate a dense time series of a single representative study area on the evolution of the network, but rather leverage the possibilities of a space-for-time substitution. Thus, we focus on data from multiple fire scars of different ages (up to 120 years between date of disturbance and date of acquisition). With our approach, we might infer past and future states of degradation from the currently prevailing spatial patterns showing how this type of disturbed landscape evolves over space and time. It further allows scientists to gain insights into the complex geomorphology, hydrology, and ecology of landscapes, thus helping to quantify how they interact with climate change.

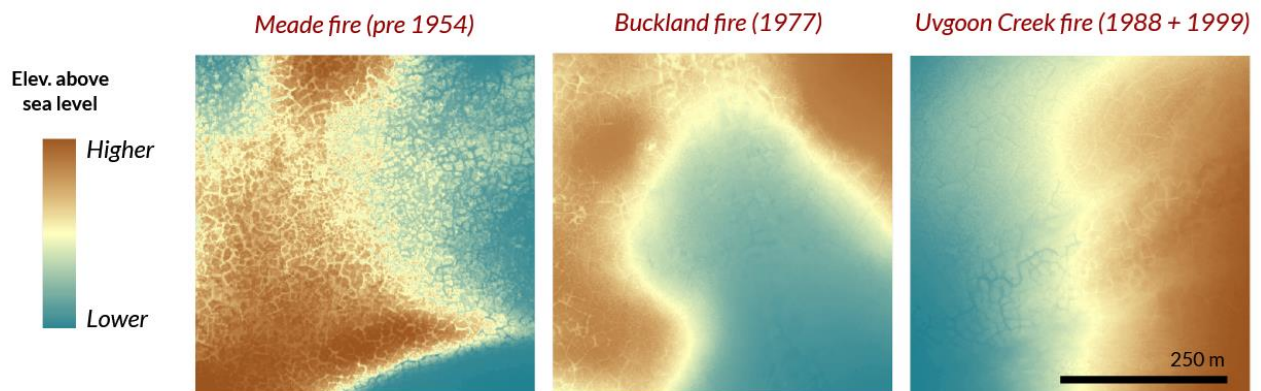


Figure 4: Ice-wedge landscapes in three Alaskan fire scars of differing ages. In brackets, the year of the burn(s) is indicated.

Keywords: permafrost, ice-wedge networks, graph analysis

References

- Jones, Benjamin M., et al. "Recent Arctic tundra fire initiates widespread thermokarst development." *Scientific reports* 5.1 (2015): 1-13.
- Liljedahl, Anna K., et al. "Pan-Arctic ice-wedge degradation in warming permafrost and its influence on tundra hydrology." *Nature Geoscience* 9.4 (2016): 312-318.
- Rettelbach, Tabea, et al. "A Quantitative Graph-Based Approach to Monitoring Ice-Wedge Trough Dynamics in Polygonal Permafrost Landscapes." *Remote Sensing* 13.16 (2021): 3098.
- Witharana, Chandi, et al. "An object-based approach for mapping tundra ice-wedge polygon troughs from very high spatial resolution optical satellite imagery." *Remote Sensing* 13.4 (2021): 558.

Acknowledgements

Financial support for conference attendance was provided by Geo.X, the Research Network for Geosciences in Berlin and Potsdam and the Potsdam Graduate School (PoGS). T.R. further acknowledges the support by the Helmholtz Einstein International Berlin Research School in Data Science (HEIBRiDS).

Kavya Sivaraj, Kurt Solander, Charles Abolt, Elizabeth Hunke, Amber Whelsky

Los Alamos National Laboratory, Los Alamos, New Mexico, USA

Abstract

Arctic sea ice plays an important role in moderating Earth's climate. On average, it experiences net negative radiation, losing more energy to the atmosphere than it absorbs, thus acting as a heat sink [1]. Sea ice is circulated and transported via the Beaufort Gyre and the Transpolar Drift Stream. The Beaufort Gyre is located in the Beaufort Sea, north of Alaska, and experiences clockwise circulation. Seasonal (first-year) ice can be trapped in the gyre for several years, growing and thickening into perennial (multi-year) ice. The multi-year ice has declined significantly in recent decades [2]. This rapid decline has severe climate implications as the melting sea ice reduces the albedo of the arctic region, thereby creating a positive feedback loop to further accelerate melting.

One important aspect of Arctic sea ice is the presence of melt ponds. Melt ponds develop on the surface of the ice, darkening it and thus affecting the total energy exchanged between the atmosphere and the ocean. Therefore, it is crucial to understand the dynamics of these features through observations. Several studies have estimated melt pond fraction and depth using either optical satellite imagery or radar [3], [4], [5]. Optical imagery is limited by the availability of cloud-free conditions and illumination. In contrast, the interpretation of the radar imagery is complicated by the effects of surface roughness, incidence angle, etc. To overcome these limitations, we synergize both optical and SAR imagery from the Sentinel-1 and Sentinel-2 missions to detect melt ponds.

In our study, we focus on a large area ($450,000 \text{ km}^2$) over the Beaufort Gyre at the height of the melt season between the months of June and August, applying algorithms to detect melt pond surface area based on both shape and color. We validate our approach by comparing the radar-based and optical-based estimates for the region. Next, we evaluate the interannual dynamics of melt pond surface area using the radar-based estimates across multiple melt seasons. Research outcomes will be used to improve observation capabilities and models of melt pond dynamics, to better understand how changes in sea ice will impact the climate system.

Keywords

Arctic melt ponds, remote sensing, sea ice

References

1. All About Arctic Climatology and Meteorology." National Snow and Ice Data Center. Accessed 17 March 2022. [/cryosphere/arctic-meteorology/index.html](https://cryosphere/arctic-meteorology/index.html).
2. Vihma, T. (2014). Effects of Arctic sea ice decline on weather and climate: A Review. *Surveys in Geophysics*, 35(5), 1175–1214. <https://doi.org/10.1007/s10712-014-9284-0>
3. Howell, S. E., Scharien, R. K., Landy, J., & Brady, M. (2020). Spring melt pond fraction in the Canadian Arctic Archipelago predicted from radarsat-2. *The Cryosphere*, 14(12), 4675–4686. <https://doi.org/10.5194/tc-14-4675-2020>
4. Rösel, A., Kaleschke, L., & Birnbaum, G. (2012). Melt Ponds on Arctic sea ice determined from MODIS satellite data using an artificial neural network. *The Cryosphere*, 6(2), 431–446. <https://doi.org/10.5194/tc-6-431-2012>
5. Tilling, R., Kurtz, N. T., Bagnardi, M., Petty, A. A., & Kwok, R. (2020). Detection of melt ponds on Arctic Summer Sea ice from icesat-2. *Geophysical Research Letters*, 47(23). <https://doi.org/10.1029/2020gl090644>

Spasova: Interoperability of remote sensing and open data for Arctic and Antarctic ice and climate change monitoring and security

Temenuzhka Spasova¹

¹Aerospace information, Space Research and Technology Institute-Bulgarian Academy of Sciences, Acad. Georgy Bonchev str., bl. 1, 1113 Sofia, Bulgaria

Abstract

Climate change and the measures that are being taken are no longer such a new and topical issue, but are part of our lives. The interoperability of multiple data sources allows for much more accurate analysis, decision making, model training and results.

Unfortunately, factors such as military action must now be taken seriously, which will also have a serious impact on climate change in some places, but will also affect the presence of snow, ice and fresh water.

However, the availability of objective information today makes it possible to at least build the right strategies and policies for climate change and security, such as reducing the carbon footprint, building sustainability policies and helping adaptation in many parts of the world.

The aim of the research is to demonstrate a model of monitoring methodology, which actively involves data from different satellites, available Open Data and Artificial Intelligence, which together give results for the dynamics and presence of different processes.

The methodology makes it possible to demonstrate the presence of vegetation in places that should normally be occupied by vegetation. Such places are the New Shetland Islands in Antarctica and arch. Svalbard in the Arctic.

Models such as TCT (Tasseled Cap Transformation), various optical and SAR (Synthetic Aperture Radar) indices, change vector index, spectral characteristics of objects and various composite images were used to show the sharp dynamics of ice, coastal seasonal ice, wet snow and snow. Last but not least, the appearance of mossy vegetation in just a few years.

As a result, interoperable independent models have been obtained for monitoring the Arctic and Antarctic latitudes, but also in areas that may be subject to military bases and actions.

These models will support the Digital Twins methodology and the work of the EC Destination Earth (DestinE) group.

Keywords: Climate change, Destination Earth, SAR

Turner: Detecting the climate-driven disturbances that are influencing aquatic environments in Old Crow Flats, Yukon, Canada

Kevin Turner¹, Michelle Pearce², Marley Tessier³

¹Department of Geography and Tourism Studies, Brock University, St. Catharines, Ontario, Canada

²Department of Earth Science, Brock University, St. Catharines, Ontario, Canada

³Department of Earth Science, Brock University, St. Catharines, Ontario, Canada

Abstract

Changes in climate across Arctic and subarctic regions are driving landscape transitions. Lake- and ice-rich permafrost landscapes are particularly sensitive to warmer and wetter conditions, with drastic and more frequent responses including retrogressive thaw slumps and thermokarst lake drainage events. We are using multiscale (spaceborne, airborne, and drone) remotely sensed data to inventory these abrupt changes in Old Crow Flats (OCF), a ~15,000-km² watershed within the traditional territory of the Vuntut Gwitchin First Nation (VGFN). Concerns of the VGFN include the impacts of these disturbance events on wildlife dynamics and downstream water quality. This research program provides insight of the location of these disturbances, how they develop over time, and the associated impacts on downstream biogeochemistry. Past research shows that the frequency of lake drainage events has increased in OCF (Lantz and Turner, 2015). This can result in drastically different catchment and aquatic biogeochemical responses (Turner et al., in press; Figure 1a). For instance, water chemistry is highly variable within the first few years following drainage until the exposed former lakebed is stabilized with encroaching shrub vegetation. We have also closely monitored areal and volumetric increases in the size of the largest active thaw slump in OCF, which initiated in June 2016 along the Old Crow River (Turner et al., 2021; Figure 1b). Our ongoing remote sensing work includes extending our records of the frequency of disturbance events. Landsat and Sentinel-2 products (e.g., water masks) can be used to identify most surface water drainage events; however, finer-scale data are required for inventorying the development of thaw slumps, which often range from 100 – 10,000 m² upon initial detachment. This presentation will feature key lake drainage and thaw slump events and the techniques we have used to document them. As well, the utility of our long-term lake and river biogeochemistry record will be presented to showcase additional evidence that climate conditions are priming OCF for continued change. For example, the 13-year lake water isotope record captures the increasing influence of rainfall and hydrological connectivity (MacDonald et al., 2021). Overall, these studies are providing comprehensive insight of the response of OCF to ongoing climate change, which complements traditional knowledge and local observations. This is relevant for

anticipating future biogeochemical responses to landscape change in OCF and other areas influenced by thermokarst processes.

References:

Lantz TC and KW Turner. 2015. Increase in the frequency of catastrophic lake drainage in the Old Crow Flats, Yukon. *Journal of Geophysical Research: Biogeosciences*, 120: 513-524, doi: 10.1002/2014JG002744.

Turner KW, BB Wolfe, I McDonald. In Press. Monitoring 13 years of drastic catchment change and the hydroecological responses of a drained thermokarst lake. *Arctic Science*.

MacDonald LA, KW Turner, I McDonald, ML Kay, RI Hall, BB Wolfe. 2021. Isotopic evidence of increasing water abundance and lake hydrological change in Old Crow Flats, Yukon, Canada. *Environmental Research Letters* 16 124024.

Turner KW, MD Pearce, D Hughes. 2021. Detailed characterization and monitoring of a retrogressive thaw slump from remotely piloted aircraft systems and identifying associated influence on carbon and nitrogen export. *Remote Sensing*, section: Remote Sensing in Geology, Geomorphology and Hydrology, special issue: Applications of UAVs in Cold Region Ecological and Environmental Studies.

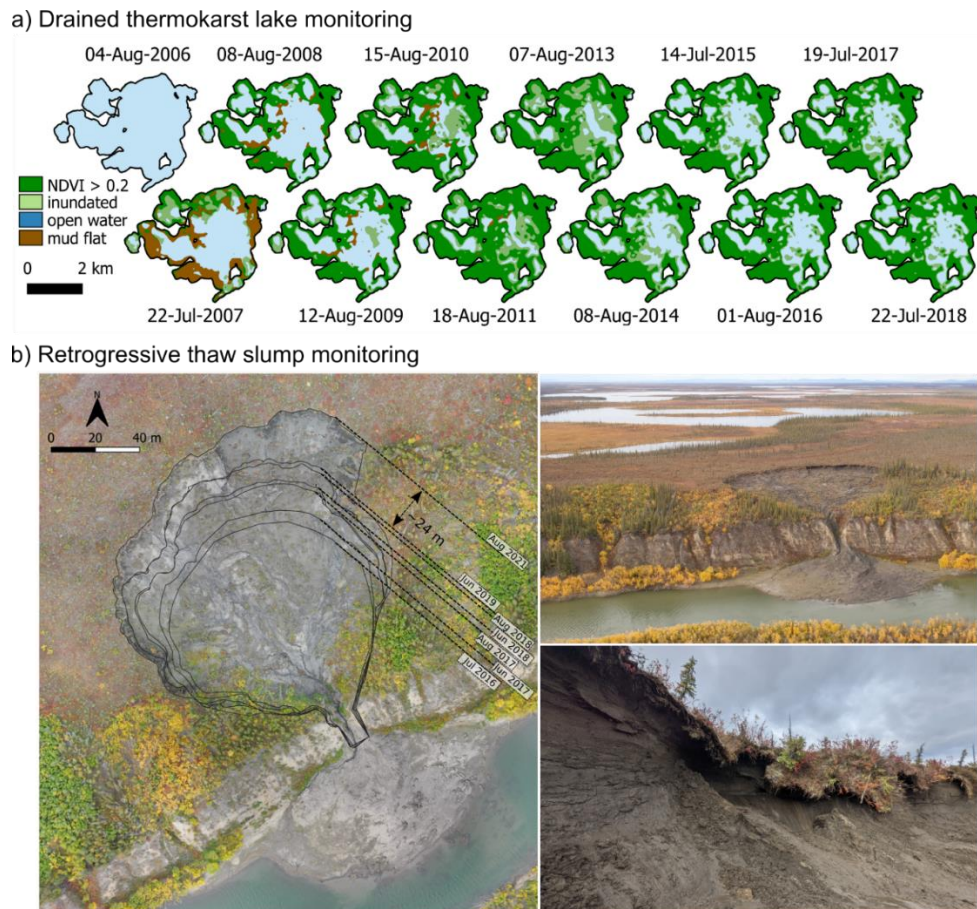


Figure 1. Time-series tracking of a) surface water and catchment land cover change within a drained lake basin, and b) the largest active thaw slump in OCF.

Keywords: thermokarst, drone, biogeochemistry

Acknowledgements:

We would like to thank the community of Old Crow and the Vuntut Gwitchin Government (VGG) for facilitating this research program. Research was also supported by Parks Canada staff and colleagues from the labs of Dr. Brent Wolfe and Dr. Roland Hall. Financial support was provided by Natural Sciences and Engineering Council of Canada (NSERC), Polar Continental Shelf Program of Natural Resources Canada, Polar Knowledge Canada, Northern Scientific Training Program of Aboriginal Affairs and Northern Development Canada, and Parks Canada. We are grateful for the NASA Arctic-Boreal Vulnerability Experiment including OCF within ongoing airborne campaigns.

Veremeeva: Yedoma surface thaw subsidence (2015-2021) depended on local geomorphological conditions, Bykovsky Peninsula, Laptev Sea region

Veremeeva A.¹, Günther F.², Kizyakov A.³, Pismeniuk A.³, Rivkina E.¹, Grosse G.².

¹ Soil Cryology, Institute of Physicochemical and Biological Problems in Soil Science, Russian Academy of Sciences, Pushchino, Russia

²Permafrost Research Section, Alfred Wegener Institute for Polar and Marine Research, Potsdam, Germany

³Department of Cryolithology and Glaciology, Faculty of Geography, Lomonosov Moscow State University, Moscow, Russia

Abstract

One of the most vulnerable permafrost landscapes in a warming climate are Yedoma landscapes formed by late Pleistocene, highly ice-rich Yedoma Ice Complex (IC) deposits covering vast lowlands of NE Siberia and Alaska. Yedoma landscapes are characterized by different geomorphological conditions leading to distinct characteristics in drainage, active layer thickness (ALT), microrelief features, permafrost soils, and vegetation cover. There is a general lack of knowledge of Yedoma landscape characteristics at local scales, in particular thaw subsidence rates and their dependence on geomorphological conditions. The aim of our study is to determine Yedoma surface thaw subsidence and to investigate the patterns and drivers of spatial differences at the local scale on Bykovsky Peninsula, Laptev Sea region. During expeditions in 2015, 2016 and 2021 we conducted field research of Yedoma upland landscapes that represent three main types of geomorphological conditions: 1) well-drained Yedoma landscapes characterized by gentle to steep slopes, 2) flat boggy Yedoma uplands, and 3) runoff hollows and stream valleys. For all Yedoma landscape types, detailed descriptions of vegetation communities and ALT measurements were carried out. To detect thaw subsidence at a subcentimeter scale, terrestrial laser scanning in 2015 and 2016 and an unmanned aerial vehicle (UAV) survey in 2021 were performed for a key site. To detect thaw subsidence in situ, 9 benchmarks were drilled into the permafrost to a depth of 4 m, which also allows to exclude the frost heave impact on benchmark position changes. To estimate the Yedoma surface elevation changes we used Sentinel-1 SAR images from 2014 to 2021. Remote sensing data of different resolution (WorldView 3, Sentinel-2, ArcticDEM) were used to characterize the vegetation cover and geomorphological analysis.

During the period from 2014 to 2021, an increase of summer air temperatures was observed while there was not clear trend of precipitation changes. Climate warming has led to ALT deepening showing an increase by about 5 cm from 2014 to 2021 at the Bykovsky Yedoma CALM site. Detailed measurements of the ALT at sites with different vegetation communities on the well-drained Yedoma surface showed an ALT variability within different vegetation types and a general increase trend of ALT from 2015-2016 to 2021 (Fig.1). Sites 2_1 and 2_2 were characterized by an initial stage of baydzhherakh relief formation: a depression between thermokarst mounds and a convex surface of the baydzhherakh respectively. Site 2_8 presents the

well-drained Yedoma slope. The five benchmarks show significant terrain surface subsidence of 1 to 3 cm per year. The highest thaw subsidence rate was observed for a Yedoma slope site (site 2_8) which settled by 15 cm from 2016 to 2021 while the ALT increased by ~8 cm from 32 cm to 40 cm in average.

Understanding the Yedoma IC thaw subsidence rates and its spatial patterns depending on geomorphological conditions at the local scale is necessary in connection with the observed significant climate warming in the Arctic to analyze and predict changes in Yedoma landscapes.

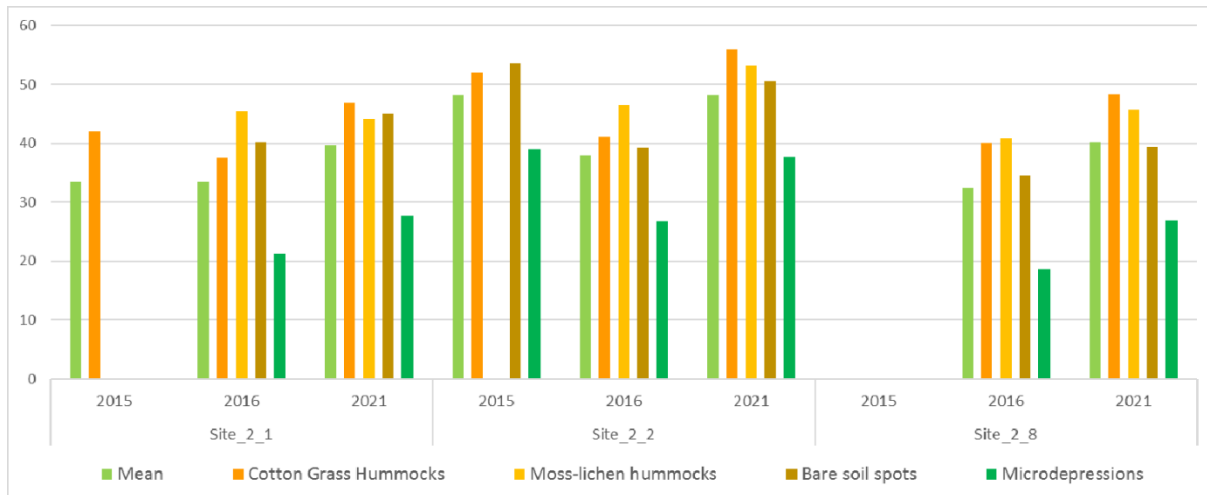


Figure 1. ALT measurements within main vegetation communities of the drained Yedoma landscapes.

Keywords: Yedoma IC, thaw subsidence, active layer thickness.

Acknowledgements: This research was funded by the ERC PETA-CARB project and the Russian Science Foundation under grant number 22-27-00731.

Wong: Calibrating 2000-2020 MODIS and Landsat greening in Northwest Alaska with 1000 km of vegetation transect data

Russell Wong¹, Dr. Roman Dial¹, Christopher Potter², Dr. Logan T. Berner³

¹Institute of Culture and Environment, Alaska Pacific University, Anchorage, AK

²NASA Ames Research Center, Moffett Field, CA 94035, USA

³School of Informatics, Computing, and Cyber Systems, Northern Arizona University, Flagstaff, AZ

Abstract

The Arctic is warming faster 2-3 times faster than average. Concurrent with warming, earth-observing satellites (e.g., MODIS and Landsat) have detected increases over time in the normalized difference vegetation index (NDVI). Increasing NDVI, a proxy for increasing plant productivity, is referred to as “greening”. MODIS and Landsat datasets show significant greening trends over the past 20 years, indicating widespread ecological changes are underway. While greening is linked to increased growth and cover of shrubs in addition to warming, there is limited research linking greening to on-the-ground observations of overstory and understory vegetation types. To inform greening, we walked a 1000km vegetation transect and documented overstory and understory vegetation classes as canopy cover, plant functional type (PFT), and taxa. While walking, we recorded the transect on iPhones as a continuous line with segments attributed by their vegetation composition. The vertices of the continuous track act as sample sites where MODIS and Landsat greening trends can be calculated. These data show which vegetation types are associated with greening and how overstory-understory interactions display different rates of greening. We can also use NDVI calculated at sample sites to train models predicting vegetation cover. By calibrating arctic greening with ground data, we can better understand and predict ecological change in these rapidly warming arctic mountains.

Keywords: MODIS, Landsat, NDVI

References

- Berner, L. T., Massey, R., Jantz, P., Forbes, B. C., Macias-Fauria, M., Myers-Smith, I., ... & Goetz, S. J. (2020). Summer warming explains widespread but not uniform greening in the Arctic tundra biome. *Nature Communications*, 11(1), 1-12.
- Holland, M. M., & Bitz, C. M. (2003). Polar amplification of climate change in coupled models. *Climate dynamics*, 21(3), 221-232.
- Mekonnen, Z. A., Riley, W. J., Berner, L. T., Bouskill, N. J., Torn, M. S., Iwahana, G., ... & Grant, R. F. (2021). Arctic tundra shrubification: a review of mechanisms and impacts on ecosystem carbon balance. *Environmental Research Letters*, 16(5), 053001.
- Potter, C., & Alexander, O. (2020). Changes in vegetation phenology and productivity in Alaska over the past two decades. *Remote Sensing*, 12(10), 1546.

Acknowledgements

This project received funding from the Alaska Space Grant Program, the Ames Research Center, the Explorers Club, and Discovery. We thank Julia Ditto, Toshio Matsuoka, Ben Weissenbach, and Maddy Zietlow for assisting in field data collection.

Wooten: Estimating Site Index in boreal forests with lidar and very-high resolution stereo imagery

Margaret Wooten^{1,2}, Christopher Neigh¹, Paul Montesano^{1,3}, William Wagner^{1,2}

¹NASA Goddard Space Flight Center (Biospheric Sciences Laboratory; Greenbelt, Maryland)

²Science Systems and Applications, Inc. (Lanham, Maryland, USA)

³Adnet Systems (Bethesda, Maryland, USA)

Abstract

In the circumpolar boreal region, the effects of climate change are increasingly evident as temperatures continue to rise at a rate faster than the global average. As a changing climate alters vegetation dynamics and the overall land atmosphere carbon budget, it is now more important than ever to understand the regrowth potential of young boreal forests and the future strength with which they may act as a carbon sink.

Site Index (SI) knowledge allows us to better understand site-specific environmental constraints on canopy structure and growth by capturing rates of forest regeneration and Carbon flux across the boreal. Here we present preliminary results and methods for estimating SI from space by pairing Landsat-derived disturbance data with canopy structure estimates from high resolution spaceborne imagery (HRSI) and lidar data from the Land, Vegetation, and Ice Sensor (LVIS).

Keywords: Climate change, Destination Earth, SAR

Special Thanks to Our Sponsors!

Massive Ice level (> \$5,000)



The National Science Foundation (NSF) is an independent federal agency created by Congress in 1950 "to promote the progress of science; to advance the national health, prosperity, and welfare; to secure the national defense..." NSF is vital because we support basic research and people to create knowledge that transforms the future. This type of support:

- Is a primary driver of the U.S. economy
 - Enhances the nation's security
- Advances knowledge to sustain global leadership

With an annual budget of \$8.8 billion (FY 2022), we are the funding source for approximately 27% of the total federal budget for basic research conducted at U.S. colleges and universities. In many fields such as mathematics, computer science and the social sciences, NSF is the major source of federal backing.

Massive Ice level (> \$5,000)



The **International Arctic Science Committee (IASC)** is a non-governmental, international scientific organization. The [Founding Articles](#) committed IASC to pursue a mission of encouraging and facilitating cooperation in all aspects of Arctic research, in all countries engaged in Arctic research and in all areas of the Arctic region. Overall, IASC promotes and supports leading-edge interdisciplinary research in order to foster a greater scientific understanding of the Arctic region and its role in the Earth system.

Rather than defining human and environmental boundaries, IASC tries to bridge those boundaries. IASC is also committed to recognizing that Traditional Knowledge, Indigenous Knowledge, and “Western” scientific knowledge are coequal and complementary knowledge systems, all of which can and should inform the work of IASC.

In-Kind Donors



MANY THANKS TO Sebastian Labour FOR DESIGNING, MAINTAINING AND HOSTING THE 16TH ICRSS WEB SITE

As a Helmholtz centre for polar and marine research the Alfred Wegener institute works above all in the cold and temperate regions of the world. Together with numerous national and international partners we are involved to decipher the complicated processes in the "system of earth". Our planet is in a radical climate change. The pole areas and seas change. At the same time they play a central role in the global climate system. How does the planet earth develop? Do we observe short-term variations or long-term trends? Polar and marine research has always been a fascinating scientific challenge. Today it is also a piece of futurology.



Inspiring discovery. Inspiring greatness. Inspiring, naturally.

MANY THANKS FOR HOSTING THE 16TH ICRSS

Land Acknowledgement

We acknowledge the Alaska Native nations upon whose ancestral lands our campuses reside. In Fairbanks, our Troth Yeddha' Campus is located on the ancestral lands of the Dena people of the lower Tanana River.

Ice Wedge (\$2,000 - \$4,999)



Alaska Climate Adaptation Science Center - A university-federal partnership

Established in 2010 as a partnership between the University of Alaska and the United States Geological Survey, the Alaska CASC is Congressionally mandated to meet state and federal needs around climate impacts, adaptation, and resilience.

Hosted by UAF's International Arctic Research Center with a USGS-hosted office in Anchorage, the Alaska CASC provides scientific information, tools, and techniques that managers and others interested in land, water, wildlife, and cultural resources can use to adapt to climate change.



Making Remote-Sensing Data Accessible

ASF is part of the [Geophysical Institute](#) of the University of Alaska Fairbanks.

- ASF downlinks, processes, archives, and distributes remote-sensing data to scientific users around the world.
- ASF promotes, facilitates, and participates in the advancement of remote sensing to support national and international Earth science research, field operations, and commercial applications.
- ASF commits to provide the highest quality data and services in a timely manner.

Aufeis (\$500 - \$1,999)



ABR, Inc. – Environmental Research and Services

Environmental Consulting Services for Alaska - We have decades of experience providing environmental consulting services and conducting ecological research safely and efficiently in one of the most challenging places on the planet—Alaska. The services we offer cover not only the complete spectrum of biological sciences, we also maintain expertise in a variety of ancillary services that our clients require. Our services take scientific expertise and pair it with leading edge technologies and methods to provide cost efficient environmental solutions.